REPUBLIC OF TÜRKİYE

ALTINBAS UNIVERSITY

Institute of Graduate Studies

Mechanical Engineering

STUDY AND DESIGN OF AN IMMERSION-COOLING SYSTEM FOR A COMPUTER USING NUMERICAL AND EXPERIMENTAL ANALYSIS

Ayad Awad Zaidan ZAIDAN

Master's Thesis

Supervisor

Asst. Prof. Dr. Yaser ALAIWI

Istanbul, 2023

STUDY AND DESIGN OF AN IMMERSION COOLING SYSTEM FOR A COMPUTER USING NUMERICAL AND EXPERIMENTAL ANALYSIS

Ayad Awad Zaidan ZAIDAN

Mechanical Engineering

Master’s Thesis

ALTINBAŞ UNIVERSITY

2023

The thesis titled STUDY AND DESIGN OF AN IMMERSION-COOLING SYSTEM FOR A COMPUTER USING NUMERICAL AND EXPERIMENTAL ANALYSIS prepared and presented by AYAD AWAD ZAIDAN ZAIDAN and submitted on 08/08/2023 has been **accepted unanimously/ by majority of votes** for the degree of Master of Science in Mechanical Engineering.

____

Asst. Prof. Dr. Yaser ALAIWI

Supervisor

Thesis Defense Jury Members:

Asst. Prof. Dr. Yaser ALAIWI	Department, Mechanical Engineering Altinbas University	____________________
Asst. Prof. Dr. Abdullahi Abdu IBRAHIM	Department, Electrical and Computer Engineering Altinbas University	____________________
Asst. Prof. Dr. Ahmed SADIK	Department, Mechanical Engineering Hasan Kalyoncu University	____________________

I hereby declare that this thesis/dissertation meets all format and submission requirements of a Master of Science thesis.

Submission date of the thesis to Institute of Graduate Studies: ___/___/___

I hereby declare that all information in this document has been obtained and presented in accordance with academic rules and ethical conduct. I also declare that, as required by these rules and conduct, I have fully cited and referenced all material and results that are not original to this work.

Ayad Awad Zaidan ZAIDAN

Signature

DEDICATION

I dedicate this humble research to my dear parents who have done everything in their power since my childhood to push me forward for educational attainment, also my beloved wife and children who have devoted their efforts to creating the appropriate environment and creating an encouraging atmosphere to continue research and analysis, also to every researcher looking forward to collecting information, which I tried as much as possible to collect as much as possible how much can be related to the topic of research.

ACKNOWLEDGEMENTS

I would like to extend my sincere thanks to Asst. Prof. Dr. Yaser ALAIWI, lecturer at Altınbaş University, Department of Mechanical Engineering, who was my supervisor during the writing of this research and who gave me the right direction by providing much correct advice, instructions, and information. Would also like to thank Assoc. Prof. Dr. Süleyman Baştürk, Head of the Mechanical Engineering Department at Altınbaş University, who in turn assisted immediately to solve all technical problems from laboratories and others. Also thanks to all the friends who supported, encouraged me and gave me valuable advice and information.

ABSTRACT

STUDY AND DESIGN OF AN IMMERSION-COOLING SYSTEM FOR A COMPUTER USING NUMERICAL AND EXPERIMENTAL ANALYSIS

ZAIDAN, Ayad Awad Zaidan
M.Sc., Mechanical Engineering, Altınbaş University,
Supervisor: Asst. Prof. Dr. Yaser ALAIWI
Date: August / 2023
Pages:123

Computer systems may be able to use electricity more effectively if cooling electronics systems is done more properly. Computer and some other electronic device could be cooled via immersion-cooling by immersing them in a thermally conductive liquid or coolant. In this study, a unique forced flow and heat sinks cooling system and technique for a single-phase immersed cooling system are presented. The CPU surface is covered with a straight fin heat-sink, and whole mainboard is immersed in 3M Novec 7100, a designed fluid that can disperse heat is utilised while utilizing immersed cooling. A simulation model created utilizing the ANSYS Multiphysics programme is validated by an experimental test. To investigate consequences of a single-phase immersed cooling system's cooling, three liquid coolant circulating speeds and two distinct heat sink material are utilized. utilizing a cross-sectional view and then a 3D isothermal surface model, the heat the model's chosen distribution was examined with different liquid coolants and material flow rates. The simulation results demonstrate that a cooler CPU would operate at a lower temperature if the liquid coolant moved more quickly. However, because of the slower circulation speed, the coolant flow was impeded. Additionally, it contributed to the uneven distribution of heat and higher temperature levels. The greatest temperature was recorded, and it was found that the model's imbalanced heat transmission. It should be noted that results are not considerably impacted by the heat sink's material. The system designer can utilize the results

to boost power densify and ensure the secure operation of an associated computer and electronic devices.

Keywords: Comsul, Ansys, Immersion-Cooling System, Computer,Heat Sing .

TABLE OF CONTENTS

Pages

LIST OF TABLES

Pages

LIST OF FIGURES

Pages

ABBREVIATIONS

CFD	:	Computational Fluid Dynamics
3D	:	Three Dimensional
3D	:	Three Dimensional
B	:	Thickness of Substrate
C_p	:	Specific Heat Capacity of Fluid
F	:	Integrated Performance Index
f	:	Proportion Factor
g	:	Gravitational Acceleration
H	:	Height
k	:	Thermal Conductivity of Solid
$L1$	:	Length
$L2$	:	Width
N	:	Number of Fins
p	:	Pressure
Rj	:	Heat Flux Range

1. INTRODUCTION

Around the globe, there are over 7,500 data centres. The number of new data centre buildings climbed by 21% in 2018 and 2019 alone, and this trend is probably going to continue in the near future. The majority of data centres are located in the United States [1]. Concern should be expressed about the growing number of data centres since they will increase the need for cooling systems, which will account for more than 4% of world energy consumption [2]. Superior methods that are more effective than traditional cooling methods like air- or water-cooling technologies must be utilized to solve this problem, including immersion-cooling. According to BIS Research, the worldwide immersion-cooling market was valued at $251.0 million in 2021. From 2022 to 2027, it is anticipated to increase at a CAGR of 36.3% and reach $1.60 billion [3].

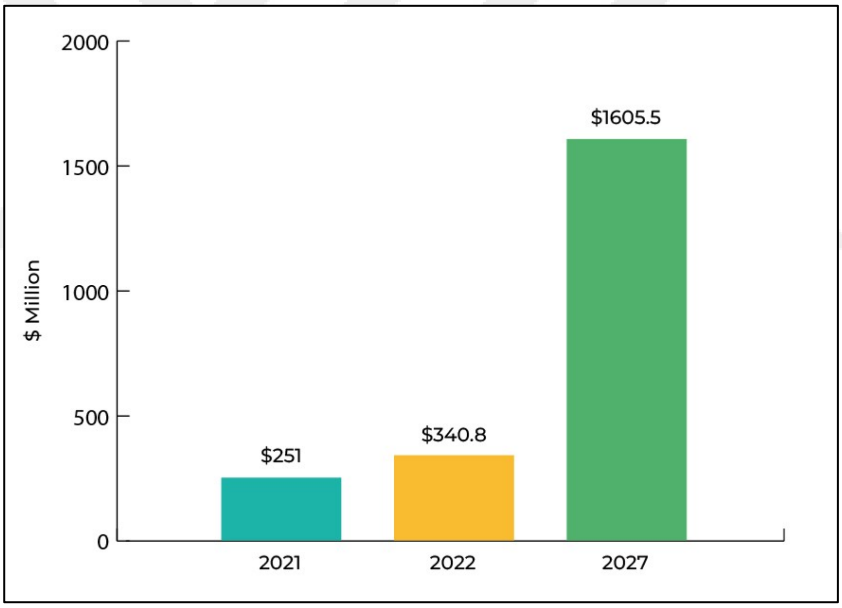

Figure 1.1: The Annual Cost Required for IT Components Cooling [4].

Air has always been the most popular means of cooling IT systems, from laptops to data centres. However, the fans, ducting, and HVAC systems needed to cool data centres with air demand a significant amount of space and power [5]. Pipes, pumps, and a substantial amount of space are needed in order to use fluid to cool IT systems, including that which may be found in cutting-edge gaming rigs or high-performance computer clusters. Additionally, fans are still required to handle the heating which the "heat pipes" and "cold plates" can't handle.

Due to immersion-cooling's greater energy and space efficacy, interest in the technology has gradually increased over time, and it has advanced significantly [6].

1.1 IMMERSION-COOLING SYSTEM

Using the heat transfer technique of immersion-cooling, a coolant is brought into close contact with a hot fluid. The most typical instance of this is when water is heated to a boil before being utilized to cool an engine [7]. Immersion-cooling has been utilized for a long time, but high-performance computer systems are just now beginning to employ it. Warm liquid is passed through one or more heating exchangers that are attached to a radiator or a fan to provide liquid immersion-cooling. Air flows thru the radiator, absorbing heating from the liquid and cooling as it does so [8].

Using a thermally conductive but electrically insulating dielectric liquid or coolant, IT components and other electronics, including whole servers and storage devices, are immersed during immersion-cooling [9]. Heating is removed from the system by moving relatively cold liquid into close contact with hot components and then moving this heated liquid via cool heat exchangers. This method of cooling servers and IT gear eliminates the need for fans, and often a heat exchanger is utilized to transfer heat from the heated coolant to the cold water circuit. The temperature of the whole system is pre-set, which helps to maintain it within safe ranges [10].

By transitioning from conventional cooling methods to immersion-cooling, data centres may efficiently prepare for future operating demands of high computing while controlling costs and environmental consequences. To prevent interfering with the computer's normal functioning, the liquid utilized should have a low enough electrical conductivity. If the liquid is particularly electrically conductive, it could be essential to insulate certain regions of components susceptible to electromagnetic interference, including the CPU. Therefore, it is ideal for the liquid to be dielectric [9].

Figure 1.2: Immersion-Cooling System [11].

By bringing the liquid in close contact with the heat source, immersion-cooling expands on this idea. In other words, the CPU is immersed in a liquid tank that allows heat from the component to be transferred into the liquid. As many researches could expect, accomplishing this calls for a lot of specialised gear, and several safety precautions should be followed to make sure that nothing bad happens [12]. An immersion-cooling PC's capacity to manage large heat fluxes without necessitating an excessive amount of surface area on the cooling apparatus and the computer is its key advantage. By increasing performance per unit space or weight, this makes it possible to run computers that would otherwise overheat when utilizing traditional air-cooling methods [13].

1.1.1 Immerse Cooling Techniques Types

Depending on the characteristics of the coolant, immersion-cooling methods in single- and two-phases applications may be categorised as follows [14]:

In single-phase, the dielectric liquid is circulated around hot electronic components via a heat-exchange process. A single-phase coolant's condition never varies; it's always liquid, never boils, and never freezes. A heat exchanger receives coolant and transfers heat to a circuit of cooler water [15].

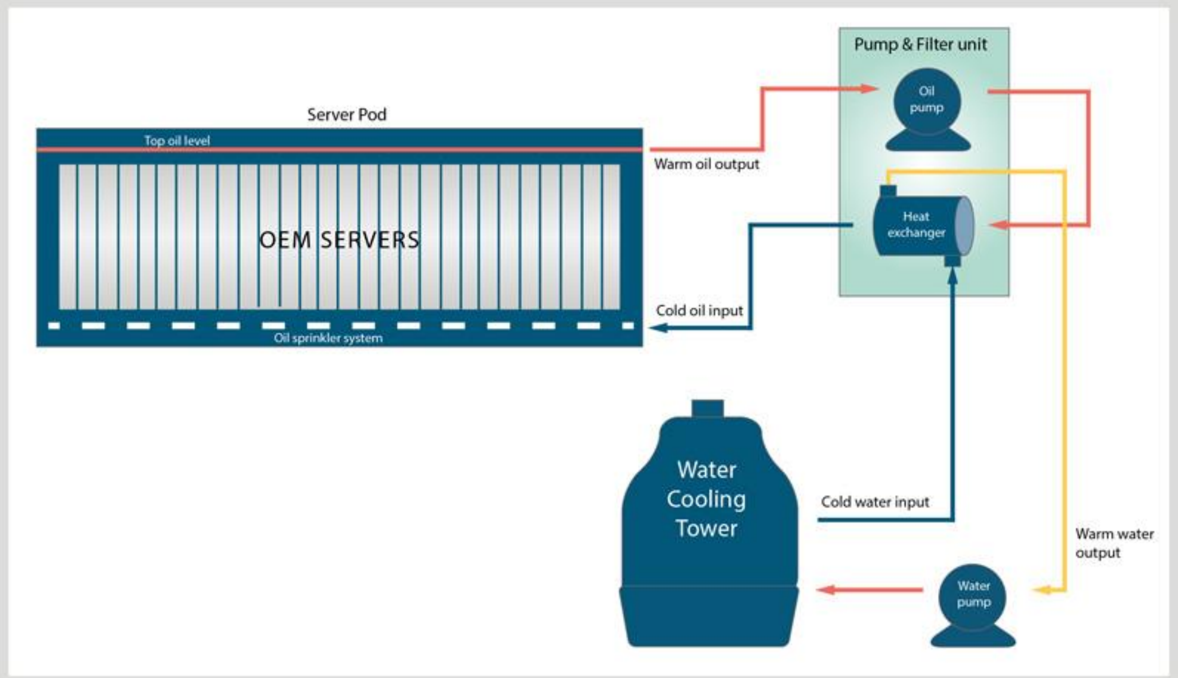

Figure 1.3: Single Phase Immerse Cooling Techniques [15].

Two-phases immersion uses low-temperature evaporation to cool hot electronics and remove heat from the liquid. The gas is once again cooled utilizing a heat exchanger to enable return passage into the bigger liquid volume. In two-phases cooling, the active fluid boils, separating into a liquid and a gas phase. The process takes use of "latent heat," or the heat (thermal energy) required to change the phase of a fluid [12].

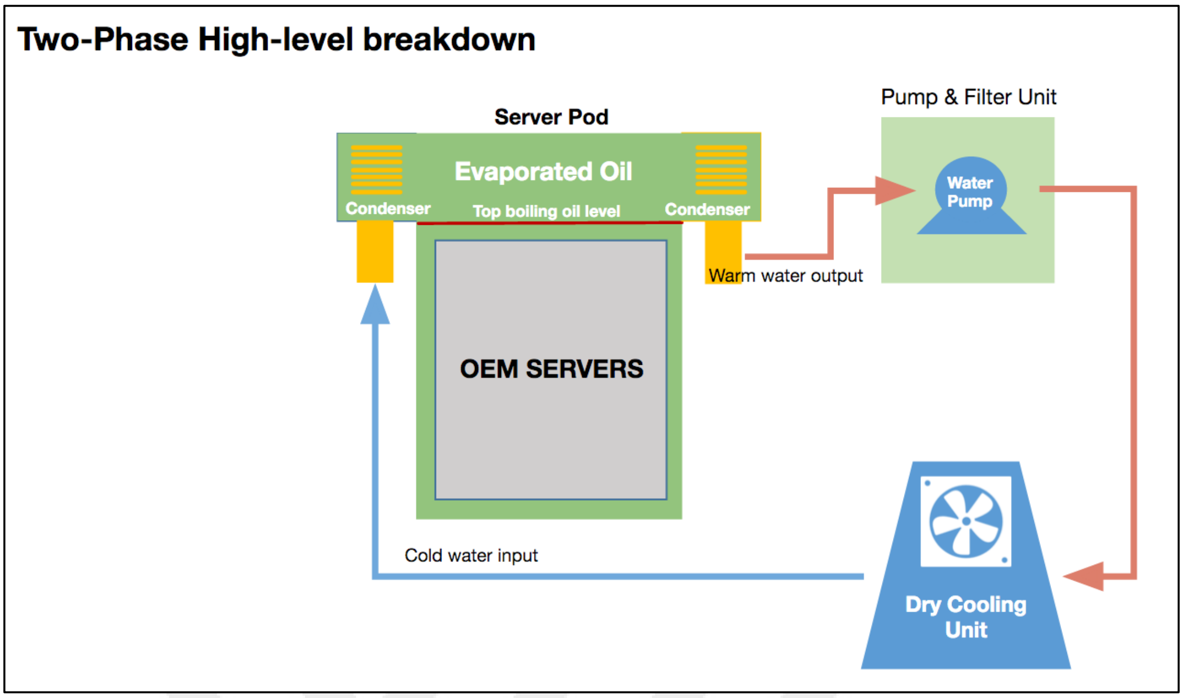

Figure 1.4: Two Phase Immerse Cooling Techniques [12].

1.1.2 Advantages of Immersion-Cooling

The use of a heat-conducting liquid in immersion-cooling allows for the resolution of energy overconsumption issues in data centres. It maximises the removal of calories lost by electronic parts while safeguarding them from outside aggressions [16]:

i. Energy use for cooling may be reduced by up to 90 percent.

ii. Fan suppression: Elimination of noise and vibration.

iii. No air contact means less oxidation and dust.

iv. Longer component lifetime.

v. Low temperature changes (due to high inertia and thermal conductivity).

vi. Significantly lower operational expenses.

The submerged servers don't need a special infrastructure and it could be deployed in any kind of structure. The whole data centre doesn't need to be cooled. Only computer hardware requires cooling. Simply extend the life and efficacy of the assets by utilising our solution.

1.1.3 Disadvantages of Immersion-Cooling

The following are a handful of the most major drawbacks [17]:

Operation complexity**:** Configuring an immersion-cooling operation in the hash center might be challenging. If you haven't done so before, then might be required to collaborate with a capable professional team. To undertake an immersion-cooling procedure, you must locate the appropriate equipment and synchronise it with the operation. It's simple to get irritated if folks can't seem to agree on anything. Consider the tools you'll have to set up immersion-cooling carefully.

The installation's price: The expense of immersion-cooling installation is another significant disadvantage. It may help you save money in the long run, but it could cost a lot up front. The cost of purchasing immersion-cooling equipment might be high, so you might want to collaborate with a group of experts who can guide you in finding the best options. Examine the cost and contrast it with the amount of money you will ultimately save. Individuals must decide if it is financially worthwhile [18].

The liquid solutions are something else we should consider since they contribute to immersion-cooling. It must make sure you choose the appropriate selection from the available alternatives. According to conventional wisdom, fluids and electronics don't mix well.

Equipment failure: It has been gotten a tone of hash boards for fixing things that were submerged. A well-done immersion may be amazing, but sometimes a backup component, like the pump, might malfunction. This kind of failure ultimately results in harm to the device, which often keeps operating in a liquid that soon warms up. However, when the whole hash board is "baked" in its mineral oil, the damage from submersion is often greater than it seems. Despite the fact that this is a fairly secure procedure, you still need to safeguard the ASICs. This entails correctly configuring it [19].

1.2 PROBLEM STATEMENT

Server power density rises in direct proportion to the demand for data processing and storage. The temperature control of servers has a substantial effect on the energy efficacy of data centres. The most popular thermal management solution in data centres right now is air cooling. Due to powerful CPUs, air cooling has begun to hit its limits. Different dielectric fluids can be utilized in liquid immersion-cooling techniques to solve these drawbacks of air cooling in data centres. The phenomenon known as "thermal shadowing" occurs when a cooling medium's temperature rises as a result of absorbing heat from a single source and consequently loses some of its heat-carrying capacity as the in between max junction and the difference in temperature, temperatures of succeeding heat sinks and incoming fluids decreases. Both low velocity oil flow cooling and air-cooling face difficulties from thermal shadowing. In this study, thermal shadowing effects in a 3rd generation public computing server utilizing different dielectric fluids are compared. The effectiveness of cooling at the server level is greatly influenced by the heat-sink. This method gives an efficient selection of heat sinks in addition to computational methods of 3rd generation public computing servers. By optimizing the heat sink, high-power density servers may be successfully cooled for only one immersed cooling applications. A parametric examination revealed a significant decrease in the vol. of such a heat-sink.

1.3 AIMS AND OBJECTS

The current study aim to develop a simulated model utilizing the ANSYS Multi-physics programme to validate the experiment's findings. To investigate the single-phase immersed cooling system's cooling effect, three coolant circulation rates and two heat sink materials—Al and Cu—were selected. However, in order to achieve the aim of the current study, the following objectives could be drawn down:

i. By modelling coolant running the temp fluctuation at different flow- rates utilizing this single-phase immersed cooling, the experiment's goal was to discover what would be the best choice for the heat-sink and circulation condition of coolant.
ii. Through XZ, YZ, and XY axis cross-sections also a 3D isothermal computer aided, the heat dispersion of the specified model was seen at varied liquid higher cooling rate and heat-sink material composition.

1.4 THESIS LAYOUT

This thesis consists of five chapters as follows:

Chapter 1: Introduction: contains background about immersion-cooling system, types of immersion-cooling system, and the issue faced immersion-cooling system and benefits.

Chapter 2: Literature review related to immersion-cooling system components, the differences between two immersion-cooling systems, and the previous studies related to immersion-cooling system.

Chapter 3: Numerical Modelling with CFD methods for immersion-cooling system and some experimental works and tests that usually utilized.

Chapter 4: Represents the results obtained from the ANSYS Multi-physics software program and the discussion of those results and compares the obtainable results and experimental results.

Chapter 5: Conclusions and recommendations for the future works.

2. BASIC CONCEPT AND LITERATURE REVIEW

2.1 INTRODUCTION

One of the most popular and extensively utilized terms in the data centre sector is server downtime. A period of time when a server could not be utilized is referred to as server downtime. It can be a result of overloaded processors, memory, etc. These circumstances result from a server that is not running or is not cooling properly. Servers are a highly important component of business and must be properly maintained for dependable functioning. The primary heat source of a server is its CPUs. Processors must be utilized within a certain range of operating temperatures to preserve operation. Servers often produce a large quantity of heat in a very small space. Fluid absorbs the heat produced by the server and releases it into the surrounding air.

The way that heat leaves a server is less consistent and is more prone to fluctuate. There are several factors that might cause electricity to not be distributed evenly. For instance, the amount of heat produced by the processor relies on the CPU's usage percentage and the duration of the high utilization period. Components which are housed in data centers are heat and humidity sensitive components. Most failures are found to occur at chip scale level. Operating temperature of the chip determines the performance of server and at the same time, it also affects the operating life of the chip.

Heat transfer in the server by method of thermal conduction and convection predominates the heat transfer by any other method. The airflow of air through the server chassis determines amount of heat that can be carried away by the air and hence resulting in affecting cooling efficacy. Conduction occurs at chip level while convection occurs at cabinet level. Different other components like heatsinks and fans are utilized to increase the amount of heat carried away by the process of convections. The amount of air flow through the server determines the cooling efficacy and in addition improve that other cooling solutions like heat pipes, heat-sinks and vapor chamber can also be utilized. [6]

2.2 DATA CENTER COOLING METHODS

Currently, there are two main methods being utilized to control the temp within acceptable ranges:

i. Air cooled servers
ii. Liquid cooled servers

The mass production of electronic gadgets over the last ten years has increased energy usage both throughout the manufacturing process and while the devices are in use. A nanotechnology method was also put forward, which decreases device size and cost but faces substantial thermal management challenges because of the high power density and resulting higher heat production. The device's productivity often suffers as a consequence of increasing heat production, which also often leads to failure. It was reported that raising the temp over 75 degree centigrade may cause the failure rate to rise exponentially [20]. Cooling systems have grown essential due to the aim to make electrical devices smaller and more productive. Due to the inadequacy of traditional ways to keep up with the ongoing demand for these devices, several alternatives were created in recent years. A few of these are listed below.

2.2.1 Air-Cooling System

A technique for eliminating heat from an item called air-cooling uses a fan and cooling fins to increase the surface area and airflow over the object [21]. Typically, it refers to automobiles, laptops, electronics, and computer rooms [22]. Forced convection is utilized in an air-cooled motorbike engine's procedure to release heat. This happens when the fan draws in the surrounding air and transmits it to the fins that are built into the engine cylinder block's external surfaces, which subsequently radiates heat into the surrounding atmosphere. In contrast, the idea behind computer air cooling is to absorb heat from the CPU and keep it away from the components. A conductive base plate, often constructed of copper or aluminum, receives the heat from the CPU's Integrated Heating Spreader (HIS) and transfers it there with the help of thermal paste before being transmitted to the heat pipes set up in the electronic cooling system [23]. The small metal fins, which make up the heat sink linked to the CPU packaging receive energy from these heat pipes in the shape of heat, which increases the heat sink's surface area. In comparison to aluminum or copper, heat sinks with heat pipes may provide approximately a 20percent boost in thermal performance [24], but they are more costly than typical active heat sinks. Additionally, the fan in the system is intended to disperse the warm air that has been fed thru the heat sink, and an increase in fan speed is anticipated to result in a larger air flow rate across the heated fin surface, hence boosting the rate of heating dissipation. Nevertheless, this increase also results in undesired vibration, a rise in noise, and an increase in power usage. [25]. Figure 2.1 illustrates utilizing air circulation to cool the computer area [26].

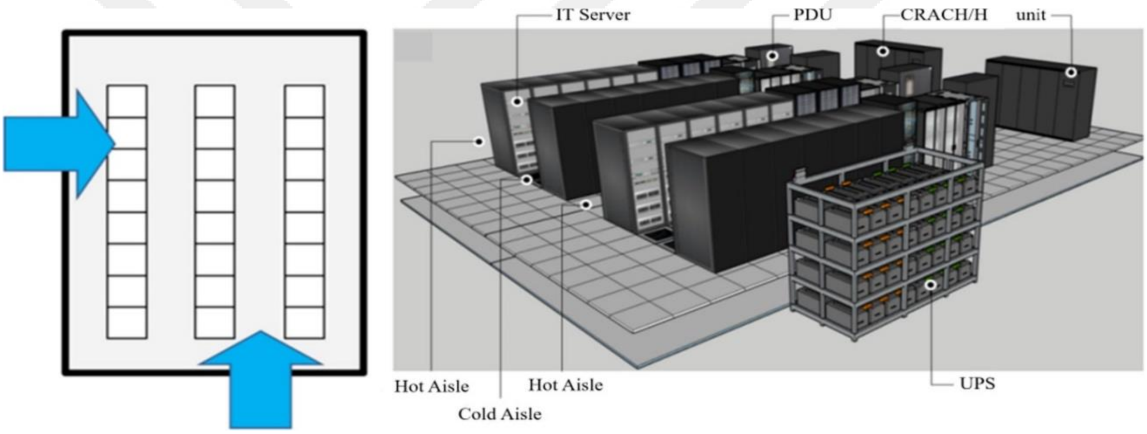

Figure 2.1: Air-Cooling System in Data Center [26].

The design, airflow proportion, room layout, heating-exchanger utilized, and energy management are few examples of variables that affect how successful air-cooling is [27]. Additionally, bigger air conditioners often disperse heat more effectively, but there isn't sufficient space for huge cooling systems, particularly in PCs with smaller capacities. It is significant to note that the air coolers constructed with fans and heating sinks are significantly less expensive than liquid cooling systems when utilized to computers. [24].

2.2.2 Water-Cooling System

The function of an automobile's water-cooling system, that seeks to move water from the source of heat to the cooling radiator, is also relevant to computer hardware and data centres.

The CPU that produces the bulk of the heat in these systems, receives coolant while the other elements have been cooled by air. For instance, the graphics processing unit (GPU) and central processing unit (CPU) of a personal computer are the parts that produce the greatest heat, as seen by the enormous heat produced during each operation. It is essential to draw attention to the fact that over the last several years, data centres have grown rapidly and energy usage has risen internationally [28]. This is due to the fast improvements in technology and communication. It is vital to focus more on data centre cooling systems since it has been suggested that these systems use more than half of the energy utilized for air conditioning, ventilation, and heating [29]. Furthermore, it was noted that the need for mechanical cooling in data centres is significantly rising as a consequence of the power density of microprocessors growing [30].

Once it comes to reducing the temp of the CPU and other elements like graphics cards, water cooling has been the top cooling technique of choice for several data centres. This is seen as necessary due to the recent rapid growth in CPU speed, which increased the quantity of heat produced. These devices are cooled by water since it absorbs heating around 30 times more quickly than air does [31], which enables the CPU to operate with low noise and greater speed. This water-cooling system is also referred to as a liquid cooling system since various liquids may be utilized in place of water. Its main benefit is a reduced temperature difference between the cooler and Central Processing Unit (CPU) due to a higher heating transfer capacity per unit [32]. It also has a higher input temp that minimises the need for active heating rejecting apparatus and for the recycling of produced heat [33]. The technique is practical and can be utilized on high-density servers [34], as the one in the accompanying picture.

The water-cooling system, as shown in Fig. 2.2, consists of two liquid loops: 1) an internal loop with a cooler that transfers heating from the server to the heating-exchanger; and (2) an external loop with internal water that enables heat transfer and through evaporation from the heating-exchanger to the outdoor water-cooling tower. It is crucial to be aware that data centres often use 7 to 10 degree centigrade cold water to cool servers [35]. After the tower has removed some heating from the water, the chiller normally continues to do so. This system uses 22percent less energy than the typical air-cooling system while being able to cool hundreds or even thousands of PCs [36]. Furthermore, it makes it possible to employ coolers that have thermophysical properties that are much superior to those of air, improving thermal resistance and reducing energy consumption in data centres through higher cooling temps and slower airflow rates. Aside from that, water cooling may be applied indirectly or directly [37], as explained in more depth in the subsections that follow.

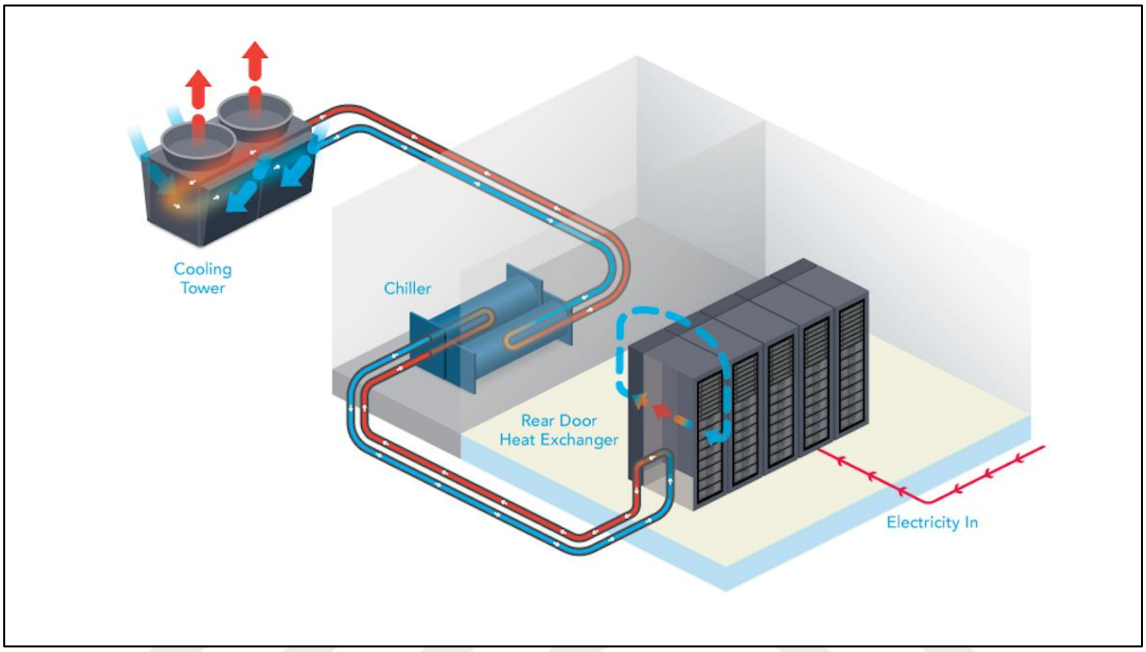

Figure 2.2: Water Cooling Scheme in the Data Center.

2.3 GENERAL DEPICTION OF IMMERSION-COOLING TECHNIQUE

With the help of a dielectric liquid [38] that absorbs heating by convection and releases it to the environment thru a two-phases and single-phase system [32], the technological development of immersion-cooling may reduce the heat component. Its benefits involve capacity to directly cool heated elements utilizing liquid, a high coefficient of heating transfer, and a steady hydrodynamic flow [39]. Virgin coconut oil (VCO) and Mineral oil (MO) are two instances of dielectric materials, which are frequently utilised nowadays [40]. Electronic equipment including power transformers [41], batteries [42], solar PVs [43], data centres [44], and computer servers frequently utilize this cooling technique [45].

Comparatively to indirect cooling, immersion-cooling has the capacity to cool the whole surface, improving temp uniformity by minimising the local heating impact on the negative and positive electrodes. Utilizing cooling media with high thermal conductivity, low viscosity, and high heat capacity may assure good efficacy [46]. Nevertheless, this technology does have certain issues, including electrochemical corrosion and electrical short circuit. Consequently, the capacity to prevent electrical short circuits [47], also non-flammability, high chemical stability, non-toxic ability, and health concerns and safety are the primary factors in the selecting of dielectric material. Mineral oil, silicon-based oil, and deionized water are some more possible cooling medium [48].

2.4 IMMERSION-COOLING APPLICATIONS

2.4.1 Solar Photovoltaic

Like other electrical components, concentrated photovoltaic cells must be properly cooled. This is a result of the necessity to effectively regulate the heating produced by the cell to prevent lowering its efficacy [37]. Consequently, a dependable heating dissipation system was necessary to guarantee the effective operation of solar cells. Placing empty cells directly in the fluid is one of the options that some experts believe to be appropriate, which prompted early investigations to concentrate on the anticipated optical and electrical impacts of liquids on cells. As time goes on, research on PV cell cooling continues with new discoveries including the potential use of thin liquid layers to surround the cells and collect light [49]. Furthermore noteworthy is the fact that cell fluid immersion permits the direct submersion of a concentrated solar cell in a liquid in addition to surface wetting and optical benefits. Additionally, the lack of a contact wall between the liquid and cell suggests that the cell may be effectively cooled. The photovoltaic panels immersion-cooling utilizing lakes water cooling is shown in Figure 2.3. [50].

Figure 2.3: Solar Photovoltaic Cooling.

As the temp rises, solar PV systems typically generate less energy. On a bright, clear, and pollution-free day, the photon energy radiates more effectively, but it also raises the PV's surface temp [51]. As a result, cooling is required to maintain optimum energy efficacy, as shown by Peng et al. [52] improvement in solar PV performance after cooling by up to 47 percent.

The energy efficacy conundrum was also suggested to make cooling of the solar cells crucial. It is crucial to remember that they may be cooled by immersion in both air and water. In addition, direct immersion is preferred over alternative cooling techniques for concentrated solar cells. A water-cooling system may also be utilized to boost the solar module's efficacy, however this method is not recommended for overcast days [53].

2.4.2 Data Center

Once the temperature rises, the processing speed of the computers and servers in the data centre decreases, which increases energy usage while maintaining the same workload [54]. The energy consumption rate for data centres utilizing traditional cooling is 38 percent. Nevertheless, a 2-kW power converter that was evaluated for immersion-cooling in deionized water was functioning at 97.2 percent efficacy. Although an unchecked temp rise might potentially harm these parts, immersion-cooling technology has been shown to boost energy efficacy [55]. Data centres may save energy and maintain the integrity of their components by utilizing mineral oil or VCO dielectric liquid. An immersion-cooling system for a data centre is shown in Figure 2.4.

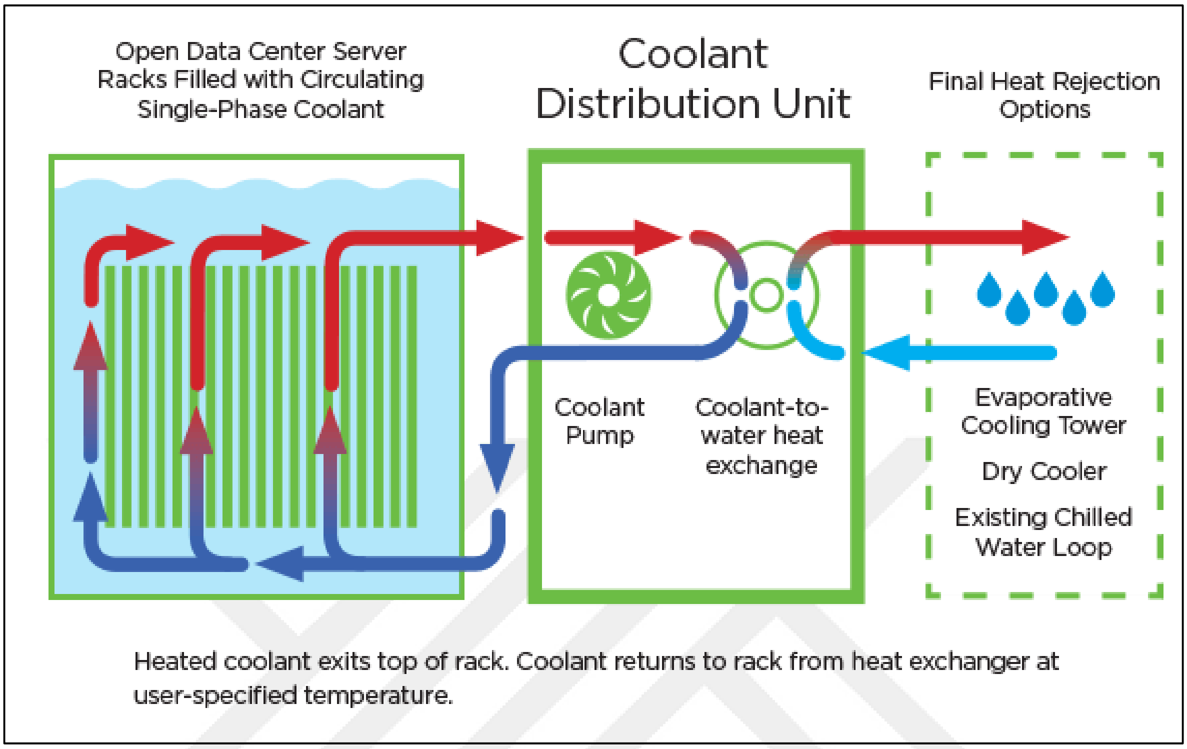

Figure 2.4: Data Center Immersion-Cooling Scheme.

2.4.3 Cryptocurrency Mining

In 2009, the peer-to-peer payment system and digital money known as Bitcoin was released as open-source software. The user may use a Bitcoin address to make and receive payments by connecting a free client or wallet to the computer. The participants, identified as miners, are in charge of employing a proof-of-work model with a secure hashing-algorithms (SHA) to validate transactions into blocks and broadcast them to the common block chain [56]. Verifying transactions with two characteristics, including capital to validate the power use and cost of the gear employed, carries costs. It is crucial to remember that increased power usage for "hashing" often results in higher profits for the colliers in the shape of significant rewards. The colliers first utilized traditional CPUs to execute SHA, but it was discovered that GPUs were more cost-effective, leading to an extra gain [57]. As Bitcoin becomes more and more popular, gamers begin to recognise that they have a "money-making machine" and begin vying to develop the most effective mining gear. The establishment of traditional air-cooled data centres is difficult due to the mining clusters' short life cycles and quickly increasing power densities [58].

Several people believe that the two-phases immersion is a practical technology that can satisfy the high-performance computer market's requirements for energy efficacy and power density. For instance, a better technology that is more efficient than direct water cooling was utilized to cool a power density that is 100 times greater than a standard air-cooled server [59]. Furthermore, despite several demonstrations in various countries, two-phases immersion-cooling was applied in the IT business by eliminating the danger; nonetheless, the new technological approach has made the process of implementation simpler. As a result, Figure 2.4 depicts the passive two-phases immersion-cooling cycle.

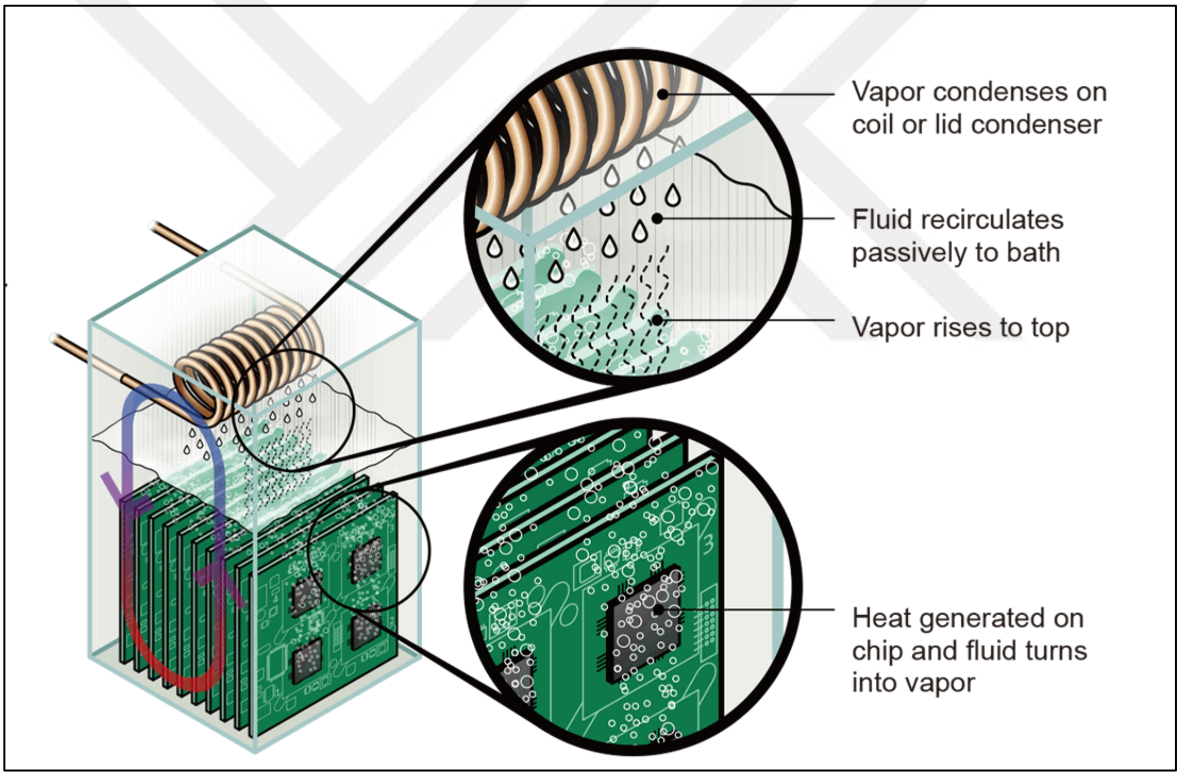

Figure 2.5: Passive Two-Phases Immersion-Cooling Cycle.

2.4.4 Electric Car Battery Cooling System

Once utilized at temps over 45 degrees centigrade, batteries perform worse because high temps reduce the pore connectivity and porosity of the material, which therefore reduces the uniformity of the battery current. Nevertheless, [60] results that a battery's charging capacity may drop by an average of 15percent once charged at 10 degree centigrade [61] suggest that an extremely low operating temp also has the power to significantly diminish battery performance. This indicates that it is crucial to manage the battery to keep it at the recommended operating temp of 20 degree centigrade, and [62] discovered that immersion-cooling is more effective for this purpose than cold-plate based cooling. When compared to indirect cooling, immersion-cooling was shown to be able to cool the whole cell surface and increase temp uniformity by minimising the local heating impact on the negative and positive electrodes [46]. A dielectric liquid immersion-cooling method for Li-ion battery thermal control is shown in Figure 2.6.

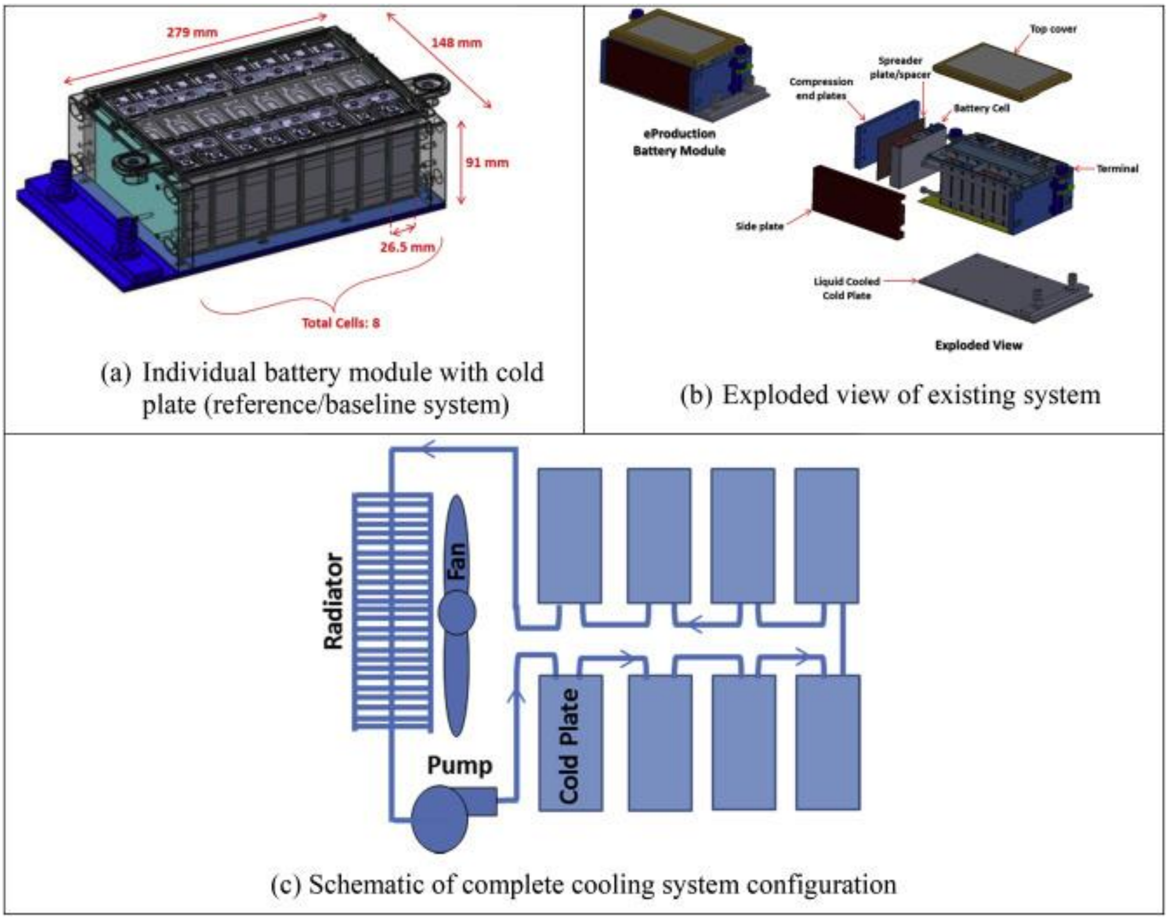

Figure 2.6: Battery Thermal Management System.

2.4.5 Power Transformers

Additional harmonic losses in power transformers raise the component temperatures, shortening the components' useful lives. The magnetic cores and windings of transformers are their primary heating sources, with the majority of the energy lost to the environment as heating when the transformer is operating. The solution to this issue is thermal energy management, specifically immersion-cooling, which was shown to be more effective than conventional air-cooling technologies [63]. Figure 2.7 illustrates the combination of immersion and fin heating-exchange cooling in power transformers.

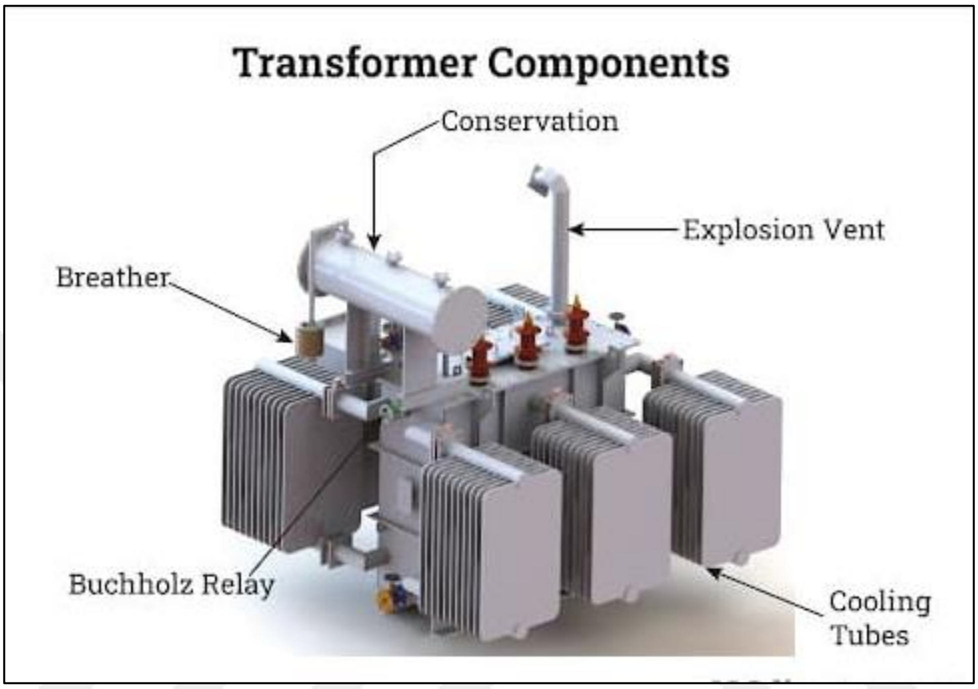

Figure 2.7: Power Transformers Components.

2.5 DIFFERENCE BETWEEN THE TWO SYSTEMS

2.5.1 Cost

The cost difference between two-phases and single-phase systems is greatest in the coolant.

2.5.1.1 Two-phases cooling

Fluorocarbon-based two-phases coolants classically cost an order of value more than hydrocarbon-based ones. Additional costs become significant when over 300 gallons of the evaporative fluid are utilized in a single rack. Moreover, fluid for two-phases immersion requires a fully sealed enclosure as to avoid losses. When it comes to maintenance, the complexity of the enclosure often creates trouble in access, let alone the costs related to fluid top-up. Furthermore, prolonged subject to the vapor could lead to environmental and health concerns since the fluorocarbon-based substance is highly regulated.

2.5.1.2 Single-phase cooling

Single-phase immersion cooling tops the complication list despite the fact it needs a pump to hold the coolant flowing thru the system. Single-phase immersion-cooling system has a simpler submerged cylinder design, making fluid containment easier to achieve, and has fewer concerns about material compatibility and contaminants in the fluid than two-phases immersion-cooling.

2.5.2 Efficiency and Operating Expenses

The efficacy levels of both techniques are much greater once comparing them to a standard air-cooled data Centre.

2.5.2.1Two-phases cooling

According to recent studies, two-phase cooling might outperform single-phase cooling by a little margin, with a PUE (Power Usage Efficiency) of 1.02 as compared to 1.03.

Even though two-phase systems use less energy, maintaining them may be challenging. As previously stated, operators should open the enclosure to access the servers whereas attempting to reduce coolant loss and vapour inhalation.

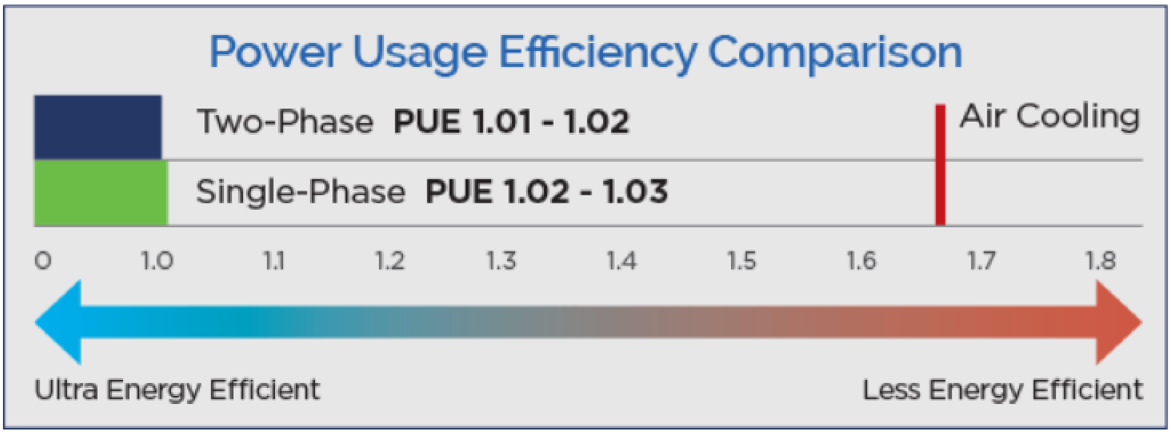

Figure 2.8: The Differences Between Power Usage Efficiency for Two and Single Phase.

2.5.2.2 Single-phase cooling

To contrast single-phase cooling with the relative energy inefficiency of non-immersion-cooled systems, 1.02-1.03 PUE is definitely convincing enough to champion the prize. In terms of fluid application, the hydrocarbon-based coolant is usually non-evaporative, odorless and non-toxic. Therefore, once maintenance levels are taken into account, the case for single-phase cooling shifts. Single-phase immersion-cooling systems typically require far less upkeep and are considerably simpler to access and fix if necessary.

2.5.3 Cooling Capacity and High-Density Performance

2.5.3.1 Two-phases cooling

Two-phases coolants can typically support extreme rack densities, higher heat transfer efficacy can be achieved through the boiling process (through state transforming from liquid to gas), some providers claim to support up to 250 kW in a single rack (kilowatts [kW] per cabinet), regardless of finding commercially available hardware that will even reach 100 kW.

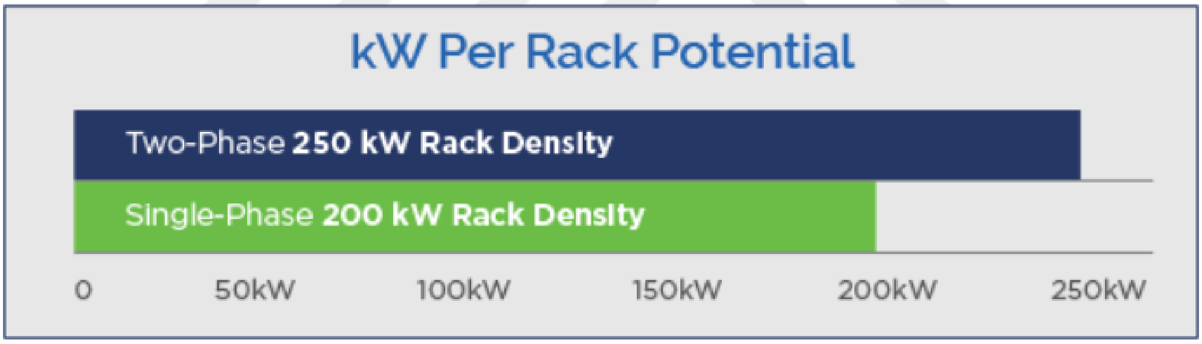

Figure 2.9: The Differences Between Cooling Capacity for Two and Single Phase.

2.5.3.2 Single-phase cooling

By contrast, some of bath tank is capable of handling 200 kW per rack (let alone only 6 ASIC machines with a maximum power of 5-6kw each, are fitted in one single tank) when attached to a chilled water system, which is more than enough cooling performance for the foreseeable industry demand to future-proof.

However, it is biased to criticize that one is better than the other between the two approaches discussed herein. However, it is fair to say that the basic principles of single-phase immersion-cooling transcend the conventional ones to the next level, but in the meantime eliminate the drawbacks of two-phases immersion-cooling which seems to be complex, costly and over-engineered for the majority of data center cooling needs today, therefore; the numerical investigation will mainly depending on the single-phase immersion-cooling.

2.6 LITERATURE REVIEW

2.6.1 Cooling System for a Computer

Board-level high efficacy flip-chip ball grid arrays packaging was the subject of research by [64]. The most fruitful of several researches on vapour chamber cooling for computers processing unit (CPU) and electrical gadgets is presented [65]–[68]. The next study by [69] focused on vapour chamber cooling for hard disc drives in PCs and provided thermal resistance data for 10 vapour chambers with various design structures and working fluid fill proportions.

[70] investigated the effects of inclination angle and nanofluids on the heat transfer performance of a CPU cooling heat pipe. It is shown that the unit's inclination angle significantly affects the cooling process since it has an immediate impact on how the evaporator functions. The capillary effect and heat pipe boiling limitations are the major causes of the impact. The findings show that there is a critical angle at which the thermal resistance of the heat pipe drastically rises for a given CPU temperature. The threshold angle is shown to fall from 60° to 30° as the CPU temperature rises. Thermal resistance has decreased as a result of the addition of 0.5 weight percent of Al_2O_3 nanoparticles to the heat pipe's water coolant. It has been shown that the thermal resistance has decreased by 22% at 25 W compared to 10% W when nanofluid is present.

In a data centre, [71] investigation looked at the heat transmission capabilities of the rack cooling system's pulsing heat pipe and internal duct. The heating transfer performance of a rack cooling system with a pulsing heat pipe and internal duct in a data centre is examined numerically in this article. Design and analysis are done on the rack's internal framework. Numerical simulation introduces the condensed thermal conductivity model of the pulsing heat pipe. The power of the rack, the status of the pulsing heat pipe, the temp of the cooling air, and the wind pressure of the rack fans are utilized to determine the temp of CPUs (Central Processing Units). The findings indicate that the temperature of the CPUs rises as rack heating power increases. The temp of CPUs drops as soon as the pulsing heat pipe (PHP) starts operating, and CPU temperatures are distributed evenly. CPU temperatures drop as the temp of the cooling air drops or when the wind pressure rises. By adding an inner duct to the rack, the temp field of the inside air is enhanced and certain "hot spots" are eliminated. In the rack cooling system with a load of 1380 W, the temp of the CPUs is no more than 60 degree centigrade.

The heat dissipation and energy usage of high heat flux chips substantially limit computer performance with the industry's fast growth. The power supply and heat dissipation are becoming more complicated due to the rise in high density server racks. Therefore, it's essential to improve computer chip cooling technologies. Heat pipe technology was utilized by [72] to improve CPU cooling performance. To help electrical equipment operate at the desired level, thermoelectric cooling technology has also been created. Various designs of heat sinks that were integrated with heat pipes were utilized, and the effectiveness of energy conservation and heat dissipation were investigated. Because of the high efficacy heat dissipation technology, the cooling performance may be improved with the new cooling systems and the energy usage could be decreased to allow the CPU to operate at its normal operating temp.

The liquid cooling in the mini-rectangular fin heating sink without and with thermoelectric for CPU was researched by [73]. Six miniature rectangular fin heat sinks with two distinct types of material and three various channel widths are made of copper or aluminum and have measurements of 3.7 cm in length, 3.7 cm in width, and 0.5 cm in base thickness. As a coolant, de-ionized water is employed. On the subject of CPU temp, consideration is given to the impacts of PC operating conditions, heating sink kind of material, coolant flow rate, and channel width. The thermoelectric liquid cooling in a mini-rectangular fin heat sink is contrasted with alternative cooling methods. The cooling of a computer's CPU is significantly influenced by the thermoelectric. Nevertheless, there is also an increase in energy use. The findings of this research should provide recommendations for designing cooling systems that would increase the efficacy of heat transfer for electronic devices.

[74] experimental study of the thermoelectric air cooler module and dual processor workstation computer's thermal cooling improvement approach. Computing load circumstances, thermoelectric air cooler module use and non-use, cooling fan turn-on/off

modes, and various cooling fan sizes are the key monitored characteristics. The operating computer load ranges from 0 to 100percent throughout the trial. The density and positioning of the passive and active elements within the device affect how hot or cold it is inside the chassis. The air and CPU temps of the dual processor computers are discovered to be significantly impacted by the thermoelectric air cooler module. Air distribution within the computer chassis is also significantly impacted by the cooling fan's working modes, locations, and sizes. However, there is also an increase in energy use. The findings of this research should provide recommendations for designing cooling systems with better heating transfer performance for electronic equipment.

For the goal of cooling the CPU, [75] presented a thermoelectric tiny cooler coupled with a micro thermosiphon cooling system. The thermoelectric module initially establishes a computational formula of heating transmission based on a one-dimensional assessment of thermal and electric power. The link between the maximum COP (Performance Coefficient) and Qc and the merit figure is shown by analytical data. The effectiveness of the cooling system has been studied utilizing full-scale tests to determine the impact of the thermoelectric operating voltage, the power input of the source of heat, and the number of thermoelectric modules. The cooling generation rises with the development of thermoelectric working voltage, according to experimental findings. With an increase in power input, the surface temperature of the CPU source of heat linearly rises, reaching a max value of 70 degree centigrade when the prototype CPU's power input was 84 W. Condensate water owing to low surface temp may be avoided via insulation between the air and heating source surface. Once the overall dimensions of the thermoelectric module and the CPU were in good alignment, the thermal efficacy of this cooling system might be improved. The design of heat dissipation for CPU units and electronic chips may benefit from this study.
Heating pipes are best suited for cooling the high power chips in electronics or computers because of the limited area and power available. [76] have studied the thermal control system of a computer with CPU cooling and a short heat pipe cooling system. On the modification of CPU temp, the impacts of the pertinent characteristics, including heat pipe inclination angle, the presence or absence of porous materials, working fluid kinds, and computer operation circumstances, are taken into consideration. In the studies, working fluids within the heating pipe with constant 50percent fill ratios include R11, R134a, and ethanol. Comparisons are made between the fluctuations in CPU temp achieved utilizing the heating

pipes cooling system and those acquired utilizing the traditional cooling method. As could be observed, the physical characteristics of the working fluids and the heat pipe's inclination angles have a big impact on the cooling capacity that affects how hot the CPU runs. The CPU temperature is lower when utilizing a heat pipe with porous medium than when utilizing one without. It is anticipated that the acquired findings would provide recommendations that would enable the construction of a thermal management system with an optimal heating pipes cooling system for CPU cooling system with the greatest cooling capacity.

2.6.2 Immersion-Cooling System

A major problem is controlling the temp of solar cells at high amounts. By utilizing efficient cooling techniques, short-term efficacy loss and long-term deterioration must be prevented. Cell performance must be improved by liquid immersion-cooling because it removes the interaction thermal resistant of back cooling. Utilizing de-ionized water for immersion-cooling, [77] evaluation of a novel CPV system made use of a 250X dish concentrator with two-axis tracking. They evaluated the I-V curves in addition to the time-dependent temp distributions of the high power back point-contact PV module. The liquid immersion method's cooling capabilities are excellent. With a 940 W/m2 direct normal irradiance, a 17 degree centigrade air temp, and a 30 degree centigrade water intake temp, the module temp may be lowered to 45 degree centigrade. Although the module's temp distribution is rather consistent, its electrical performance begins to deteriorate after spending a considerable amount of time submerged in deionized water.

Solar cells' or panels' efficacy significantly declines when the surface temp rises. The water immersion-cooling method, which involves submerging the solar cell in water to preserve its surface temp and give improved efficacy at severe temps, may be utilized to prevent the heating of the solar cell surface. The electrical characteristics of a solar cell were estimated by [78], who found that the cooling parameter is crucial for improving electrical efficacy. Under actual environmental circumstances, the temperature of a solar cell submerged in water was regulated between 31 and 39 C. Cell electrical performance improves significantly. Findings are discussed; at 1 cm of water depth, panel efficacy has improved by roughly 17.8pcenter . The Concentrated Photovoltaics System may be supported by the research by immersing the solar cells in various media.

It was shown that ultrasonic irradiation may speed up the processes of heat transfer. A stationary copper sphere (k = 386 W/m.K, Cp = 384 J/kg.K, ρ = 8660 kg/m^3) was subjected to ultrasonic irradiation for the purpose of studying the heat transfer phenomena, namely the heat exchange at the surface by [79]. The ultrasonic cooling system, which featured a chilled circulator, a flow metre, an ultrasound generator, and an ultrasonic bath, submerged the sphere (0.01 m in diameter) in a solution of ethylene glycol and water (10 degree centigrade). Utilizing a data logger fitted with a T-kind thermocouple in the sphere's centre, the temp of the object was measured. Four thermo-couples placed in the bath at various locations also monitored the temp of the cooling medium. The centre of the sphere served as the reference system's centre, and the sphere was placed at various heights (0.06, 0.04, and 0.02 m) above the transducer surface of the bath and subjected to a range of ultrasonic intensities (4100, 3400, 2800, 1800, 890, 450, 190, 120, and 0 W m2) while cooling. The ultrasound had a 25 kHz frequency. It was shown that ultrasonic irradiation may greatly speed up heat transfer, leading to noticeably faster cooling times. Greater intensities resulted in faster cooling rates, and Nu magnitudes climbed from around 23–27 to 25–108 based on the ultrasound's power and the sphere's location. Nevertheless, intense ultrasound generated heat at the sphere's surface, limiting the lowest end temp that could be reached. An analytical solution that took into account heat production was created, and it was fitted to the experimental data with R2 magnitudes between 0.910 and 0.998. Visual observations showed that the heat transfer event required both cavitation and acoustic streaming. The primary factor producing the heating impact were cavitation clouds near the sphere's surface. According to the findings, cooling rates were greater at closer distances from the transducer surface. On the other hand, even though the sphere was further away from the transducer, the improvement factor for heat transfer was larger once it was nearer to the gas-liquid interface. When utilized for immersion-cooling, ultrasound irradiation improved convective heating transfer rate in a promising way. More research is necessary to clarify the behavior of ultrasound-assisted heating transfer and determine the right approach to use ultrasound to speed up the freezing or cooling processes.

Utilizing dielectric fluid immersion-cooling (DFIC) technology, [42] examined the direct cooling performance properties of Li-ion batteries and battery packs for electrical cars. The experiment's findings demonstrated that Li-ion pouch cells immersed in flowing dielectric fluid and assisted with tab cooling performed better in terms of cooling performance, with a max temp at the positive tab that was reduced by 46.8percent when compared to natural convection at a 3C discharge rate. Utilizing the Multi-Scale Multi-Domain (MSMD) technique and the Kim (NTGK), Gu, Tiedemann, and Newman model, an electrochemical-thermal model of a Li-ion pouch cell submerged in flowing dielectric fluid was created. The findings of the numerical investigation and the experimental data showed an excellent agreement to within 5 percent. At the optimal pumping power of 81.7 W, the 50 V battery pack max temp was kept below 40 for 5 degree centigrade discharge. The max battery pack temp was 9.3percent lower with the suggested DFIC aided with tab cooling technology utilized, demonstrating enhanced cooling performance comparison with the traditional cooling approach. Under thermal abuse conditions with an internal short circuit, the battery pack's peak temp of 341.7 degree centigrade was recorded, although thermal runaway was avoided with the exception of the afflicted cell. In the use of high-density and high-capacity Li-ion batteries in electrical cars, this research showed that the DFIC supported by tab cooling is a secure and effective thermal management solution.

For linear CPV (concentrating photovoltaic) systems, [80] proposal for direct liquid-immersion-cooling of solar cells employing dimethyl silicon oil as a heating dissipation solution. A thin rectangular channel receiver was created to lessen liquid holdup, and its heating transfer efficacy was tested experimentally at an energy flux proportion of 9.1 suns. Under actual climatic circumstances, the long-term durability of mono-crystalline concentrator silicon solar cells submerged in dimethyl silicon oil with a viscosity of 2 mm2/s was observed. The liquid-immersion-cooling capability of the intended receiver is good, according to experimental data. With a 910 W/m2 DNI (direct normal irradiance), a 15 degree centigrade silicon oil input temp, and a range of Re numbers (Reynolds) from 13,602 to 2720, the cell temp may be regulated to be between 20 and 31 degree centigrade. A broad connection of the Nu number (Nusselt) was discovered, and the temperature distribution inside the cell is relatively uniform. After being submerged for 270 days, the electrical efficacy of the cells in the silicon oil remains steady, and no noticeable efficacy deterioration was seen.

High power density batteries' performance, longevity, and safety depend on effective temperature control. Direct mineral oil jet impingement cooling of the lithium-ion (Li-ion) battery pack was experimentally examined by [81]. The experimental findings of battery cooling utilizing mineral oil are disclosed for the first time. The effects of a Li-ion pack's temp uniformity and charging and discharging properties are taken into account. Experimental measurements of temp homogeneity inside and between cells are made. The battery pack is also said to be cooled by free-convective airflow as a baseline. Direct-jet impingement and submerged jet are two alternative jetting configurations that are taken into consideration. Mineral oil almost maintains constant skin temp both inside and between cells at the greatest charge-discharge rates taken into account (3C discharge and 2C charge). According to the findings, modular jet oil cooling is a fantastic lithium-ion pack cooling solution that may be utilized in stationary electrical storing and transport applications.

2.6.3 Immersion-Cooling System for PC

Computer systems may be able to use electricity more effectively if cooling electronics systems is done more properly. Computers and other electronics might be cooled via immersion-cooling by immersing them in a thermally conductive liquid or coolant. The cooling structure and process of a single-phase immersion-cooling system employing a heat sink and forced circulation were given by [11] in their publication. The CPU surface is covered with a straight-finned heat sink, and the whole mainboard is immersed in 3 M Novec 7100, a designed fluid that can disperse heat and is utilised in immersion-cooling applications. A simulation model created utilizing computer simulation software is tested experimentally to ensure its accuracy. To investigate the cooling impact of a single-phase immersion-cooling system, three liquid coolant circulation rates and two distinct heat sink materials are utilized. Through the use of a cross-sectional view and a 3-dimensional isothermal surface model, the heating distribution of the specified model was studied at varied liquid coolant and material flow rates. The simulation findings demonstrate that a cooler CPU might operate at a low temp if the liquid coolant moved more quickly. Nevertheless, because of the decreased circulation speed, the coolant flow was impeded. Additionally, it contributed to the uneven distribution of heat and higher temp levels. The greatest temps were recorded, and it was found that the model's imbalanced heat distribution. It should be noted that the findings are not considerably impacted by the heat sink's composition. The system designer may utilise these results to boost power densification and ensure the secure functioning of the associated computer, server, and communication systems.

Approximately 40percent of the total energy needed for cooling a standard information technology system is consumed by the system itself. Water cooling, closed-loop liquid cooling, and immersion-cooling systems are the three main subcategories of cooling systems. It was noted that the newest development in cooling solutions for IT devices is immersion-cooling. It is a cooling process that involves submerging all of the computer's parts in a dielectric coolant. Utilizing this immersion approach, [82] investigated the cooling procedure of the GPU. Due to its high dielectric strength, mineral oil is utilized as a medium fluid. A benchmark piece of software was then utilized to gauge the temp variation between immersion-cooling and fan usage. The outcome demonstrated that the GPU temp was lower with immersion-cooling than with a traditional fan. When the immersion approach was utilized, the GPU's operating temp was 70 degree centigrade, compared to 80 degree centigrade when the traditional fan technique has been utilized.

Since 46percent of the world's population now uses the internet and creates up to 8 zettabytes of data flow every day, the value of the global internet is increasing. Data centre infrastructure has expanded as a communication system, storage, and processing in the digital world as a result of this expansion. The data centre has already contributed 1.5percent of the world's total power usage, and it is anticipated that this percentage will rise over time. 52percent of the energy required in the data centre goes toward information technology (IT) devices, 38percent goes toward cooling, and 10% goes toward auxiliary equipment. The information technology (IT) cooling elements has been one of the issues these centres have had throughout the years. A cooling model with the potential to increase data centre energy efficacy is described by [14]. Many researches were conducted, and one of them looks at the usage of the immersion-cooling method since it promises to increase the energy efficacy of data centres by utilising dielectric fluids with large heat capacities. This document identifies and discusses a number of the fluid kinds employed in this procedure.

One of the solutions for the problems with the present data centre cooling system was the development of immersion-cooling has been suggested by [38]. Therefore, the purpose of this work was to identify the variables influencing the performance of mineral oil immersion-cooling. Creating an immersion-cooling unit and operating the server by loading the software were further steps in the experiment. The Technique with Orthogonal Array L8 was utilized to calculate the contribution and impact of each component. The CPU temp and Energy

Usage are two of the performances that are monitored, with the inlet-outlet position, flowrate, and cooling fan speed acting as the Taguchi parameters. The findings demonstrated that energy usage and cooling fan performance had a combined effect of 71.278percent and 75.034percent on CPU temp.

An effective data centre cooling system may improve server performance and encourage energy conservation. [83] investigate the effectiveness of a two-phases cooling system utilizing a lab experiment and computational fluid dynamics (CFD) simulation. Under different IT (Information Technology) loads, the suggested system's partial power consumption effectiveness (pPUE) and performance coefficient (COP) were assessed. The minimal intervals that might keep the temp of the server surfaces below 85 degree centigrade were determined by doing a CFD study on the connection between the interval of the two submerged servers and their surface temperatures. According to experimental findings, COP rises and pPUE drops as server power increases. In one trial, the pPUE dropped from 1.053 to 1.037, but the COP rose from 19.0 to 26.7. The tank side is where the majority of the exergy degradation occurs, and the exergy efficacy of this system varies from 12.65percent to 18.96 percent. Under 1000 W of power, 20 W under 1500 W, and more than 30 W under 2000 W and beyond, the minimal distances between servers are 1.5 cm, 2 cm, and 3 cm, respectively. The findings and recommendations in this research might serve as useful resources for the investigation of cooling systems in data centres.

The construction of reconfigurable computing systems depending on cutting-edge UltraScale+FPGAs and Xilinx UltraScale; and a design technique of immersion-cooling systems for computers having 96–128 chips were both taken into consideration by [84]. They provide essential technological solutions' selection criteria for building highly effective computer systems with liquid cooling. The prototype computing block's building process and the findings of its experimental heat testing are discussed. The findings demonstrate the suggested open cooling system's great energy efficacy and the presence of a power reserve for FPGAs of the future generation. The fundamental component of the system under consideration is efficient cooling of 96–128 FPGAs with a total thermal power of 9.6–12.8 kW in a 3U computing module. The benefits of the created technological solution include insensitivity to leaks and their effects also compatibility with conventional water cooling systems depending on industrial chillers. These characteristics enable the installation of liquid-cooled computer systems without substantially altering the architecture of the computer hall.

In their study of reconfigurable computing systems depending on Xilinx Virtex UltraScale+ series high integration fields programming gate arrays (FPGAs), [85] found that all electronic components are cooled utilizing immersion liquid cooling systems. For the thermal interface, cooling liquid, radiators, and the complete reconfigurable computing system, novel technical and technological solutions are taken into account. These qualities make it feasible to fit a maximum of 128 FPGAs for a 3U computing module into a typical 19"x19" computer racking, an unparalleled layout density. The findings of experimental testing and development of an energy-efficient compute module with immersing liquid cooling system are presented in the study. With the aid of the new computing module, it is conceivable to operate at 1 Pflops in a typical 47U rack while utilizing no more than 150 kW of total power. The immersion liquid cooling system is compatible with conventional water cooling systems depending on industrial chillers, has a power reserve for previously created and for next-generation high integration FPGA series, and is resistant to leaks and associated effects.

Because of their increasing performances and reducing sizes, power electronics' heat flux is sharply rising. One of the main problems impeding the advancement of power electronics is reliable and effective heating dissipation. A very effective two-phases direct immersion-cooling system with direct contact between the heat source and the coolant was experimentally tested by [86]. As the working fluid, three distinct dielectric liquids—ethanol, FC-72, and R113—were utilized, and their thermal properties have been contrasted. The findings shown that under a 1000 W heat load for ethanol, the minimal total thermal resistance of 0.073 °C/W was reached under forced air convection. With ethanol, the minimal total thermal resistance was also reached under natural convection; the minimal value is 0.2 °C/W. (at the heat load of 300 W). Additionally, the critical heat fluxes for the three coolants' related heat transfer limitations and boiling hazards have been theoretically examined. The revised Rohsenow boiling heat transfer equation's coefficients were fitted, and the reliability of mathematical modelling for direct immersion-cooling was greatly improved.

The complete submersion of servers in artificial dielectric fluids is quickly growing in popularity as a method to reduce the amount of energy needed by data centres for cooling. Since synthetic dielectric fluids have large heat dissipation capabilities that are around 1200 times higher than air, immersion-cooling generally provides notable benefits over traditional air-cooling techniques. The consistent temperature distribution across chips, the decrease of noise, and the flexibility to address operational improvements such whisker formation and electrochemical migration are further benefits of dielectric fluid immersion-cooling. However, the majority of data centre operators are hesitant to use this technology due to the paucity of published data and the scarcity of long-term dependability statistics on immersion-cooling. [87] uses computational fluid dynamics utilizing 6SigmaET® to evaluate the thermal performance of an air-cooled server vs a single-phase oil immersion-cooled HP ProLiant DL160 G6 server firstly. The Baseboard Management Controller, Input Controller Hub (ICH), Input/Output Hub (IOH) chip, Dual In Line Memory Module (DIMM), and Central Processing Unit (CPU) are the study's primary focus (BMC). The second section of this study focuses on optimising the thermal performance of servers that are cooled by oil immersion by adjusting the oil's input temp and volumetric flow rate.

3. CHAPTER THREE: SIMULATION AND MODEL DESCRIPTION

3.1 INTRODUCTION

For the models that have been completed in the following chapters, this chapter discusses the mathematics and Computer Fluids Dynamics (CFD) modelling. This chapter provides an introduction to computational fluid dynamics as well as the steps involved in solving a simulation model. There is a description of the boundary conditions for the immersed server model simulation using two software (ANSYS and COMSOL). The laminar or turbulent fluid behaviour employed for the immersed servers model is described. The equations for the turbulence model that might be used to analyze the turbulent flow are shown.

3.2 COMPUTATION FLUIDS DYNAMICS (CFD)

Thru a computer-based simulations that solves the formulas governing fluid flows, heat transport, and the pertinent chemical processes, computation fluids dynamics (CFD) evaluates an engineering system [88]. CFD is a new subject that combines computer science with fluid dynamics. To establish the physical properties of fluid movement, mathematical formulas may be created, often in the kind of partial differential formulas that involve the energy governing, momentum, and continuity formulas [89]. These mathematical formulas ions are transformed into computer software and programmes by scientists using sophisticated programming languages, including ANSYS, and OpenFOAM COMSOL. ANSYS was mostly utilized in the present project to run simulations and forecast the outcomes [90].

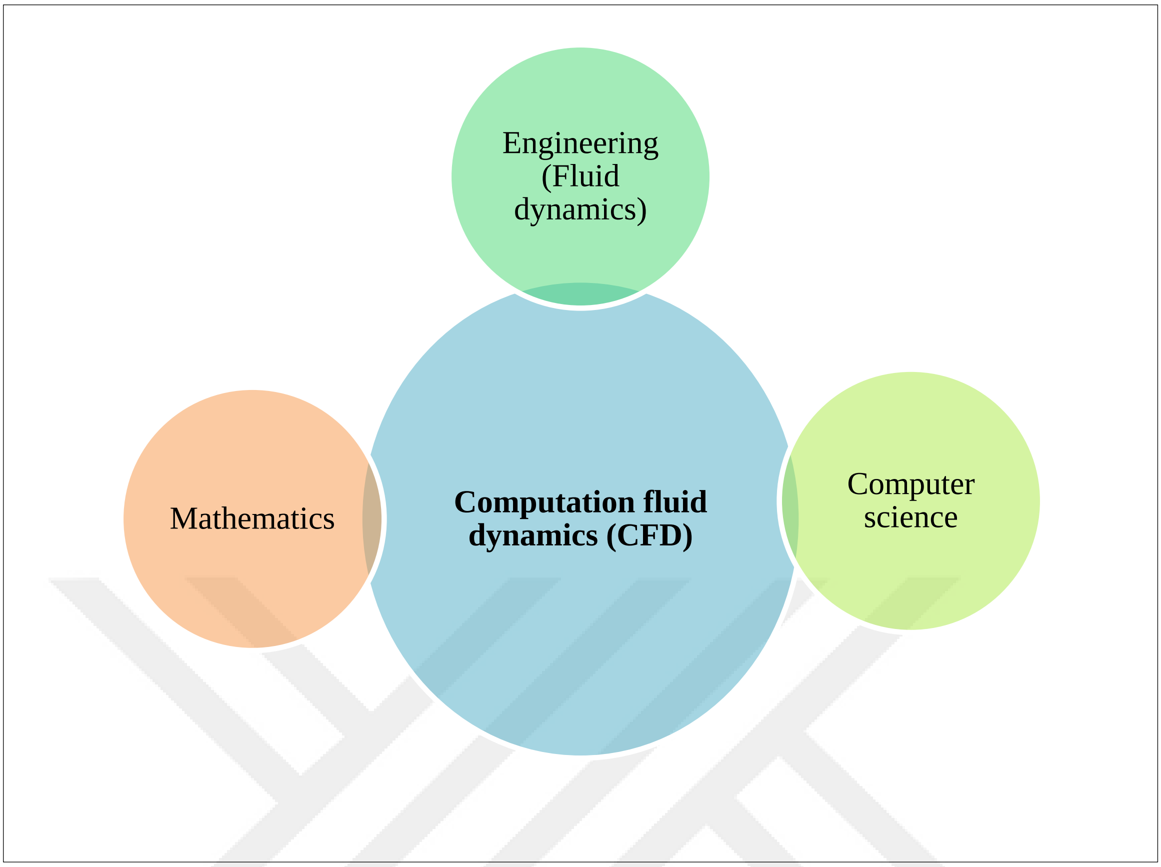

Figure 3.1: CFD Combinations [91].

Engineering fields such as aerospace, biological engineering, environmental engineering, and more recently modelling flow of air inside electronic data centres, employ CFD extensively [92]. Depending on Almaneea [93], the CFD code has three key components:

i. Pre-processors.

ii. Solvers.

iii. Post-processors.

Pre-processors seem to be a method for entering a particular liquid flow's properties into CFD software that is subsequently changed into a shape more suitable for the mathematical algorithm (solver) [94]. The operator operations at the pre-processing step need an operator-friendly interfaces, which includes:

i. Geometry description.

ii. Meshes production.

iii. To identify the model characteristics including the physical and chemical characteristics.

iv. Identify the fluid/physical characteristics.

v. To provide suitable boundary condition for the initial solution.

So as to solve a single or a collection of partial differential formulas regulating fluid movement, there seem to be three most typical techniques to express a mathematical formulation in terms of the solvers. These include the finite differences, the finite elements, and the finite volume. They enable the discrete algebraic counterpart of the continuous issue denoted by partial differential formulas, which is applicable at all nodes within such a solution space [95].

The CFD programme generates a large quantity of data for the post-processor stage, that when analysed has produced several advantages from the recent advancements in the capabilities of the graphic workstation. The top commercial CFD systems now include visualisation software capabilities that help the user better grasp the fluid flow and its related geometry [96]. These might involve:

i. The meshing/ grid Views display.

ii. Vector plots.

iii. Surface plots of three dimensional and two dimensional.

iv. Flow’s animations.

v. Shaded and line counter draws.

vi. Colors production.

vii. Particles tracking.

viii. View manipulation (translation, rotation, scaling, etc.)

3.2.1 Finite Element Technique

The numerical approach known as the Finite Element Methods (FEM) has been utilised to approximation the solution across a particular element. This element allows any two adjacent components to interact, changing a variety of characteristics continually. In general, FEM works well for issues in which the solid domain impacts the patterns of heat and fluid movement [97].

The governing formulas for all physical events take the form of partial differential formulas, or PDEs. Numerical solution techniques do not recognise these types of equations. The FEM does this by converting PDEs to useful algebraic form. The governing formulas' algebraic forms are discretized throughout the whole domain.

FEM seems to be the foundation of ANSYS, which uses its methods for several applications involving heat transfer and fluid movement. For instance, there is a clear contact between the heated surface and the coolant while cooling electronic components. It may also be utilised to cool electrical motors and solve a variety of phase transition issues [98].

3.3 CFD-BASED DATA CENTER MODELING

The CFD may be utilised in a data centre to forecast fluid flow at many levels, including rack, chip, and room levels. The designers would be capable of recognizing potentially dangerous hot spots and find suitable cooling system solutions with the aid of an accurate data simulations. Additionally, this would enable research into the architecture of the next data centre buildings [99].

For energy efficiency, precise data centre fluid flow and CFD modelling may be used to justify the new facility's design. facilities. It is the most economical way to lower data centres' energy use [100].

The first time the datacentre flow modelling findings were released was in the year 2000. The parameters of the datacentre heat transfer and flow were evaluated by a number of modelling research using CFD [101].

3.4 BOUNDARY CONDITIONS

The boundary conditions play a crucial role in the creation of the governing formula. In order to reflect the flow as accurately as possible, the boundary conditions are selected and have a significant impact on the flow [102]. In the next sections, the entrance, outflow, wall, and symmetry were discussed.

3.4.1 Inlet and Outlet

There are boundary conditions at the entrance and exit of the flow path in the cold plate above the submerged server. Generally, the temp, pressure, flow rate, and velocity are described by the inlet boundary conditions. The intake for the flow path in the server cold plate utilised in this project. Water in the cold plate flows via a channel with a circular cross section. The speed or flow rates at the circumstances known as fully developed flow at the intake boundary. According to Figure 3.2, the fluid evolved entirely after a certain distance from the entry, known as the entrance length (L_{entr}). The L_{entr} ought to be much greater than 0.06ReD since the laminar profile was attained at a long entry length [93].

$L_{entr} >>> 0.06ReD$

Whereas: the diameter of the inlet is D and the number of Reynolds is Re.

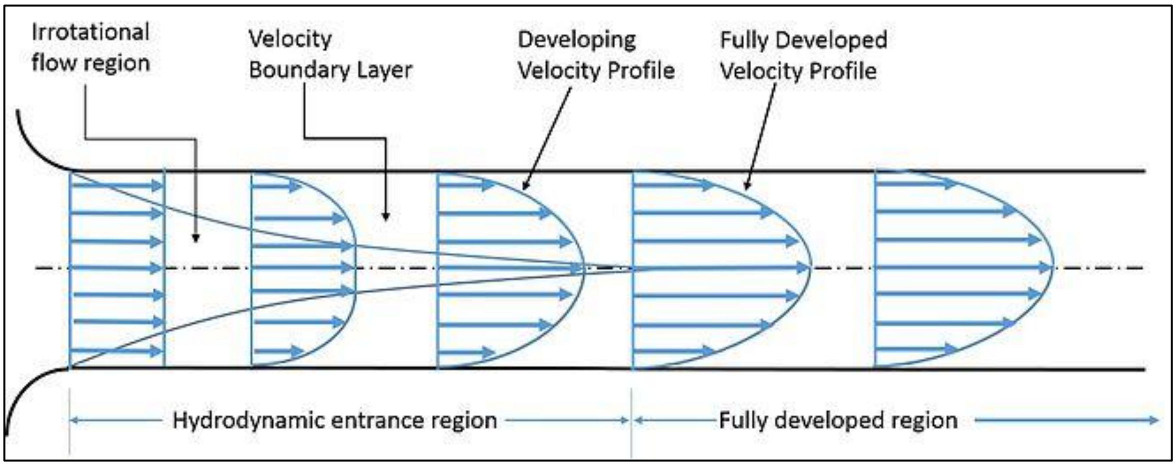

Figure 3.2: the Developing of Velocity Layer Within the Pipe [103].

Velocity and Pressure for the flowing fluid may be used to establish the boundary conditions of the output. At the outflow boundary, the outflow provides acceptable boundary conditions for the heat transfer convective domain. The formula employed in the outflow process of heat transfer involves [104]:

$$-\boldsymbol{n} \cdot (-\lambda \nabla T) = 0 \tag{3.1}$$

Whereas, the thermal conductivity of the fluid is λ and normal vector is n.

3.4.2 Walls

The simulation model's most typical boundary is a wall. At stationary walls without slip condition, the velocity is 0. Due to the chaotic character of turbulence on a small scale, it is difficult to determine the velocity for turbulent flow close to the walls. There seem to be two methods for resolving the turbulent flow close to a wall. The first strategy entails resolving the whole flowstream from the wall to the fluid. This called for a boundary layer with a close-to-the-wall high density meshes. The second strategy is known as walls function [105], and it is predicated on using an analytical solution to bridge the space between both the turbulent flow and wall. The wall functional, as illustrated in Figure 3.3, begins the mathematical model from the walls at a distance δ_w.

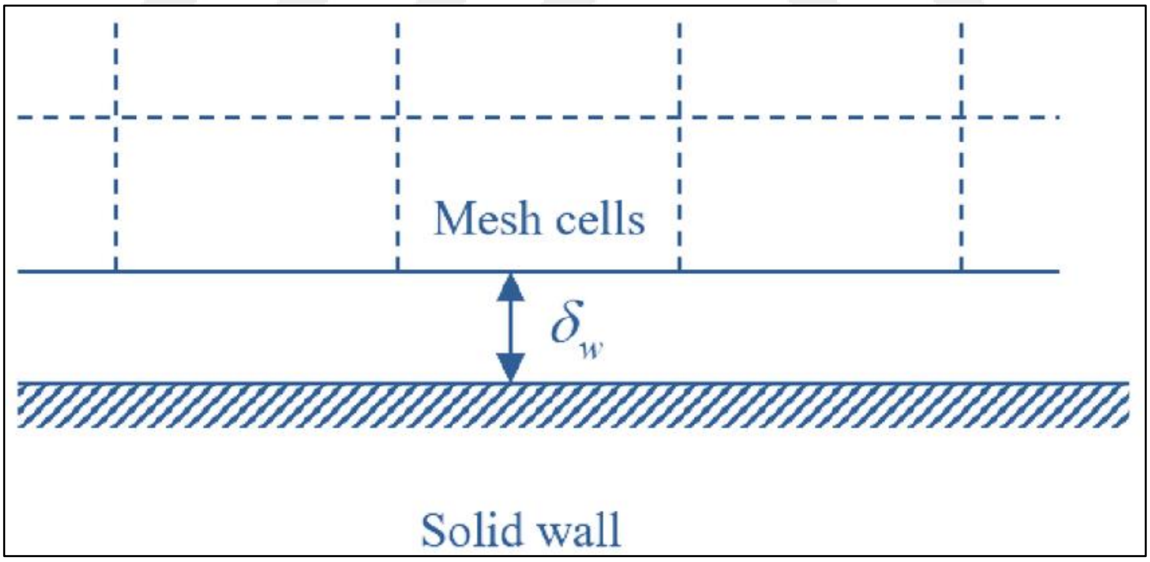

Figure 3.3: The Distance Between Wall $\boldsymbol{\delta_w}$ and Computations Domains [106].

$$\delta_w^+ = \frac{\rho u_\tau \delta_w}{\mu} \tag{3.2}$$

Whereas, the density fluid is ρ, the distance between the wall and the computations domains meshes is δ_w, the dynamics fluid viscosity is μ and the frictional velocity is u_τ and it could be found from [107], [108].

$$u_\tau \stackrel{\frac{1}{4}}{=} \overline{C}_\mu \sqrt{\kappa} \tag{3.3}$$

Whereas κ is the Karman constant, which for walls lift off would be equivalent to 0.41. $C\mu$ is an experimental constant that has the value 0.09 in math. To ensure that the correctness of the answer is really not impacted by the δ_w^+ variations along the walls, it should be verified. In order to get more accuracy, the magnitude of walls lift off (δ_w^+) must be as near to 11.06 as feasible. [82-84]

3.4.3 Symmetry

There are two boundary conditions in the symmetric as boundary conditions. Heating asymmetry is the first, while flow symmetry is the second. The boundary condition is identical to thermal insulation when the boundary for heating symmetry is present. In other words, the thermal symmetry has not been crossed by any heat flow. The formula utilized to determine thermal symmetry is:

$$-\boldsymbol{n} \cdot (-\lambda \nabla T) = 0 \tag{3.4}$$

Whereas: the normal vector is n and the thermal conductivity of fluid is λ.

Just the fluid flow was utilized to characterize the symmetrical boundary using the symmetric flow boundary condition. The following formulas resolve the boundary conditions for symmetric flow:

$$u \cdot n = 0 \tag{3.5}$$

$$K - (K \cdot n) \cdot n = 0 \tag{3.6}$$

$$K = \mu(\nabla u + (\nabla u)^T) \cdot n \tag{3.7}$$

Whereas, velocity is u, dynamics viscosity is μ, normal vector n and viscos stress vector is K on the symmetric boundaries.

3.4.4 Conjugate Heat Transfer

Conjugated heating transfer seems to be the simultaneous transmission of heating between a solid and a fluid. Conduction heating transfer predominates in solids, while convection prevails in fluids. A diagram illustrating the conjugated heating between fluids and solids is shown in Figure 3.4. There seem to be two temps on the wall that separates the solid from the fluid: T_f for the fluid and T_s for the solid. Since the temps would be equalized in conjugated heating, $T_s=T_f$, and the heating flux in the wall between the solids and fluids is continuous as indicated by Fourier's law, have no need to apply the heating transfer coefficient.

$$-n \cdot (-\lambda_s \nabla T_s) = -n \cdot \left(-\lambda_f \nabla T_f\right) \tag{3.8}$$

Whereas, the thermal conductivity for solids are λs, and fluid thermal conductivity is λf.

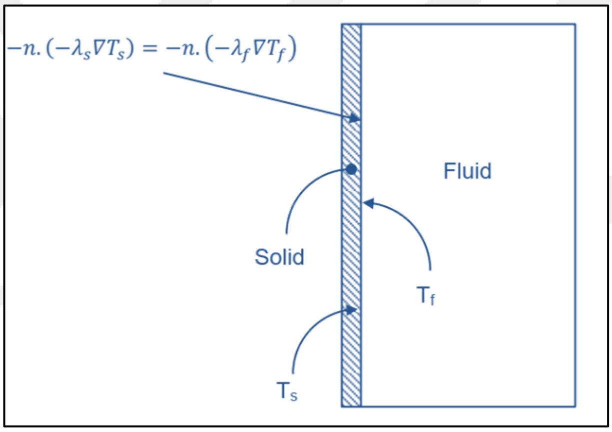

Figure 3.4: The Conjugated Heating Transfer for Fluid and Solid Domains.

3.5 MODELING OF LAMINAR FLOW

Figure 3.5, in which plates is stationary while the other is flowing, illustrates a fluid flow between the two surfaces with laminar flow. The laminar layers solely on a single plate flows over other laminar surface without interfering with others.

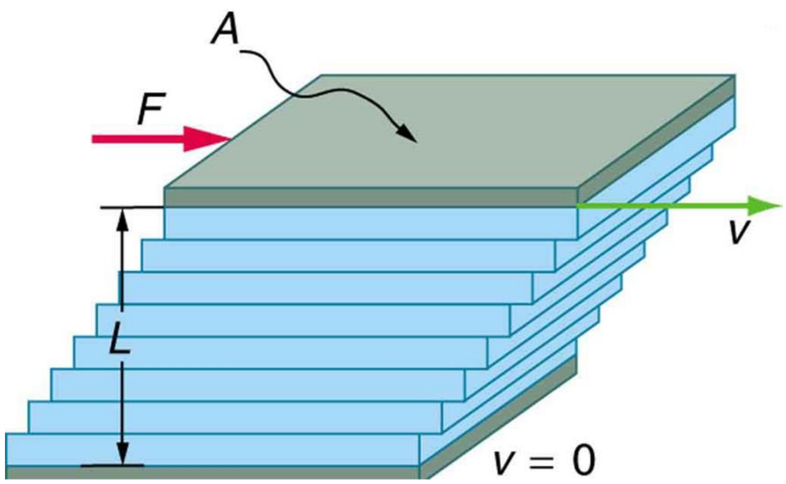

Figure 3.5: Two Panels in Laminar Flow: One Moves and the Other Remains Fixed [85].

Before beginning to solve the equation in CFD, the flow status—laminar or turbulent—should be established. There are two characteristics that show whether the flow is turbulent or laminar. Reynolds number was the first used for forced convection (Re). It consists of the inertia force split by the viscous force, resulting in a non - dimensional mix of four factors [86]:

$$\mathrm{Re} = \frac{\rho u \mathrm{D}}{\mu} \tag{3.9}$$

whereas: D is the pipe's diameter, the fluid's viscosity is μ, ρ is its density, and u is its average velocity. Because once the Re$\leq$ 2300 is present, the flow behaviour in the condition of the pipe was laminar [86]. The fluid was laminar because the Re of the flow path of the cold plate equals 276 and is less than 2300. The Rayleigh number (Ra) in natural convection may be used to determine whether the flow is turbulent or laminar. Ra seems to be the steady differential temp ΔT =(Th-Tc), in which the buoyancy to viscous forces proportion is 87.

$$Ra = \frac{c_p \rho^2 g \beta \Delta T L^3}{\mu \lambda} \tag{3.10}$$

Whereas, characteristic length is L, fluid's density is ρ, dynamics viscosity is μ, thermal expansion coefficient is β, thermal conductivity is λ, and specific heating is Cp.

Exploring was the fluid flow behaviour of the rectangular enclosure in Figure 3.6 for a Prandtl number (Pr) range of 1 to 20 and a rectangular aspect proportion (L/W) ranging of 1 to 40 for various T1 and T2. Figure 3.7 depiction of the study's findings demonstrates that the fluid in a rectangular channel was laminar when Ra 106 and turbulent if Ra 107 [15]. The submerged server in Chapters 5 and 6 seems to have an aspect proportion of 13, a Pr of 18, and a Ra of 10^8, that is within the original study acceptable range. As a result, the fluids flow behaviour was turbulent since Ra is larger than 10^7.

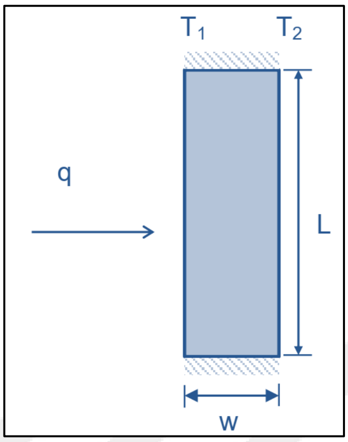

Figure 3.6: Geometry of Enclosure Rectangular Channel [15].

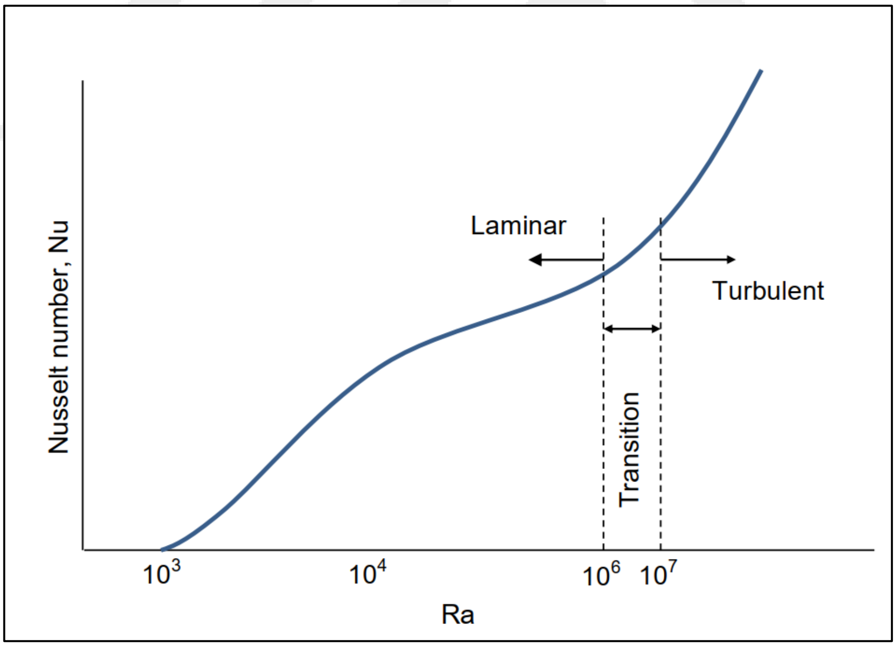

Figure 3.7: Natural Convection Fluid Flow Behaviour in A Rectangular Enclosure [15].

3.6 TURBULENCE MODELLING

Figure 3.8 illustrates turbulent flow, a phenomenon called as chaotic and random flow movement that causes disorder in the fluid flow path for laminar flow. To analyze a turbulent system, one must not utilize a laminar solver since Turbulent was unsuitable for laminar applications and would not need an accurate solution.

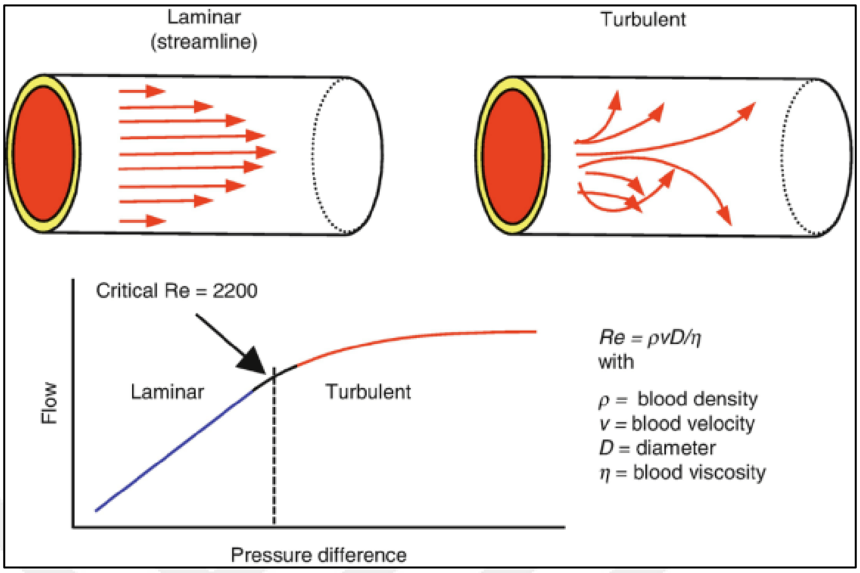

Figure 3.8: The Laminar and Turbulent Fluid Flow Behaviour [84].

Turbulence was brought on by a system's low viscous force, rough surfaces, or high flow rate. Eddies are produced by the rotating of the flow in turbulent flow. Eddies move at a varying speeds and are shorter. Large eddies are created by the inertia force. Transport eddies are created in the flow as a result of the phenomenon known as vortex stretching. This phenomenon causes the huge eddies to split into smaller eddies. The viscose impact becomes significant when the eddies shrank till they were negligible [88].

Some techniques, including Large Eddies Simulations (LES), Directly Numerical Simulations (DNS), Reynolds Averages Navier-Stokes (RANS), and may be used to model turbulent flow. The large Eddies Simulations (LES) method usages subgrid-scale models to capture tiny eddies in order to solve turbulent flow problems using explicit large eddies. Since the meshes grid size required to calculate the Navier-Stokes equation must be smaller than the lowest scale of turbulence, Direct Numerical Simulation (DNS) was highly costly and necessitates the utilization of extremely powerful computers for the majority of situations [89]. The following section explains Reynolds Average Navier-Stokes (RANS), which is utilised in ANSYS.

3.6.1 Turbulent Flow – RANS

The Reynolds average Navier stoke (RANS) solution has been the most popular approach to solving turbulent flow because it can accurately represent turbulence utilising components that are much bigger in size by average is it occurring thru the component rather than capturing localised fluctuation. In order to do this, parameters are split into two categories: fluctuation and mean. The fluctuating category really expresses the Navier-Stoke formula at two distinct velocities, while the mean category gives a smooth behaviour [73].

$$U = u + u' \tag{3.11}$$

whereas: the unfiltere velocity is u and u' is the vector representing velocity variations. For incompressible fluid, the Navier-Stokes formula is written as [73]:

3.6.1.1 Continuity formula

$$\rho\, \nabla \cdot \boldsymbol{u} = 0 \tag{3.12}$$

Reynolds Average Momentum formula

$$\rho \frac{\partial u}{\partial t} + \rho(u \cdot \nabla)u + \nabla \cdot (\overline{\rho u' \otimes u'}) = \nabla \cdot [-pI + \mu(\nabla u + (\nabla u)^T)] + F \tag{3.13}$$

Whereas, the forcing term is **F** that could for instance account for buoyancy or gravity.

Reynolds stress tensor is $\nabla \cdot (\overline{\boldsymbol{\rho}\mathbf{u}' \otimes \mathbf{u}'})$ and the outer product vector is $\otimes$.

The Eddy Viscosity Model for RANS is

$$\nabla \cdot (\overline{\rho \mathrm{u}' \otimes \mathrm{u}'}) = \mu_T(\nabla \mathrm{u} + \nabla \mathrm{u}^T) - \frac{2}{3}\delta k I \tag{3.14}$$

Models that are specified in the following sections must be computed in order to determine the magnitude of the additional turbulence.

3.6.2 K-ε Turbulence Model

Launder and Spalding [90] created k-, one of the first turbulent models employed. The kinetics energy (k) and the rate of dissipation (ε) for turbulent are the two unknowns in the k-ε model. In order to compute two new unknown factors, 2 extra formulas are introduced.

Using Reynolds Averages Navier-Stokes (RANS) formulas, the following extra equations must be solved: Transport formula for kinetics energy in turbulent flow, k:

$$\rho \frac{\partial k}{\partial t} + \rho \boldsymbol{u}. \nabla k = \nabla \cdot \left[\left(\mu + \frac{\mu_T}{\sigma_k} \right) \nabla k \right] + p_k - \rho \varepsilon \qquad (3.15)$$

The rate of dissipation for turbulent transport formula, ε:

$$\rho \frac{\partial \varepsilon}{\partial t} + \rho \boldsymbol{u} \cdot \nabla \varepsilon = \nabla \cdot \left[\left(\mu + \frac{\mu_T}{\sigma_\varepsilon} \right) \nabla \varepsilon \right] + C_{e1} \frac{\varepsilon}{k} P_k - C_{e2} \rho \frac{\varepsilon^2}{k} \qquad (3.16)$$

You may find the production phrase from:

$$p_k = \mu_T \left[\nabla \boldsymbol{u} : (\nabla \boldsymbol{u} + (\nabla \boldsymbol{u})^T) - \frac{2}{3} (\nabla \cdot \boldsymbol{u})^2 \right] - \frac{2}{3} \rho k \nabla \cdot \boldsymbol{u} \qquad (3.17)$$

The definition of the turbulent viscous forces is:

$$\mu_{\mathrm{T}} = \rho C_\mu \frac{k^2}{\varepsilon} \qquad (3.18)$$

whereas k is the Prandtl number of k, u seems to be the average velocity, uT is the mean velocity transport, T is the turbulent viscosity, and u is the density. The constant variables of the experimental turbulent model are:

$\sigma_{\mathrm{k}} = 1, \sigma_{\mathrm{e}} = 1.3, \mathrm{C_{e1}} = 1.44$ and $\mathrm{C_{e2}} = 1.92$

A variety of industrial applications have been properly modelled using the turbulent model k-ε [78]. Nevertheless, when rotational flow or non-circular ducts are present, employing the turbulent model k-ε yields erroneous results [78]. Because k- is an useful turbulent model to utilise for open and vast areas, Cho et al. [53] employed the turbulent simulation k-ε in the data centre to discover the temp field.

3.6.3 k-ω Turbulence Model

Wilcox seems to be the creator of the K-[81]. It resolves turbulent kinetic energy (k) and specific dissipation rate (ω). Dynamic viscosity of turbulence is:

$$\mu_{\mathrm{T}} = \rho \frac{k}{\omega} \qquad (3.19)$$

Transport formula for the kinetic energy of turbulent flow, k:

$$\rho \frac{\partial k}{\partial t} + \rho u \cdot \nabla k = \nabla \cdot [(\mu + \mu_T \sigma_k^*)\nabla k] + p_k - \rho \beta_o^* k\omega \quad (3.20)$$

Formula of transport for the turbulent particular the rate dissipation, ω:

$$\rho \frac{\partial \omega}{\partial t} + \rho \boldsymbol{u} \cdot \boldsymbol{\nabla} \omega = \nabla \cdot [(\mu + \mu_T \sigma)\nabla \omega] + \alpha \frac{\omega}{k} p_k - \rho \beta_0 \omega^2 \quad (3.21)$$

You may find the manufacturing phrase from

$$p_k = \mu_T \left[\nabla \boldsymbol{u} : (\nabla \boldsymbol{u} + (\nabla \boldsymbol{u})^T) - \frac{2}{3}(\nabla \cdot \boldsymbol{u})^2\right] - \frac{2}{3}\rho k \nabla \cdot \boldsymbol{u} \quad (3.22)$$

Whereas the constant factors,

$$\alpha = \frac{13}{25}, \sigma_k^* = \frac{1}{2}, \sigma_\omega = \frac{1}{2}, \beta_0 = \frac{9}{125}, \beta_0^* = \frac{9}{100}$$

The fluid behaviour within the submerged server is turbulent and follows the same physical principles as the fluid flow inside a cavity, in which the fluid is controlled by the temp differential. In order to determine the optimal turbulence that offers a solution that is near to the findings of the investigation, Rundle [91] built a turbulence simulation of a cavity. The research found that the k-turbulence model offers better findings when compared to other turbulent flows. The findings of another research by Zitzmann [92] have shown that utilising k-ω may produce a good agreement with experiment for a turbulent natural convection in square cavity. This study looked at a variety of turbulent models for this situation. Additionally, Amounallah [93] investigated a variety of turbulence models for a turbulent flow in a hollow with a single wavy wall, and the findings demonstrated that the k-ω model provides the highest predictions in comparison to experimental. These experiments suggest that the k-ω option seems to be a promising one for this thesis' solution to the turbulent flow within submerged servers.

3.6.4 Low Reynolds Number k-ε Turbulence Model

If the precision of the k-turbulence model was insufficient, the Low Reynolds Number turbulence model is used. The region close to the wall was estimated using the Low Reynolds Numbers k-ε turbulence models. The dampening function is introduced to the turbulence transport formulas using the Low Reynolds Numbers k-ε turbulence models [94]. Transportation formula for kinetic energy in turbulent flow, k:

$$\rho \frac{\partial k}{\partial t} + \rho \boldsymbol{u} \cdot \boldsymbol{\nabla} k = \nabla \cdot \left[\left(\mu_D + \frac{\mu_T}{\sigma_k} \right) \nabla k \right] + p_k - \rho \varepsilon \tag{3.23}$$

Formula of transportation for the rate of turbulent dissipation, ε:

$$\rho \frac{\partial \varepsilon}{\partial t} + \rho \boldsymbol{u} \cdot \boldsymbol{\nabla} \varepsilon = \nabla \cdot \left[\left(\mu_D + \frac{\mu_T}{\sigma_\varepsilon} \right) \nabla \varepsilon \right] + C_{\varepsilon 1} \frac{\varepsilon}{k} p_k - f_\varepsilon C_{\varepsilon 2} \rho \frac{\varepsilon^2}{k} \tag{3.24}$$

The definition of the production phrase is

$$p_k = \mu_T \left[\nabla u : (\nabla u + (\nabla u)^T) - \frac{2}{3} (\nabla \cdot u)^2 \right] - \frac{2}{3} \rho k \nabla \cdot u \tag{3.25}$$

The definition of the turbulent dynamics viscosity was

$$\mu_T = \rho f_\mu C_\mu \frac{k^2}{\varepsilon} \tag{3.26}$$

$$f_\mu = \left(1 - e^{-\frac{l}{14}} \right)^2 \cdot \left(1 + \frac{5}{R_t^{3/4}} e^{-\left(\frac{R_t}{200} \right)^2} \right) \tag{3.27}$$

$$f_\varepsilon = \left(1 - e^{-\frac{l}{3.1}} \right)^2 \cdot \left(1 - 0.3 e^{-\left(\frac{R_t}{6.5} \right)^2} \right) \tag{3.28}$$

$$l = \frac{(\rho u_\varepsilon l_w)}{\mu}, R_t = \frac{\rho k^2}{\mu \varepsilon}, u_\varepsilon = \left(\frac{\mu \varepsilon}{\rho} \right)^{\frac{1}{4}}$$

The constant variables of the turbulent models

$C_{\varepsilon 1} = 1.5, C_{\varepsilon 2} = 1.9, C_\mu = 0.09, \sigma_k = 1.4, \sigma_\varepsilon = 1.4$

Whereas, Prandtl number of k is σk, Prandtl number of ε is σε, density is ρ, viscosity turbulent is μT, mean velocity is **u** and the distance close to wall is l_w.

3.7 MODEL DESCRIPTION

A three-dimensional model has been created utilizing computer simulation software so as to test the impact of the immersion cooling with flowing liquid and heat sink installed on the CPU surface of a computer (PC). The model has a flat finned heating sink on top of the CPU, which generates the most of the heating in a computer. The CPU measures 40 mm square in size. Copper and aluminium (Al) have been the materials used for the heating sink (Cu). The PC box's top left corner served as the exit point for the liquid coolant, which entered the

Computer box from the bottom of the heating sink. The model has been predicated on a laminar, stable, incompressible flow. As seen in [25,26], the momentum formula is as follows:

$$\rho(\mathrm{DV}/\mathrm{Dt}) = -\nabla P + \rho \mathrm{g} + \mu \nabla^2 \mathrm{V} \tag{3.29}$$

A 2D model will be sufficient to depict the cooling for the project scope after it was decided to simulate only one rack since the flow was only going thru the servers in one direction. The fact that this choice will operate better with ANSYS Student's restricted meshing capabilities and with the restricted amount of available computing time at the institution was also seen as a benefit.

Even though two dimensional modelling doesn't provide a full view of everything taking place in the data centre, it would provide a very clear illustration of what was occurring for the purposes of the project. If further work was required based on promising findings, this can be accomplished within a three dimensional model at a later time as part of additional research, if required.

3.7.1 Computer Aided Design Model

The integrated CAD programme inside ANSYS Fluent has been used to produce the AutoCAD software for the two dimensional simulation, with the model parameters set to two - dimensional Instead of modelling the space and rack for the two dimensional ANSYS simulation, the fluid is modelled, and the proper boundary conditions were therefore applied to this model during the meshing step. Figure 3.9's simulation of the 15kW air-cooled engine provides an illustration of this concept in action. Figure 3.10 shows a meshed model.
The floor and roof of the datacentre seem to be the top and lower borders of the model in the image above. The model's right edge has been designated as the exit, while the left side served as the inlet. Blanking panel and the cabinet top were modelled in the huge outdoor space, and the partition that emerged to the right of it served as the heated aisle containment area. The remaining gaps have been produced to simulate the servers, and the simulations' heat production had been placed to the margins of these gaps.

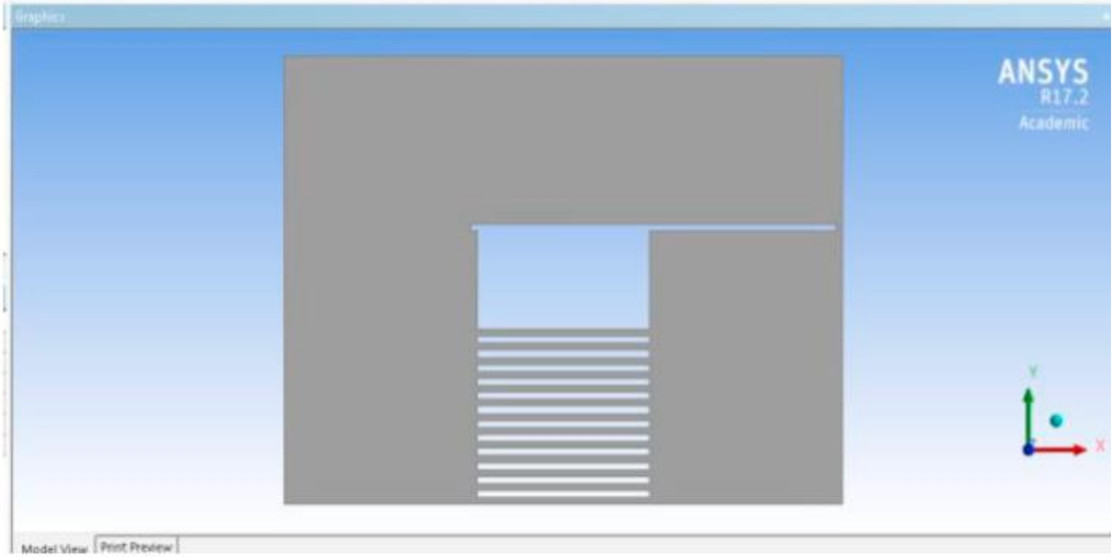

Figure 3.9: Two-Dimensional Autocad Model for Air-Cooling Simulation.

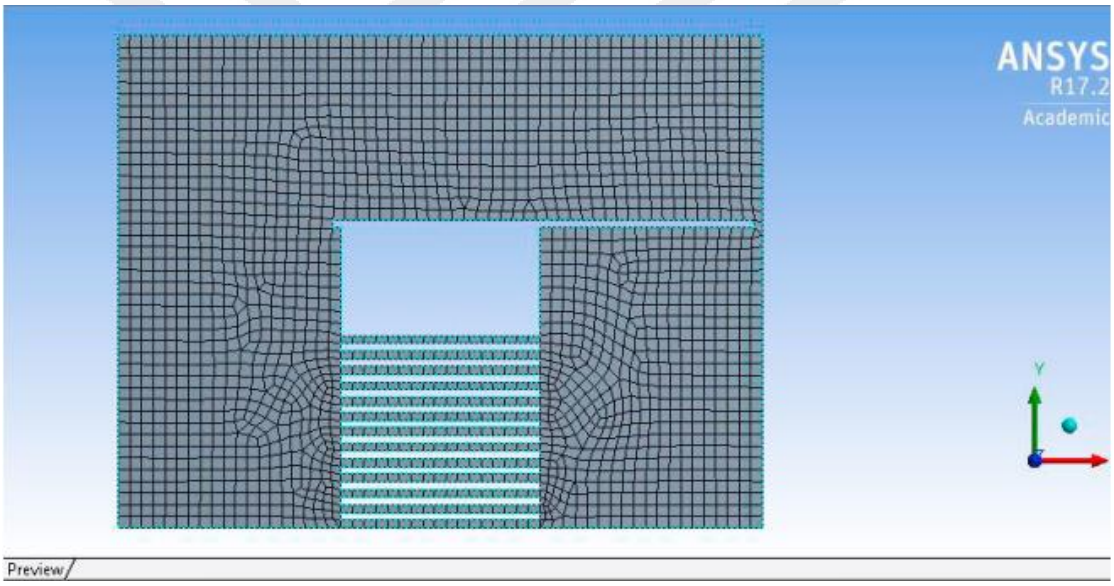

Figure 3.10: Air-Cooling Meshes (Elements).

3.7.2 Simulation

Each simulation displays the overall temp in Kelvin inside the datacenters with a steady state operation. The outlet and inlet variables were maintained constant and set as shown in Table 3.1 for each simulation.

Table 3.1: Initial Boundary Conditions Set.

Physical Properties	Magnitude
For the inlet	
Velocity	0.25m/s
Pressure	15Pa
Temp	298K (25 degree centigrade)
For the outlet	
Pressure	15Pa
Temp	298K (25 degree centigrade)

The initial step was to figure out how much of the overall heating was produced by each server in so that we could calculate the heating produced for every one of the rack sizes. By splitting heating generated by the rack by the servers' number, it was discovered that the 15kW rack generated 1250W per server and the 30kW rack 1579W for every server.

The volume of one server has been computed based on the AutoCAD model and the specified width of the servers (since the AutoCAD model had only been two dimensional), and it was discovered that this volume was 1.3x0.05x0.8= 0.0455m3 in order to model this in ANSYS. Following the volumetric division of the heat produced for every server model, the heat produced for every server for the 15kW racks and the 30kW racks was calculated to be 27472W/m3 and 34702W/m3, respectively.

The cooling medium for the air-cooled racking were air, that was chosen using the pre-set settings in ANSYS Fluent 19.2 Academic.It was originally planned to enter characteristics for the cooling fluid utilised by Submersify for the water cooling racks, nevertheless the data base did not include the information needed by ANSYS, thus Novec 3M 649, the fluid utilized in the Two-Phases system referenced in the existing literature, has been utilised instead.

3.7.3 Mathematical Formulation

This rectangular cavity's flow is turbulent and is thought to be incompressible. In the Cartesian coordinates, the continuity formula is expressed by:

$$\frac{\partial u}{\partial x} + \frac{\partial v}{\partial y} = 0 \tag{3.30}$$

Applying the momentum formula in the X-axis with a Boussinesq buoyancy assumption;

$$\rho\frac{\partial u}{\partial t} + \rho\left[u\frac{\partial u}{\partial x} + v\frac{\partial u}{\partial y} + w\frac{\partial u}{\partial z}\right] = -\frac{\partial p}{\partial x} + \mu\left[\frac{\partial^2 u}{\partial x^2} + \frac{\partial^2 u}{\partial y^2} + \frac{\partial^2 u}{\partial z^2}\right] + \rho g_x \beta(T - T_o) \tag{3.31}$$

Y- axis

$$\rho\frac{\partial v}{\partial t} + \rho\left[u\frac{\partial v}{\partial x} + v\frac{\partial v}{\partial y} + w\frac{\partial v}{\partial z}\right] = -\frac{\partial p}{\partial y} + \mu\left[\frac{\partial^2 v}{\partial x^2} + \frac{\partial^2 v}{\partial y^2} + \frac{\partial^2 v}{\partial z^2}\right] + \rho g_y \beta(T - T_o) \tag{3.32}$$

Z- axis

$$\rho\frac{\partial w}{\partial t} + \rho\left[u\frac{\partial w}{\partial x} + u\frac{\partial w}{\partial y} + w\frac{\partial w}{\partial z}\right] = -\frac{\partial p}{\partial z} + \mu\left[\frac{\partial^2 w}{\partial x^2} + \frac{\partial^2 w}{\partial y^2} + \frac{\partial^2 w}{\partial z^2}\right] + \rho g_z \beta(T - T_o) \tag{3.33}$$

When, the steady condition flow

$$\frac{\partial u}{\partial t} = \frac{\partial v}{\partial t} = \frac{\partial w}{\partial t} = 0$$

$g_x = g_z = 0$

Since absence acceleration gravity in both *x* and *z* axis

Therefore, formula would be,

$$\rho\left[u\frac{\partial v}{\partial x}+v\frac{\partial v}{\partial y}\right]=-\frac{\partial p}{\partial y}+\mu\left[\frac{\partial^2 v}{\partial x^2}+\frac{\partial^2 v}{\partial y^2}\right]+\rho\,\underbrace{g_y\beta(T-T_o)} \tag{3.34}$$

The energy formula

$$\rho c_p\left[\frac{\partial T}{\partial t}+u\frac{\partial T}{\partial x}+v\frac{\partial T}{\partial y}\right]=k\left[\frac{\partial^2 T}{\partial x^2}+\frac{\partial^2 T}{\partial y^2}\right] \tag{3.35}$$

The following non-dimensional parameters are necessary for the non-dimensionalization of the governing formula.

$$\begin{aligned}
x' &= \frac{x}{L} \text{ or } x = x'L\\
y' &= \frac{y}{L} \text{ or } y = y'L\\
v' &= \frac{\rho L}{\mu} v \text{ or } v = \frac{\mu}{\rho L} v'\\
u' &= \frac{\rho L}{\mu} u \text{ or } u = \frac{\mu}{\rho L} u'\\
p' &= \frac{\rho L^2}{\mu^2} p \text{ or } p = \frac{\mu^2}{\rho L^2} p'\\
T' &= \frac{T-T_c}{T_h-T_c} \text{ or } T = T'(T_h-T_c)+T_c\\
T'_o &= \frac{T_o-T_c}{T_h-T_c} \text{ or } T_o = T'_o(T_h-T_c)+T_c
\end{aligned} \tag{3.36}$$

3.8 MODEL BY COMSUL

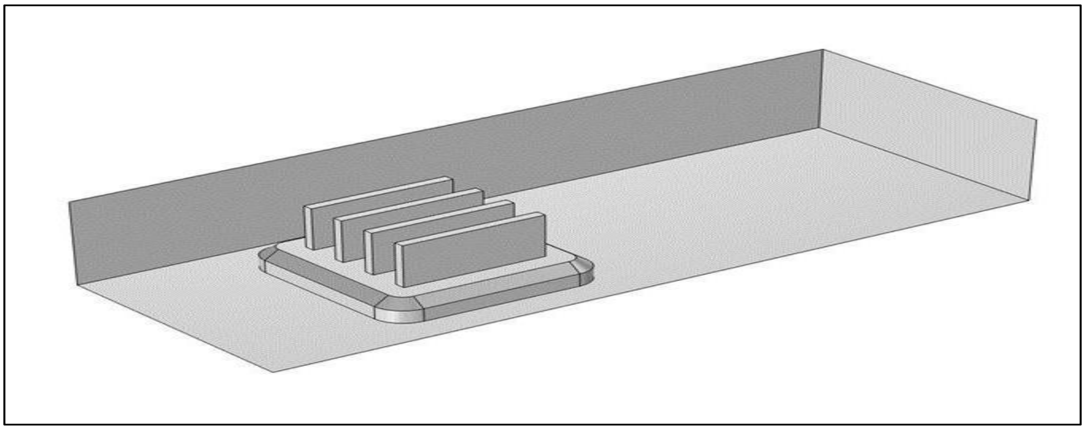

Figure 3.11: Two-Dimensional Autocad Model for Air-Cooling Simulation.

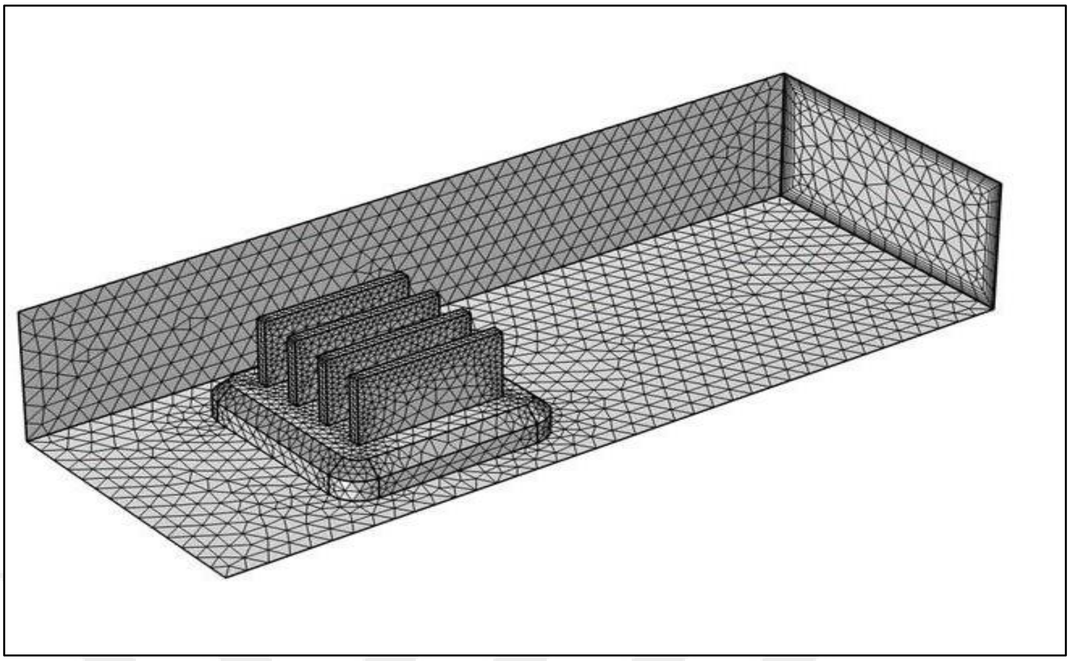

Figure 3.12. Air-Cooling Meshes (Elements).

3.8.1 Simulation

Each simulation displays the overall temp in Kelvin inside the datacentres with a steady state operation. The outlet and inlet variables were maintained constant and set as shown in Table 3.2 for each simulation.

Table 3.2: Specifications and Boundary Conditions of Forced Air Cooling With Heat Sink.

Heat Sink Base		
Depth	3	cm
Length	3	cm
Thickness	5	mm
Corner fillet radius	2	mm
Chamfer length, angle 45°	2	mm
Box		
Inlet distance	2	cm
Outlet distance	6	cm
Lateral distance	0.5	cm
Top distance	0.5	cm
Heat Sink Fin		
Heat sink type	Straight	-
Hight	1	cm
Thickness	1.5	mm
Number of fins	5, 6, 7, 8, 9	-
Boundary conditions		
Inlet velocity	1	m/s
Inlet temperature	22	°C

4. RESULTS AND DISCUSSION

Once developing cooling systems for data centers, several different variables are considered. These factors include the design of low-level chips and heat sinks, thermally-aware software, the physical arrangement of servers, fans, and a building's cooling systems, as well as site design decisions that take advantage of a data center's surrounding climate. Heat sinks, fans, liquid-cooling systems, and chillers that rely on compression are the standard components of traditional cooling designs. They work out how to operate the data center securely at greater temps, how to organize their computers to get ideal ventilation, and how to make better use of the peculiarities of the local environment (like when you open your windows in the Fall instead of running an air conditioner). There are also investigations being conducted into more extreme options, including Microsoft's Project Natick, which places data centers beneath the sea in order to benefit from the cooling and other advantages of this location.

The current chapter present obtained results from both COSOL software and ANSYS software that related to design of heat sink. Heat sinks are devices that facilitate the transfer of heat from a hot surface, which is often the housing for a heat-generating element, to a cooler ambient, which is typically air. Heat sinks are also known as heat exchangers [109]. For the sake of the subsequent talks, it will be assumed that the cooling fluid is air. Heat transfer via the interface between the solid surface and the coolant air is the least efficient within the system, and the solid-air interface represents the biggest barrier for heat dissipation. This is true in the majority of instances [110]. This barrier may be decreased with the help of a heat sink primarily because it expands the surface area that is in direct contact with the coolant. This makes it possible for more heat to be dissipated and/or decreases the temp at which the gadget operates [15]. The fundamental objective of a heat sink is to keep the temp of the device at or below the max temp that is safe for operation, as determined by the makers of the device. therefore, the obtained results that study the effect of heat sink design as following:

4.1 COMSUL SOFTWARE RESULTS

4.1.1 Effect of Fins Number on Temperature of Heating Sink

Based on the obtained results demonstrated in Figures 4.1 and 4.2, the increasing the fins number for heat sink from 5 to 6 reduce the cooling efficiency for the system, where the temperature in case of using 5 fins was 45 degree centigrade. While increasing the fins number more than 6 lead to increase the outlet temperature to be 47.5 degree centigrade. The lowest temperature of the outlet heat sink is 20 degree centigrade when using 5 fins and the lowest heat sink temperature increased to be 25 degree centigrade when use 6 or more fins number. Cooling systems, particularly those involved in cooling the data center building, should be adjusted if the outside temp changes (for example, a hotter than typical summer day). "Work harder" to keep the temperature in the safe room. Working harder often results in more energy (and hence, more money) being used to cool down. Nevertheless, in more severe situations, it would be essential to throttle or shut down a portion of the data center if trying harder to cool it doesn't work that would have an influence on the data center's performance and overall effectiveness.

When a data center is overheating, it must either reduce the amount of heat it produces or increase the pace at which heat is removed from the data center. It is indeed possible that if you generate less heat, you'll also complete less computer work, which might make the customers of the data center less happy with the service they get. Transferring more away the heat from the data center may involve turning on additional cooling equipment (including air chillers) that could result in an increase in the amount of electricity used by the data center as well as an increase in its operating cost. When a data center does not handle concerns related to overheating, it may lower the lifetime of its components as well as the performance of its computing, which will result in both unsatisfied customers and higher operating expenses. However increasing the fans number lead to increase the realized temperature due to increase the surface area, but at the same time increase the fins lead to increase the air velocity that directly will reduce the overall heat of the whole system.

The most cutting-edge data centers, according to ASHRAE [111] should not exceed temps between 20 and 25 degrees Celsius. It is often believed that running at the higher end of this range or higher than it would make the data center's cooling system more efficient, which will result in a reduction in the overall amount of electricity used by the facility. An examination of the system's thermodynamics reveals that elevating the temp of the heat source with the high temp, whilst also maintaining the temp of the heat sink with the low temp, will result in an improvement in the removal of heat from the system's overall efficiency. Unluckily, the simplistic model does not capture all of the elements of the entire system, which may lead to an incorrect conclusion being drawn as a result. In point of fact, raising the temp in the data center might cause some systems and components to use more power, which in turn raises the overall power consumption of the facility. As the temp in the room rises, the total use of energy might still decrease little, or it may even increase. In this study, we investigate the full energy picture, from the facility's connection to the utility to the process of rejecting heat into the surrounding environment. Additionally, researchers investigate the effect that an increase in the temp of the surrounding environment could have on each link in the energy chain. This analysis suggests that there is a temp that is optimal for the operating condition of data centers, but that temp would then vary from one data center to the next depending on its specific features. These features include the IT equipment, cooling system architecture, and location of the data center (for example, the outside ambient conditions). In this article, additional effects of a rising ambient inlet temp, including problems with dependability and increased operating complexity, are described. It has been determined that just increasing the temp of the data center's ambient air might not have the expected impact of lowering the amount of energy that is used.

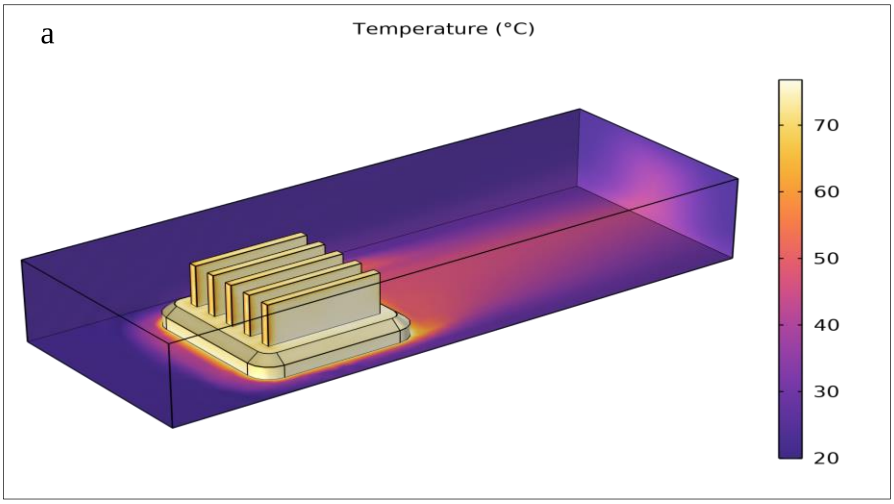

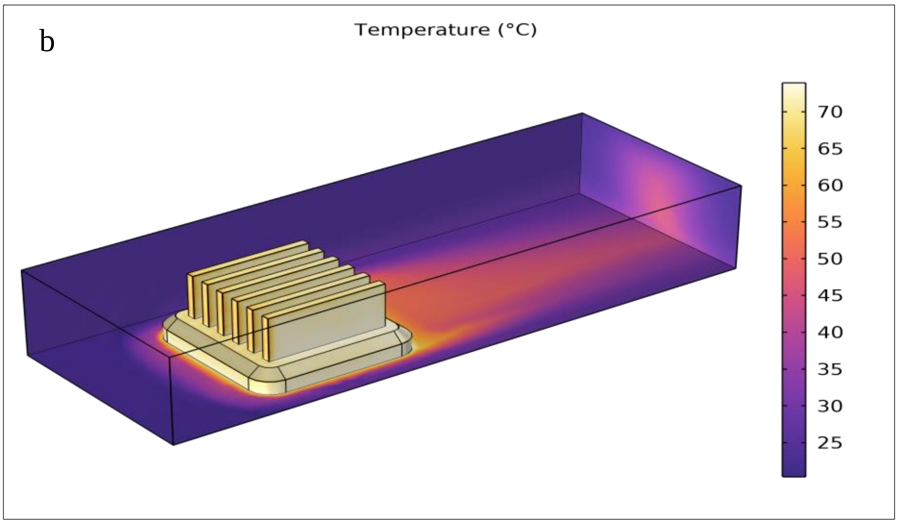
b
Temperature (°C)
70
65
60
55
50
45
40
35
30
25

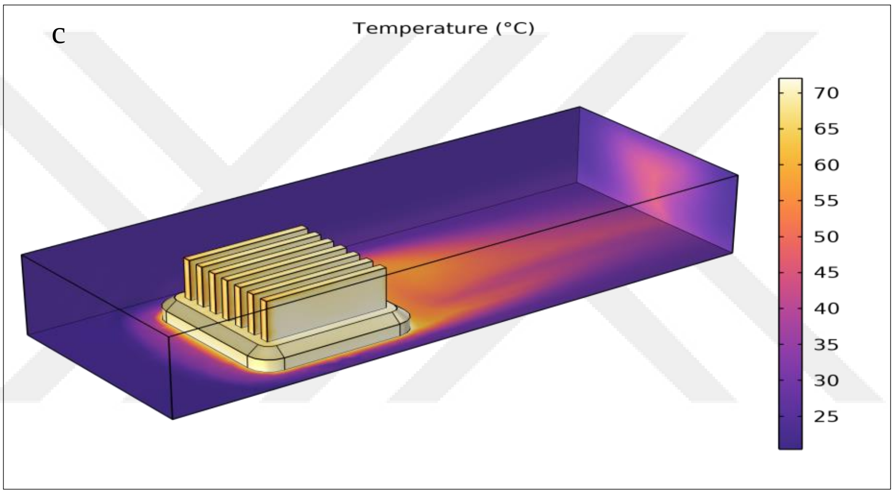
c
Temperature (°C)
70
65
60
55
50
45
40
35
30
25

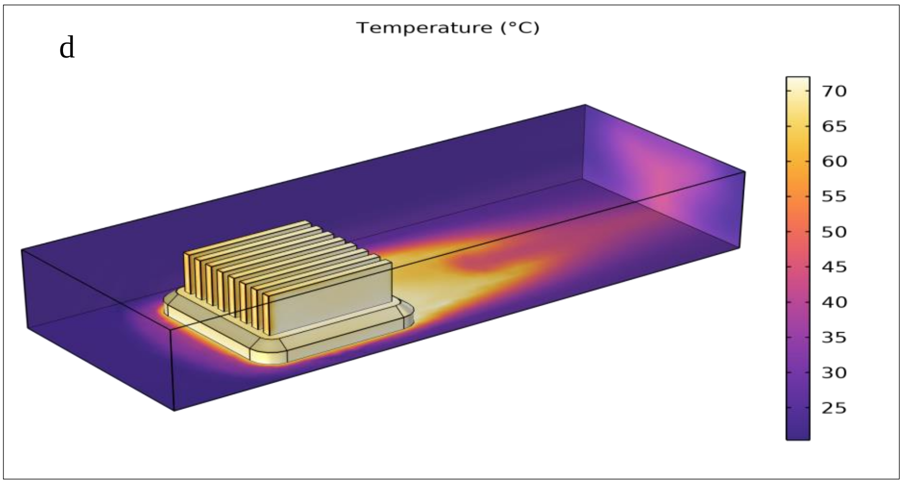
d
Temperature (°C)
70
65
60
55
50
45
40
35
30
25

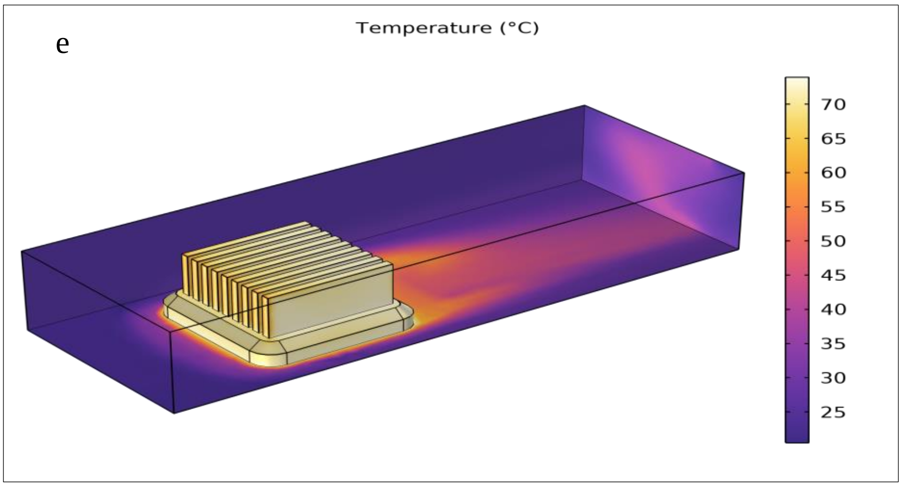

Figure 4.1. Temperature Profiles of Heat Sink With Multiple Fin Numbers (a= 5 fins, b=6 fins, c=7 fins, d=8 fins, and e=9 fins).

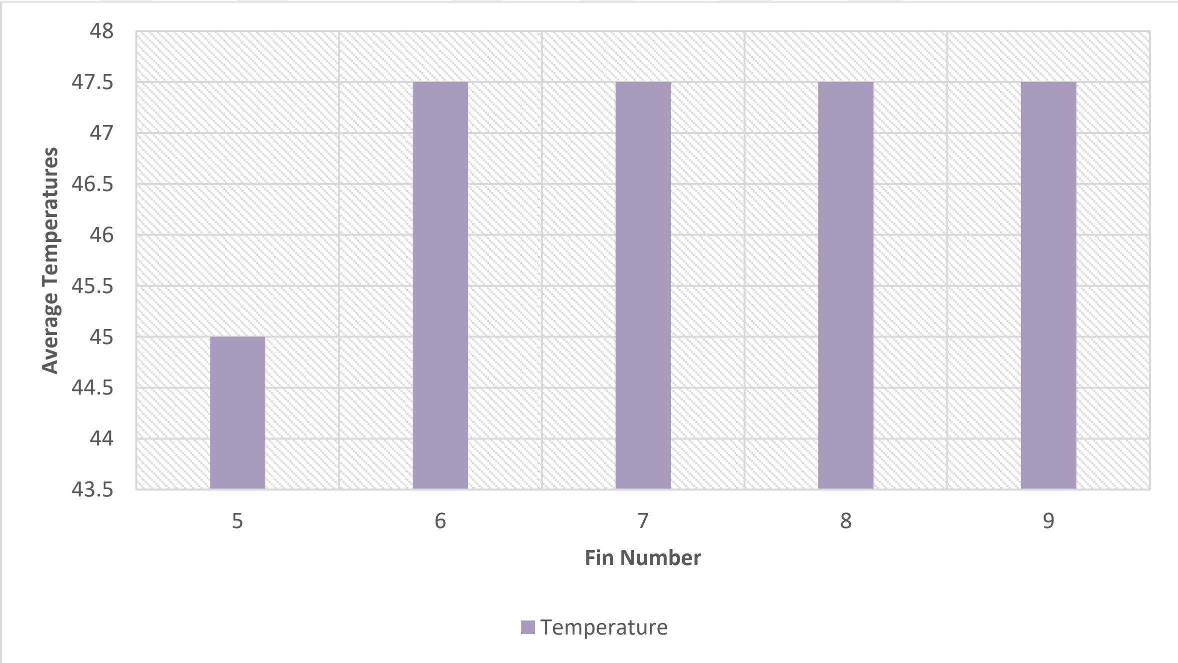

Figure 4.2. The Effect of Fins Number on Average Temperature in Immersion Cooling System.

4.1.2 Effect of Fins Number on Velocity

The average velocity was increased with increasing the fins number due to increasing the fluid flow path as demonstrated in Figures 4.3 and 4.4, the increasing the fins number for heat sink from 5 to 6 lead to increase the average velocity. While increasing the fins number more than 8 has no effect on the average velocity of the heat sink due to reduce the path area that resulting from fins area. The highest and lowest average velocity magnitude was changed based on the fins number, in case of using 5 fins the highest velocity was 1.8 m/s and lowest velocity was 0.2 m/s. Moreover, using 6 and 7 fins have similar lowest and highest velocity, also using 8 and 9 fins have the same velocity in lower and upper case.

Air is often used in the process of cooling the hardware that is housed in a data center. The hot air that is produced by the machinery is often directed toward a heat exchanger, which is then used to cool the air before it is recirculated back into the room [112]. Instead, the air might be routed straight to the surroundings and replenished with air from the outside. If a heat exchanger is employed, the cold may be obtained via a variety of methods, including but not limited to outside air, cooling machines, dry coolers, or cooling towers [113]. The requirements that must be met for the needed cooling source are determined by the geographical location at which the data center is situated. In regions that have a climate that is favorable, it is possible to make use of free cooling for a significant portion of the year. The most frequent source of free cooling in data centers is outside air, however it is possible to utilize other sources of free cooling, such as water from rivers, lakes, oceans, and other comparable bodies of water. Outdoor air is the most popular source of free cooling in data centers [114], [115].

By far the most typical method involves making use of a heat exchanger to bring the temperature of the air that is continually being recirculated within the building down to a more comfortable level [116]. In many cases, the external air may be used even when it does not immediately fulfill the needs. This issue may be remedied by treating the air outside using evaporative cooling, dehumidification, or humidification until the air's characteristics are satisfactory and it can be provided to the area in investigation [117]. The latest generation of information technology equipment can function at extremely high temps, which opens the door to the possibility of using free cooling for a greater proportion of the year.

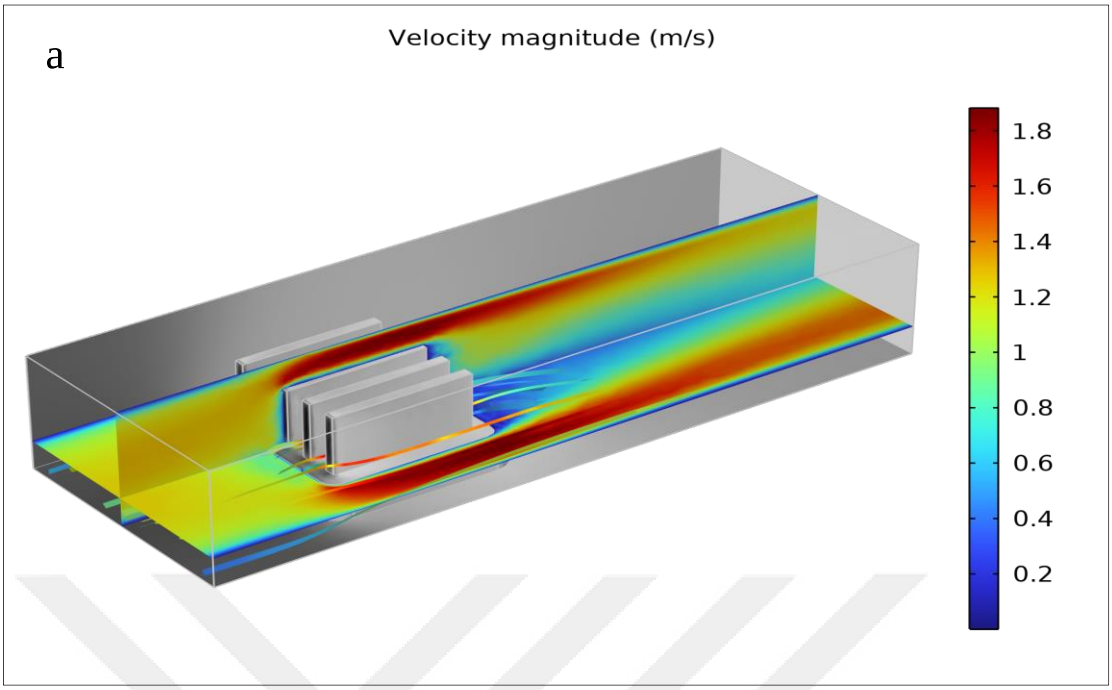
a
Velocity magnitude (m/s)
1.8
1.6
1.4
1.2
1
0.8
0.6
0.4
0.2

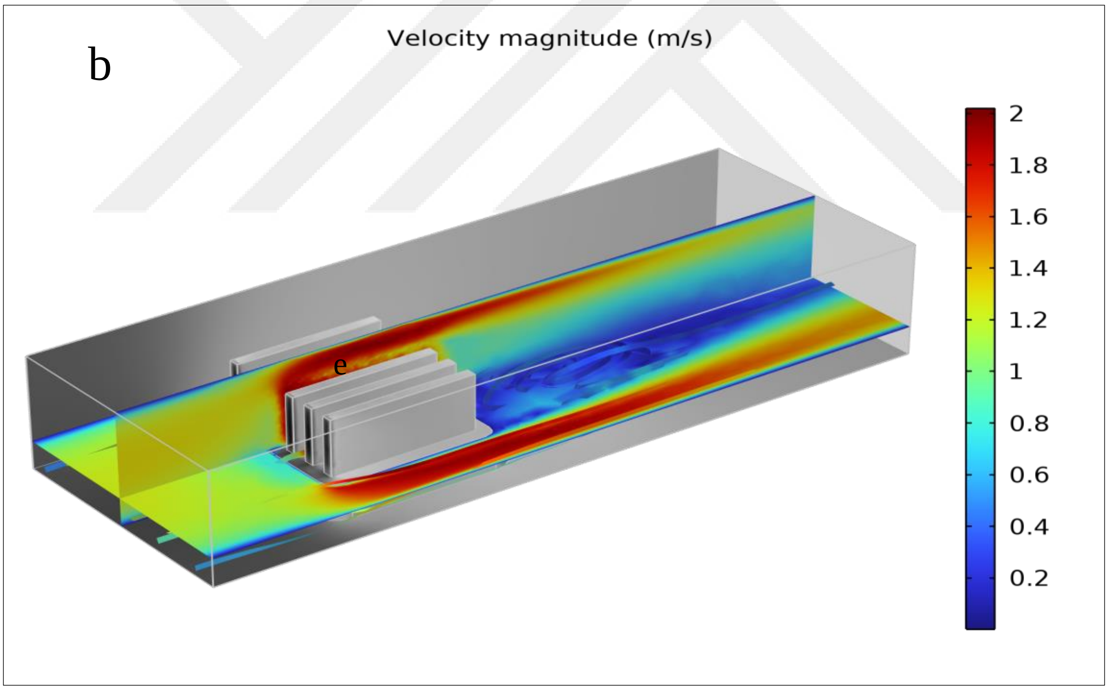
b
Velocity magnitude (m/s)
2
1.8
1.6
1.4
1.2
1
0.8
0.6
0.4
0.2

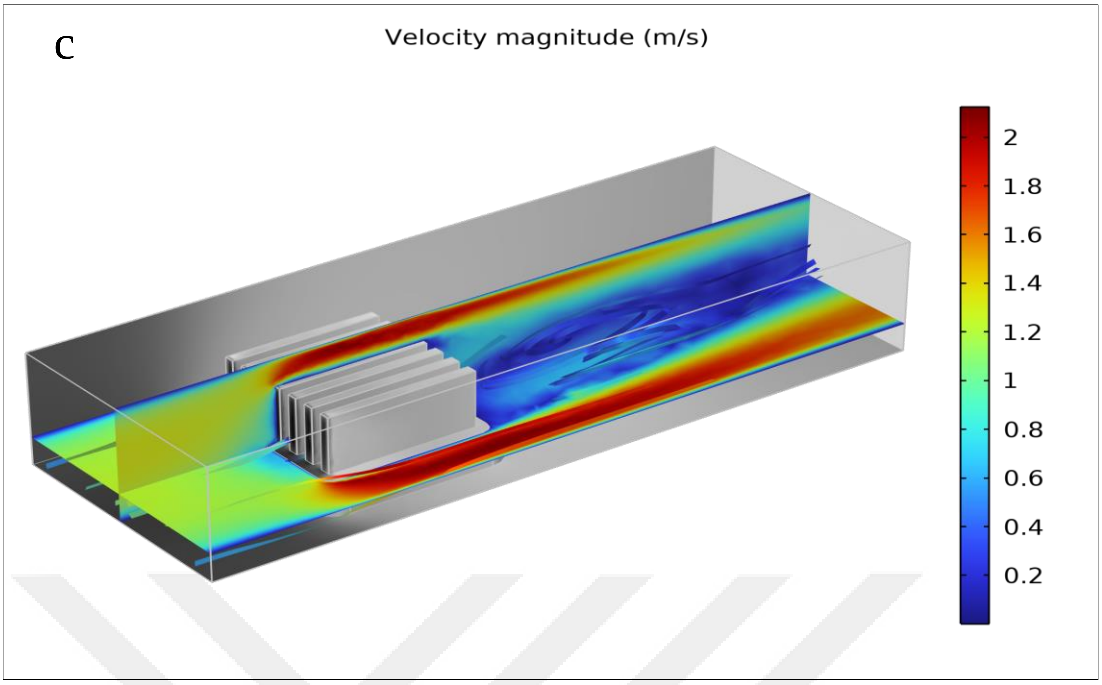
c
Velocity magnitude (m/s)
2
1.8
1.6
1.4
1.2
1
0.8
0.6
0.4
0.2

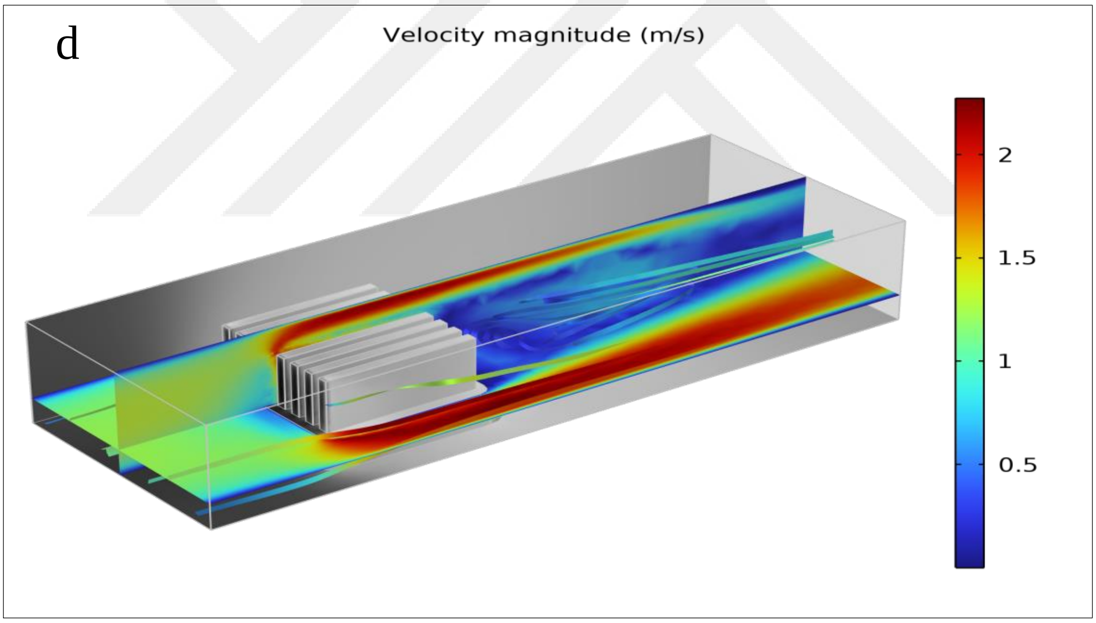
d
Velocity magnitude (m/s)
2
1.5
1
0.5

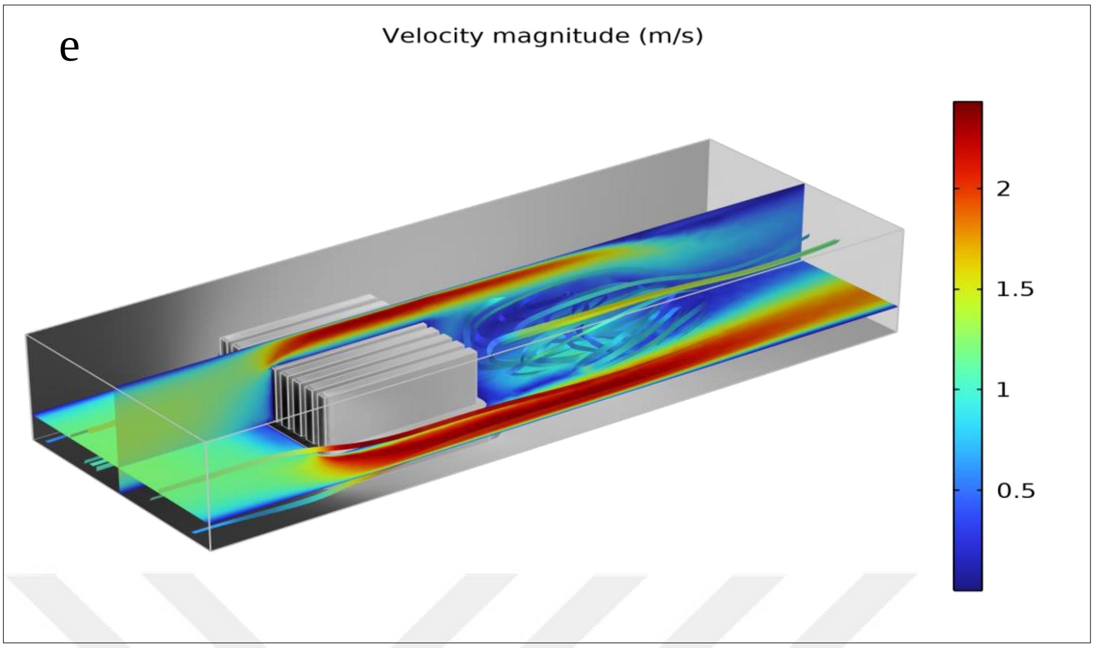

Figure 4.3. Velocity Profiles of Heat Sink With Multiple Fin Numbers (a= 5 fins, b=6 fins, c=7 fins, d=8 fins, and e=9 fins).

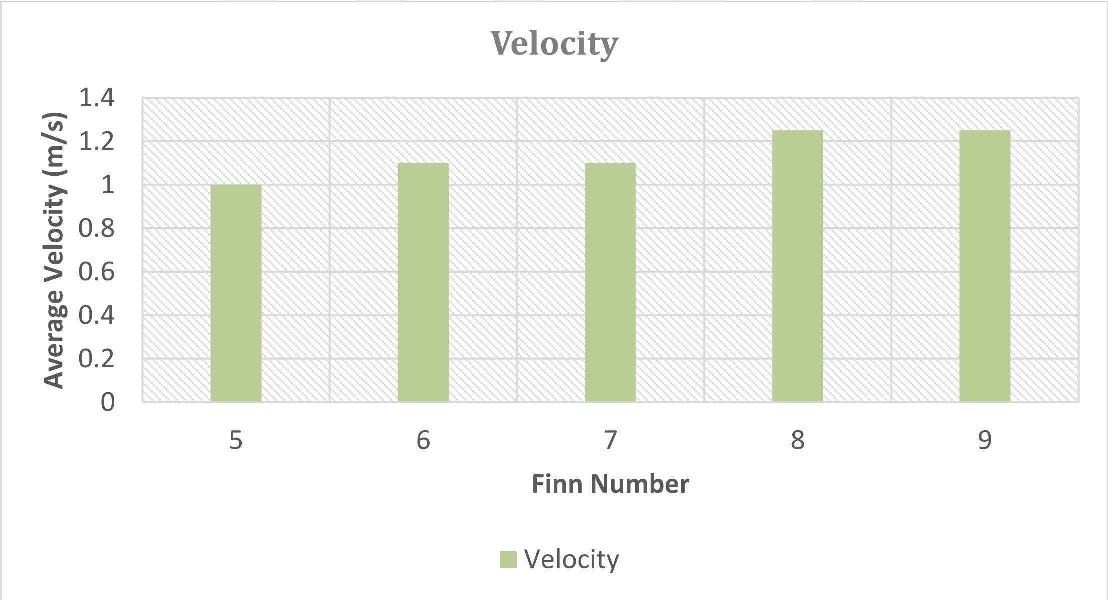

Figure 4.4. The Effect of Fins Number on Average Velocity in Immersion Cooling System.

4.1.3 Effect of Fines Number on Pressure

Figure 4.5 shows that the pressure value and variation of pressure was changed based on fins number, when using 5 fins the highest pressure value was 2 Pa and lowest value was -0.5 Pa. Increasing fins number to 6 and 7 lead to increase the pressure variation value along with increasing the highest pressure value with similar lowest pressure value, while increasing the fins number to 8 fins lead to increase the highest pressure value without any change on the lowest one that resulting in increasing the average pressure value as shown in Figure 8. Schmidt et al. [118] made allowances for the pressure fluctuations that occurred in the under-floor area, but they utilized a depth-averaged model in order to reduce the complexity of the issue from three dimensions to two dimensions. It was proved that there was a good agreement with the measurements for the examples that they looked at. On the other hand, more recent research has demonstrated that the depth-averaged model is sufficient to use when the height of the elevated floor is quite modest (normally less then 0.15 m or 6 in.). Floor heights in data centers typically vary between 0.3 and 0.75 meters in practicality. As a consequence of this, even this simplification cannot be accepted, and one is required to carry out the whole calculation in all three dimensions.

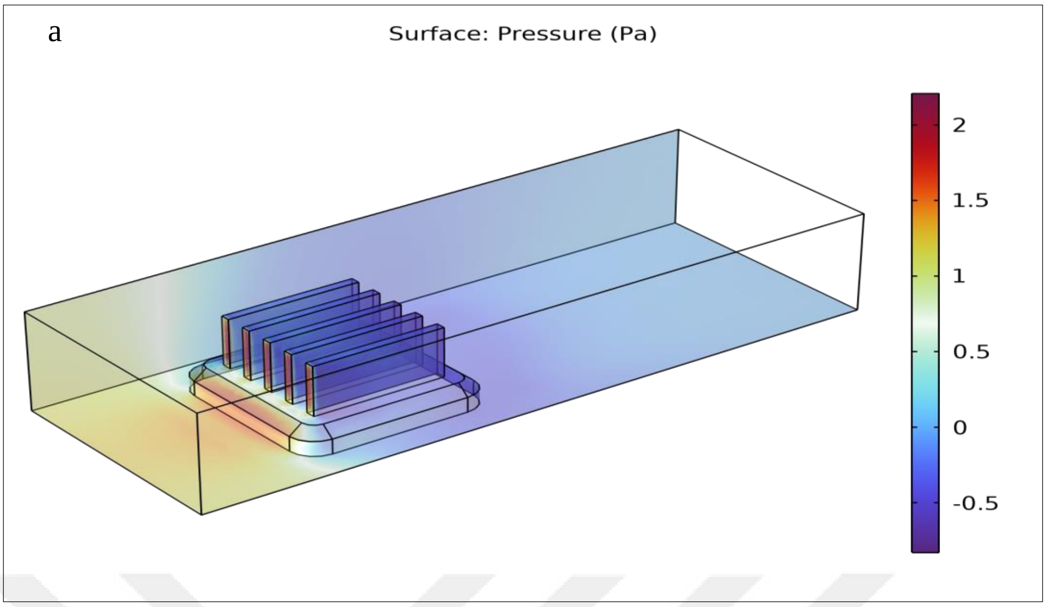
a
Surface: Pressure (Pa)
2
1.5
1
0.5
0
-0.5

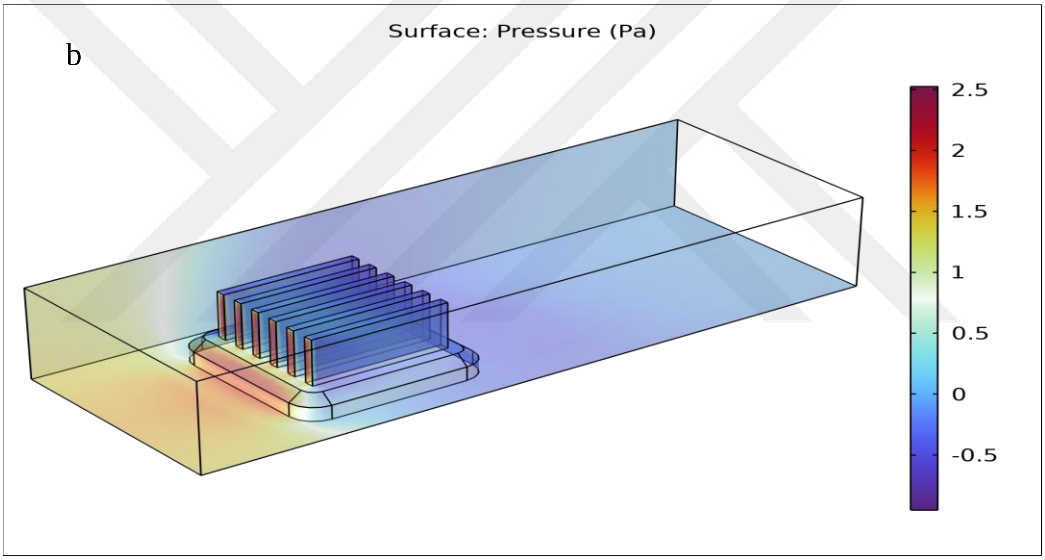
b
Surface: Pressure (Pa)
2.5
2
1.5
1
0.5
0
-0.5

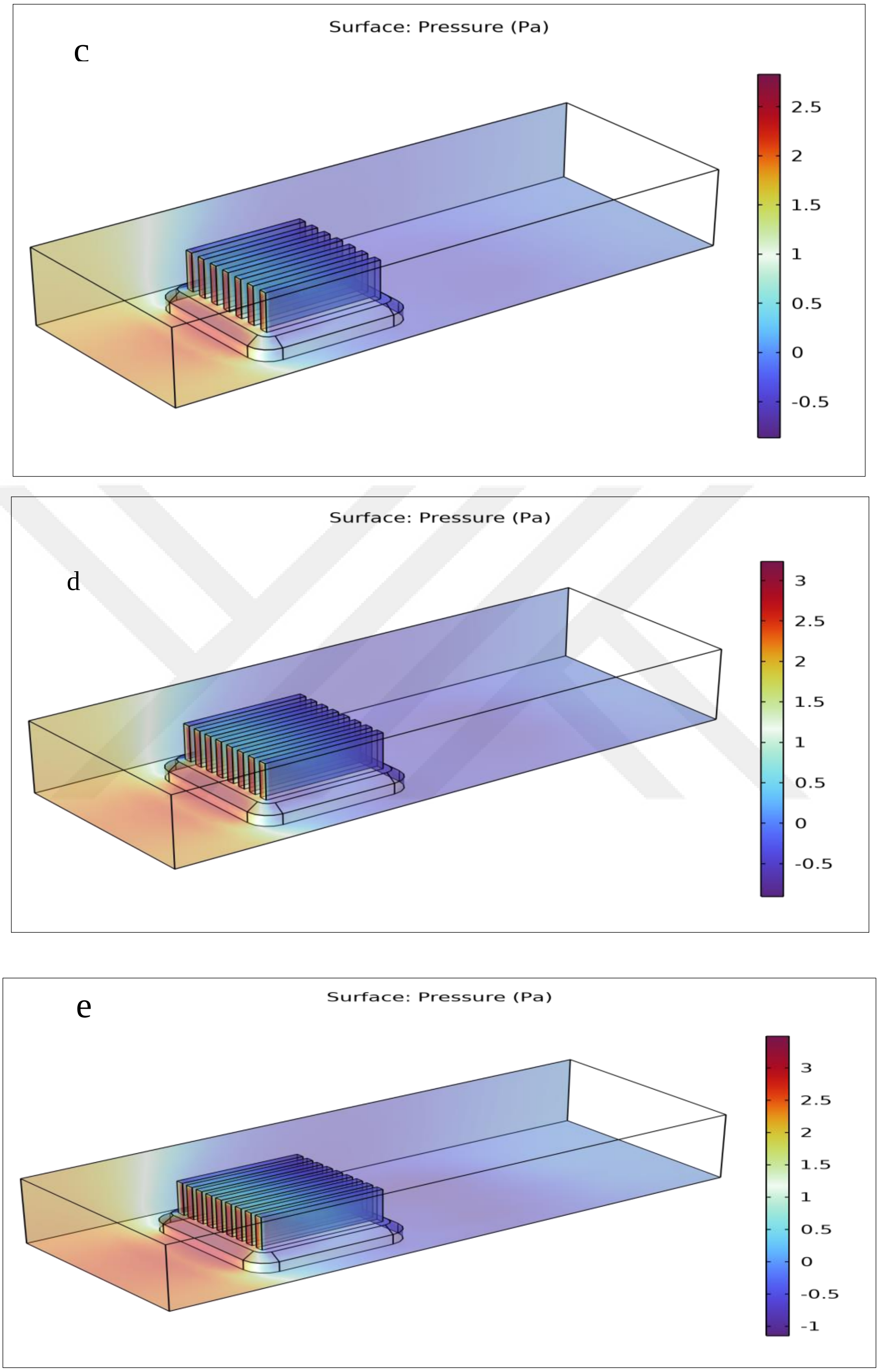

Figure 4.5. Pressure Profiles of Heat Sink With Multiple Fin Numbers (a= 5 fins, b=6 fins, c=7 fins, d=8 fins, and e=9 fins).

The hotter inside air from the data center travels thru the wheel to heat the pathway (several special corrugated Metal substance) of the wheel, whereas the hotter path is then gradually rotated to the outdoor side to give up heat to the cooler air, thereby decreasing the temp of the passage appropriately. In order to flow air over the wheel, several high-volume, low-pressure fans that are both efficient and effective are deployed. This design has the capability of including an internal DX system with numerous cooling phases in order to accommodate hot ambient temperatures. Nevertheless, in order to maintain their efficiency, air-to-air heat exchangers and heat wheels need to be cleaned or replaced on a regular basis. This is due to the fact that over time, significant amounts of pollutants that are present in the air that is transferred thru the heat exchanger may accumulate, hence reducing the heating exchangers efficiency [119]. Based on Figure 4.6 model with five fins records the lowest pressure, therefore it is mostly the most efficient case.

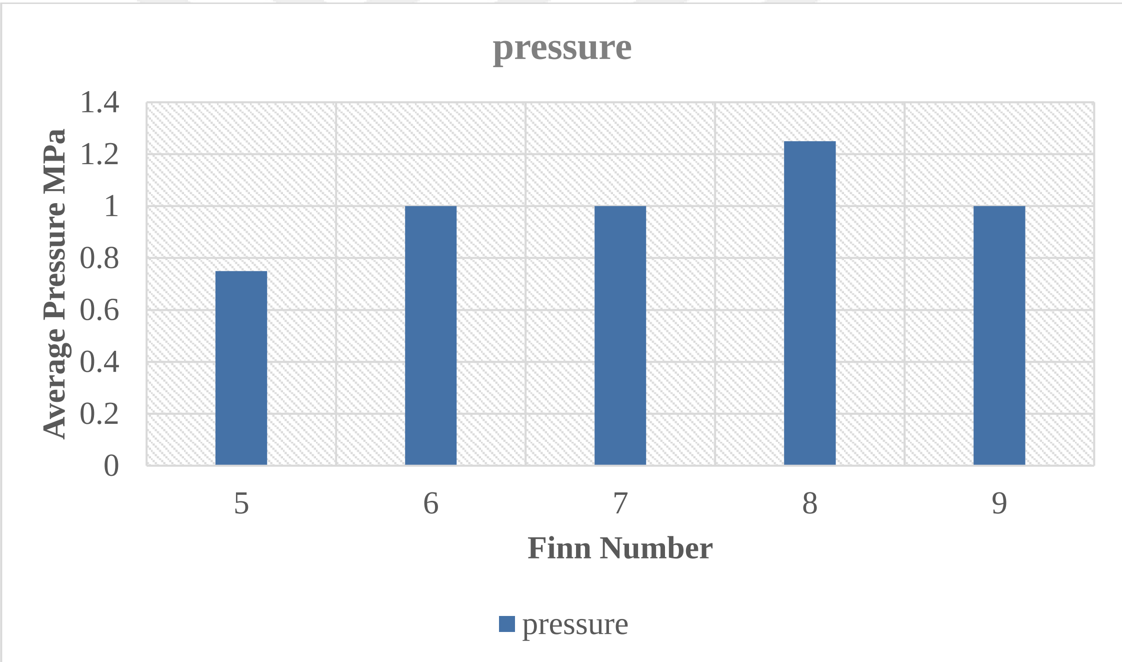

Figure 4.6. The Effect of Fins Number on Average Pressure in Immersion Cooling System.

Table 4.1: Summary of Obtained Results.

Number of Fins = 5	
Dissipated Power	6.311 W
Pressure drop	1.121 Pa
Number of Fins = 6	
Dissipated Power	7.0275 W
Pressure drop	1.3859 Pa
Number of Fins = 7	
Dissipated Power	7.5239 W
Pressure drop	1.757 Pa
Number of Fins = 8	
Dissipated Power	7.5334 W
Pressure drop	2.1011 Pa
Number of Fins = 9	
Dissipated Power	7.1887 W
Pressure drop	2.3696Pa

Figure 4.7 show relationship between dissipated power and pressure drop for different fins number. Increasing the fins number lead to increase the dissipated power and the highest power dissipation has been obtained when using 7 and 8 fins number. While increasing the pressure drop is compatible with increasing the fins number.

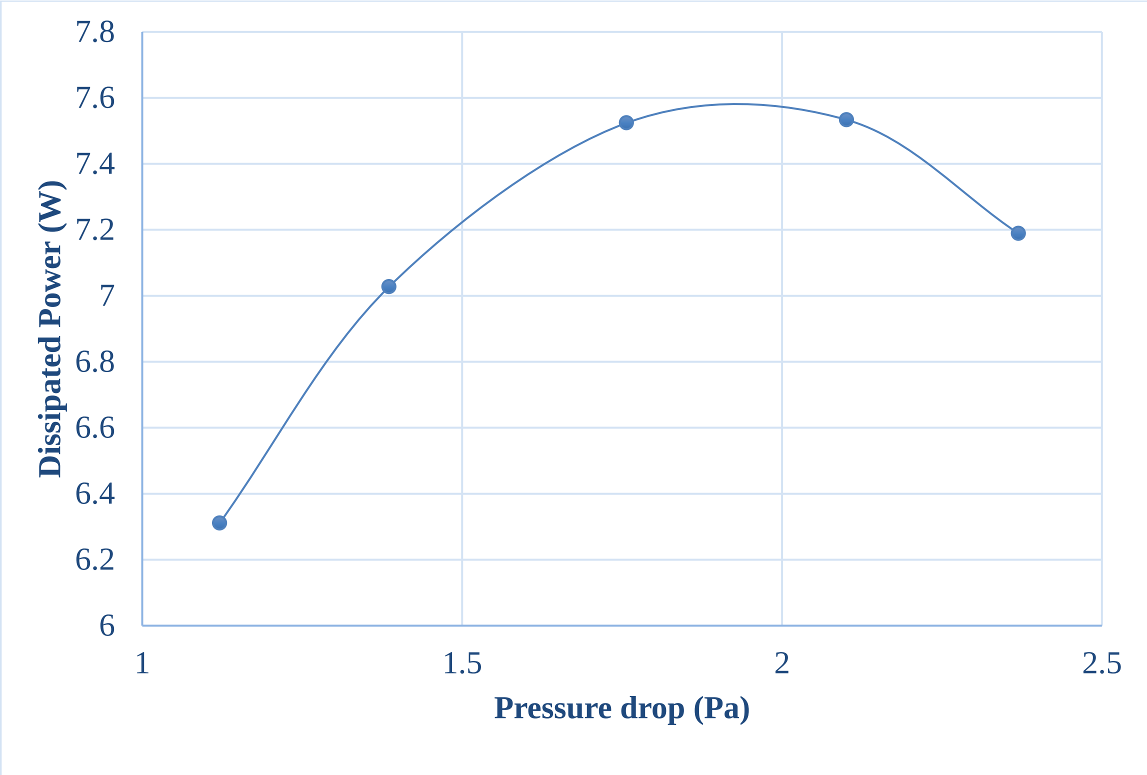

Figure 4.7. The Relationship Between Dissipated Power and Pressure Drop for Different Fins Number.

4.2 ANSYS

The using of ANSYS software program is to compare the obtained results from COMSUL software with ANSYS results.

4.2.1 Effect of Fins Number on Temperature of Heating Sink

Figures 4.8-4.12 shows the temperature contour for each case with different temperatures values that obtained from ANSYS software that cases differs in fins number first case with five fins and case five with nine fins.

The temperature and velocity contours at the horizontal center plane of the server demonstrate that there are larger velocities of fluid over the serve in the case where there is no bypass of fluid. This leads to enhanced forced convection, which in turn results in lower temps of the server when compared to the case where there is bypass of fluid.

Both the performance of the system with dielectric fluids and the performance of both configurations are improved by the fans. A more substantial improvement is achieved by simultaneously lowering the temperature and the thermal resistance. As comparison to when there is no fan present, the thermal resistance of the system and the temperature of the server drop by about 9.3 and 3.8%, respectively, when there are two fans present [120].

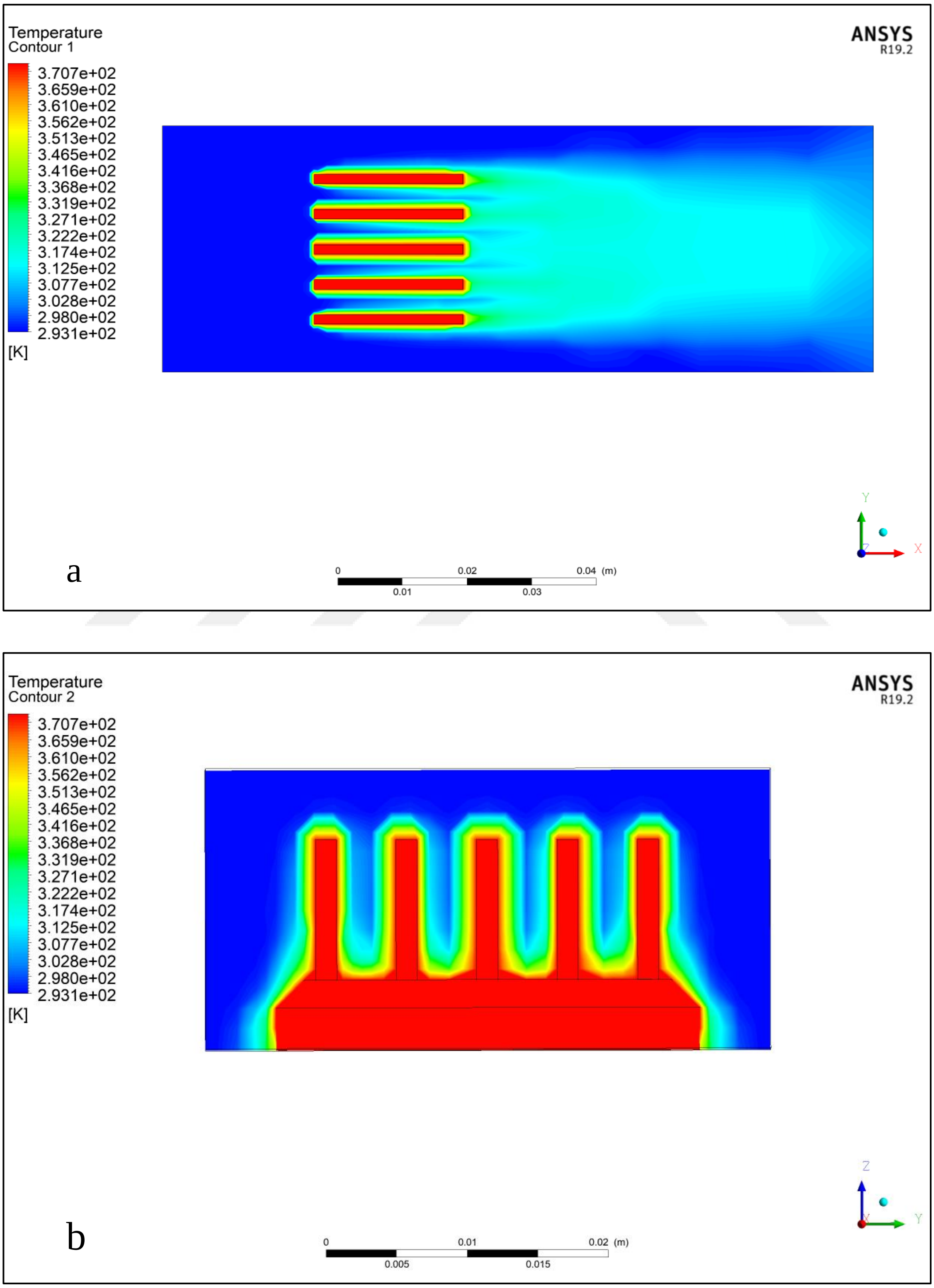

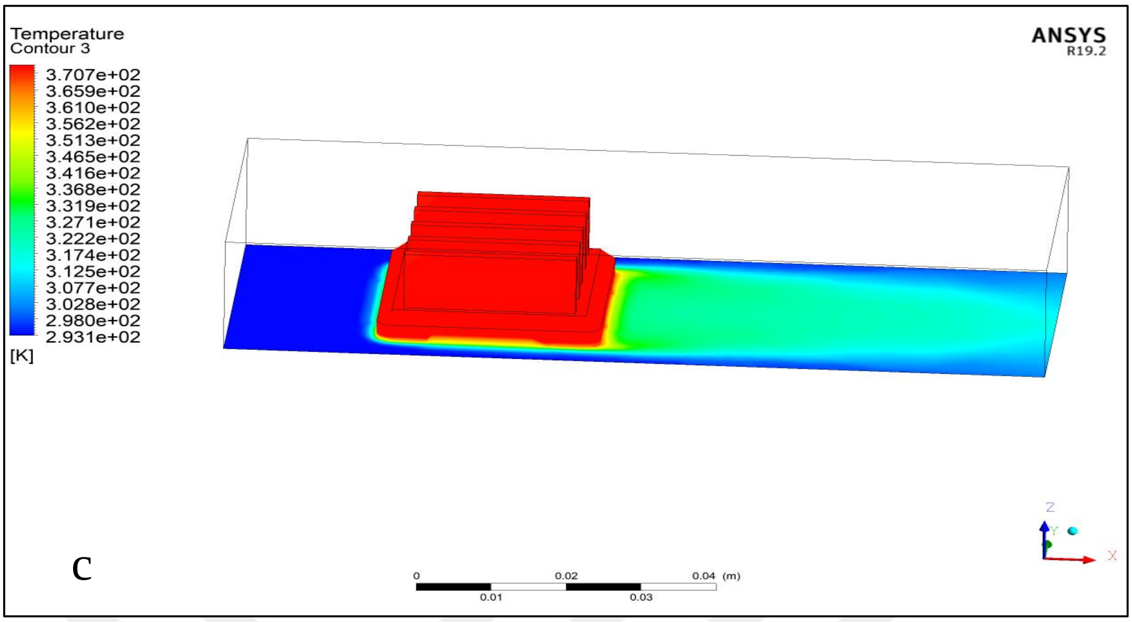

Figure 4.8: Temperature profiles of Heat sink with f**ive** fin numbers (a) top view; b) Temperature contour along the wall and heat sink and c) overview).

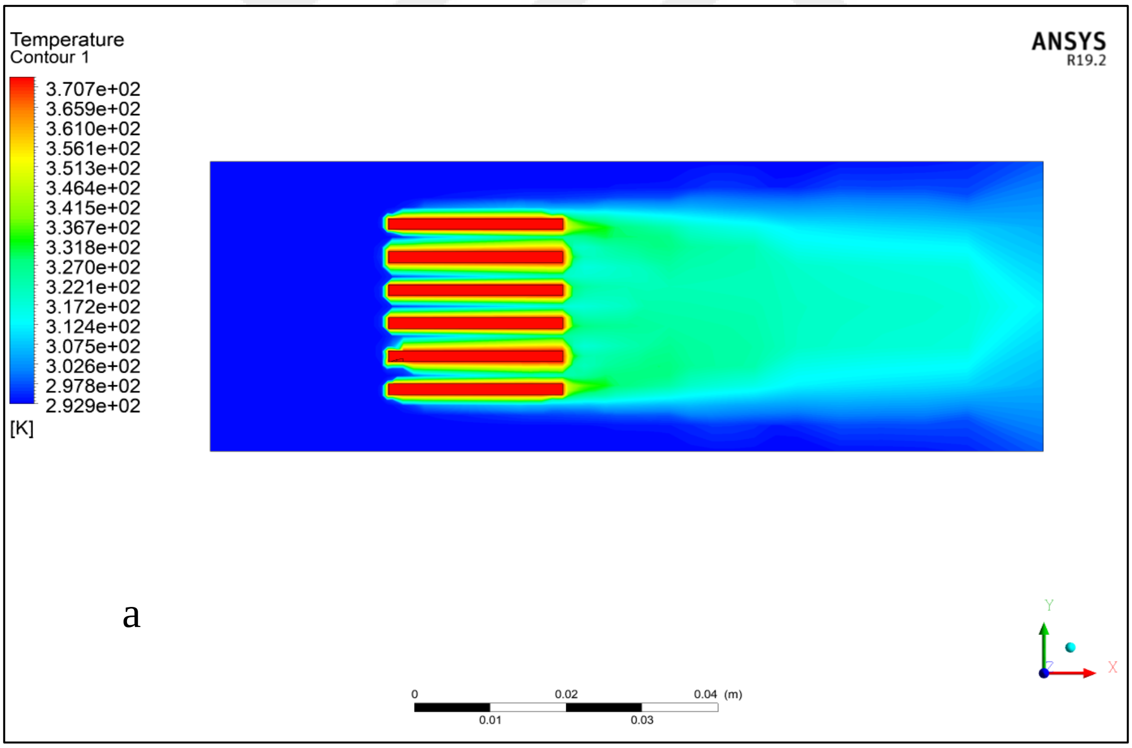

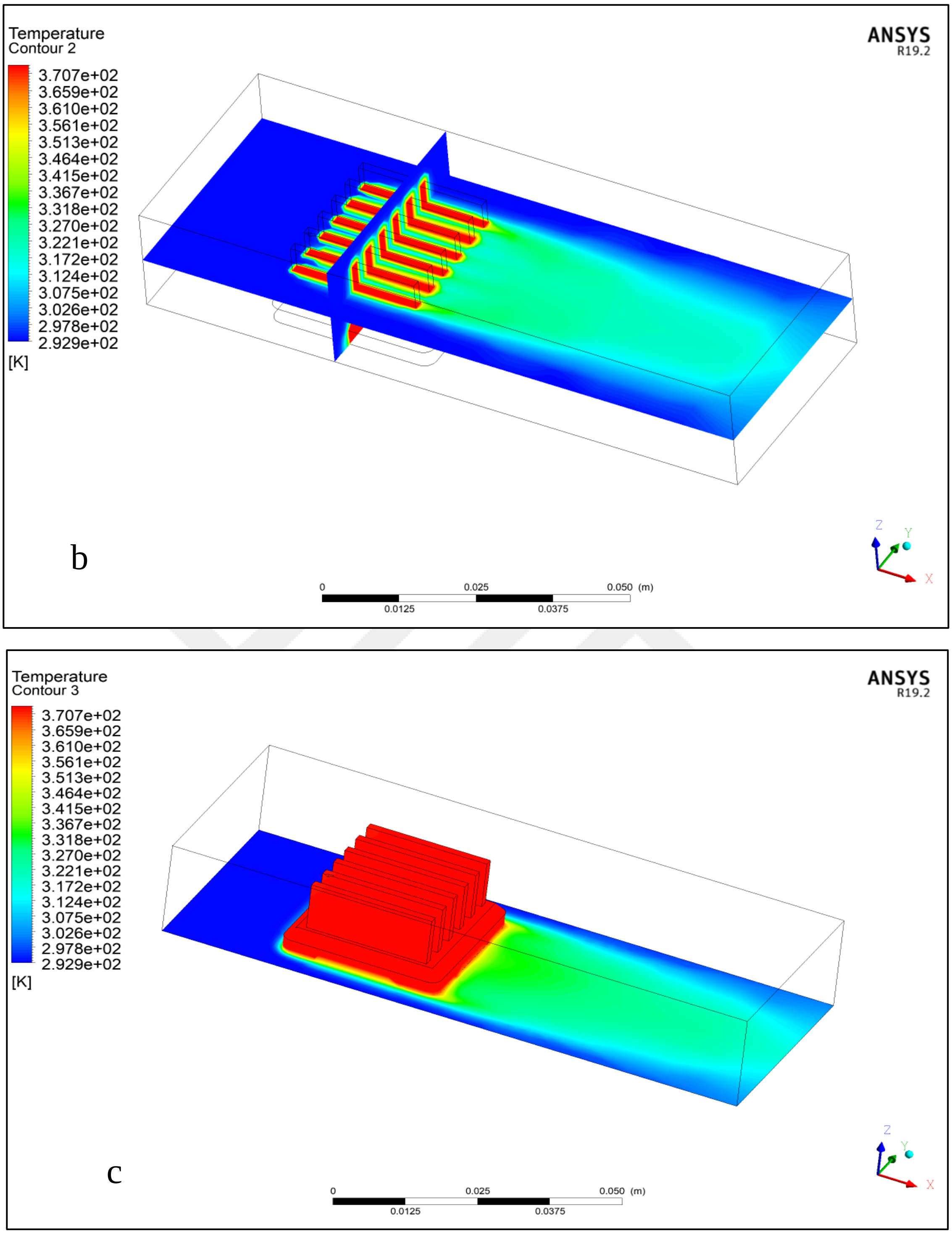

Figure 4.9: Temperature Profiles of Heat Sink With Six Fin Numbers (A) Top View; B) Heat Sink Bottom Side and c) Overview).

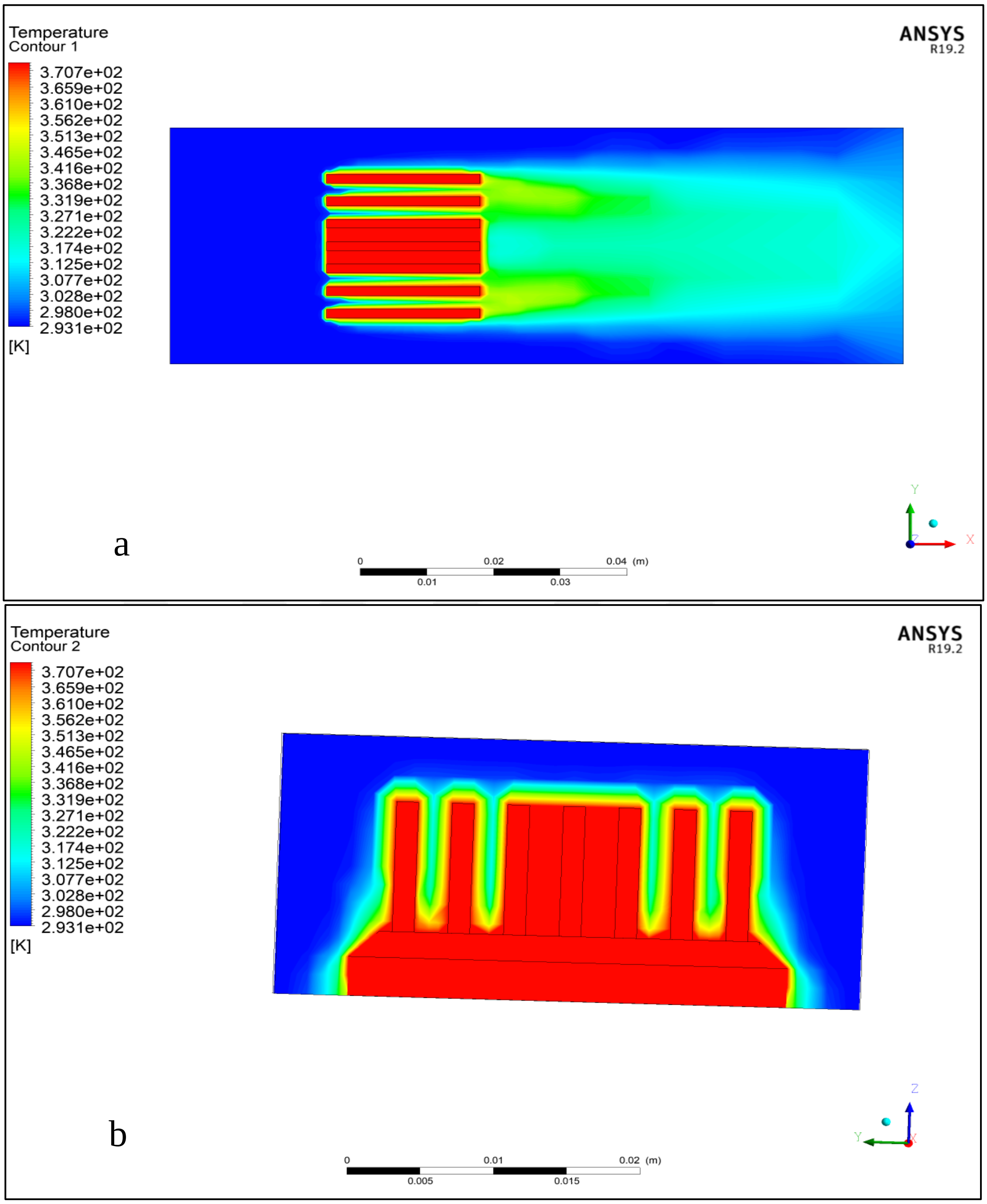
Temperature
Contour 1
3.707e+02
3.659e+02
3.610e+02
3.562e+02
3.513e+02
3.465e+02
3.416e+02
3.368e+02
3.319e+02
3.271e+02
3.222e+02
3.174e+02
3.125e+02
3.077e+02
3.028e+02
2.980e+02
2.931e+02
[K]
ANSYS
R19.2
a
0
0.01
0.02
0.03
0.04 (m)
Temperature
Contour 2
3.707e+02
3.659e+02
3.610e+02
3.562e+02
3.513e+02
3.465e+02
3.416e+02
3.368e+02
3.319e+02
3.271e+02
3.222e+02
3.174e+02
3.125e+02
3.077e+02
3.028e+02
2.980e+02
2.931e+02
[K]
ANSYS
R19.2
b
0
0.005
0.01
0.015
0.02 (m)

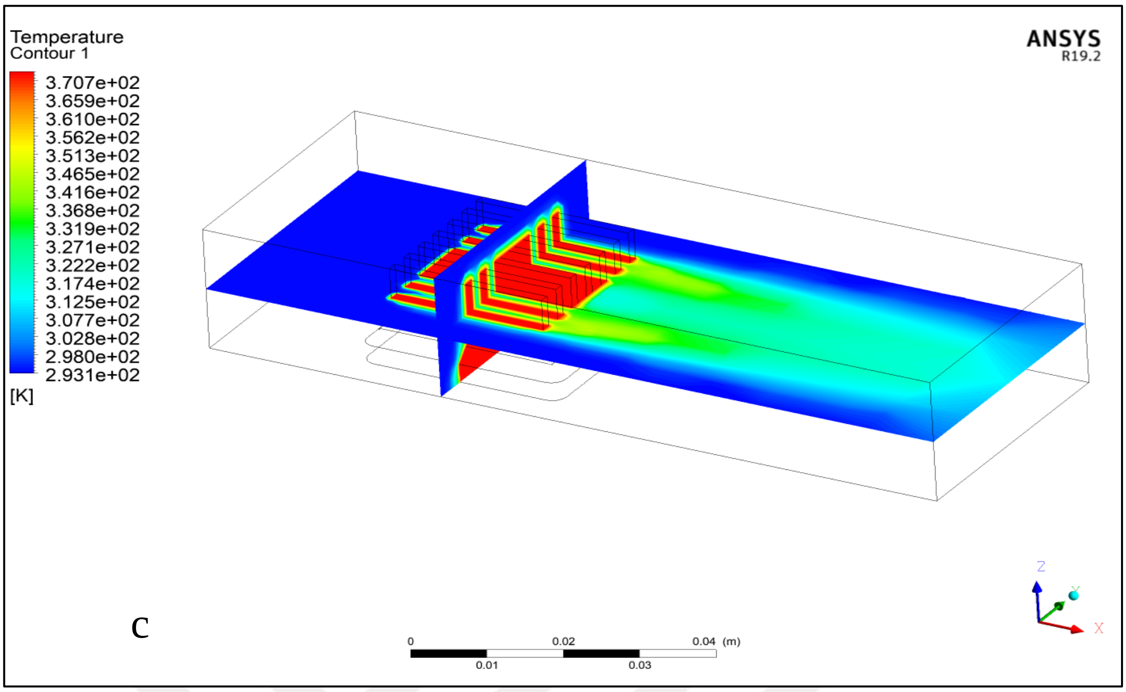
Temperature
Contour 1
3.707e+02
3.659e+02
3.610e+02
3.562e+02
3.513e+02
3.465e+02
3.416e+02
3.368e+02
3.319e+02
3.271e+02
3.222e+02
3.174e+02
3.125e+02
3.077e+02
3.028e+02
2.980e+02
2.931e+02
[K]
ANSYS
R19.2
c
0
0.02
0.04 (m)
0.01
0.03
Z
X

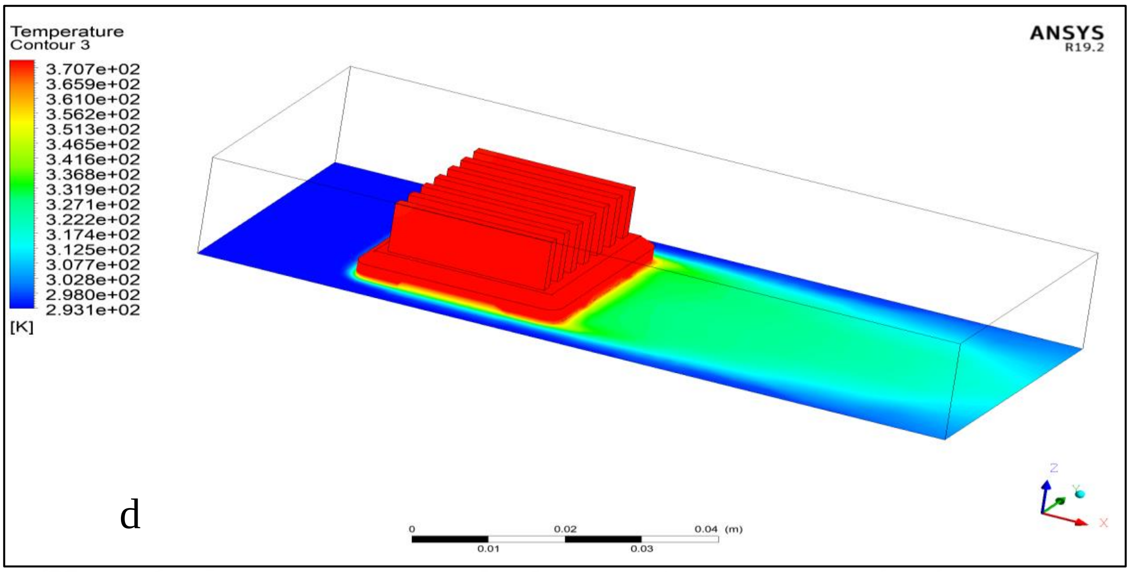

Figure 4.10: Temperature Profiles of Heat Sink With Seven Fin Numbers (A) Top View; B) Temperature Contour Along The Wall, C) Heat Sink Bottom Side and D) Overview).

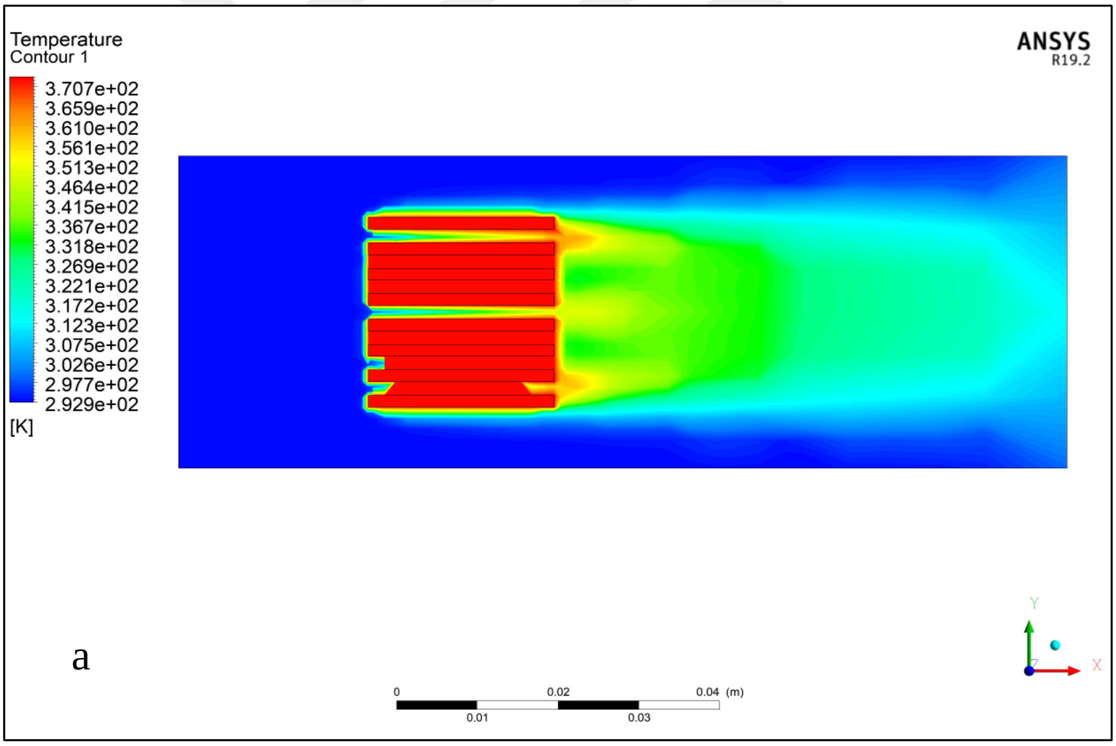

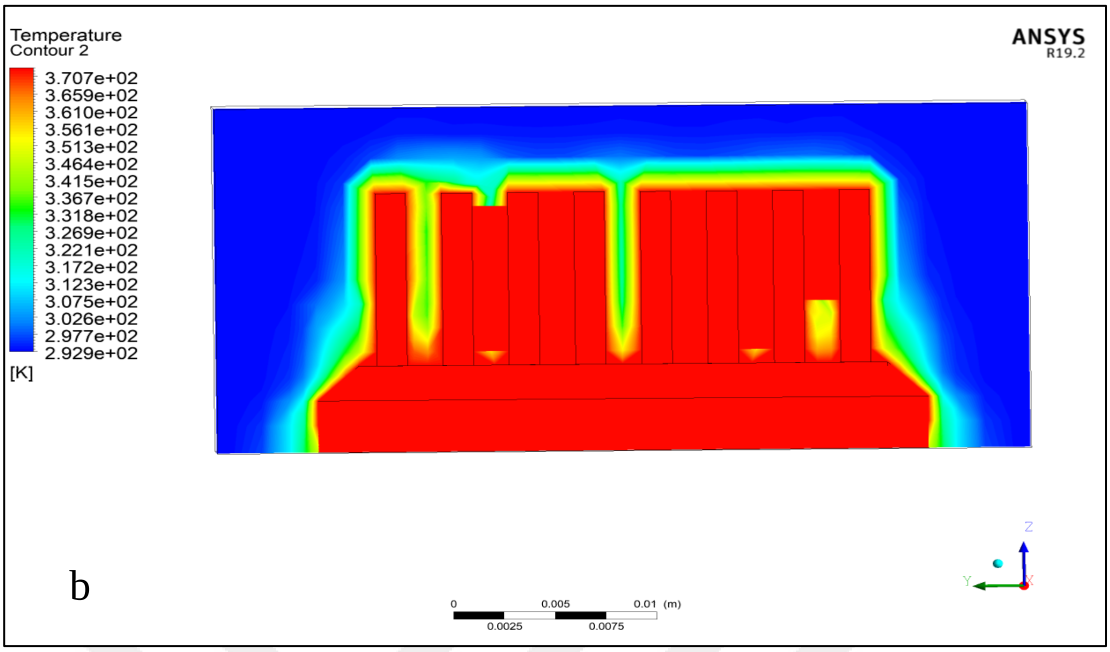
Temperature
Contour 2
3.707e+02
3.659e+02
3.610e+02
3.561e+02
3.513e+02
3.464e+02
3.415e+02
3.367e+02
3.318e+02
3.269e+02
3.221e+02
3.172e+02
3.123e+02
3.075e+02
3.026e+02
2.977e+02
2.929e+02
[K]
ANSYS
R19.2
b
0
0.005
0.01 (m)
0.0025
0.0075

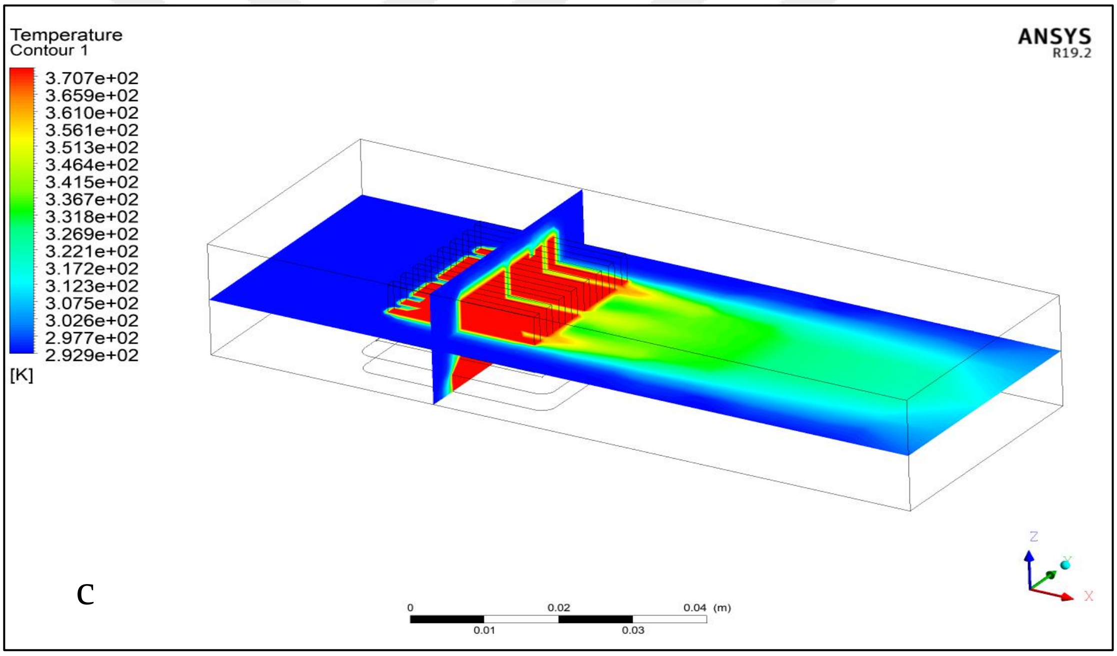
Temperature
Contour 1
3.707e+02
3.659e+02
3.610e+02
3.561e+02
3.513e+02
3.464e+02
3.415e+02
3.367e+02
3.318e+02
3.269e+02
3.221e+02
3.172e+02
3.123e+02
3.075e+02
3.026e+02
2.977e+02
2.929e+02
[K]
ANSYS
R19.2
c
0
0.02
0.04 (m)
0.01
0.03

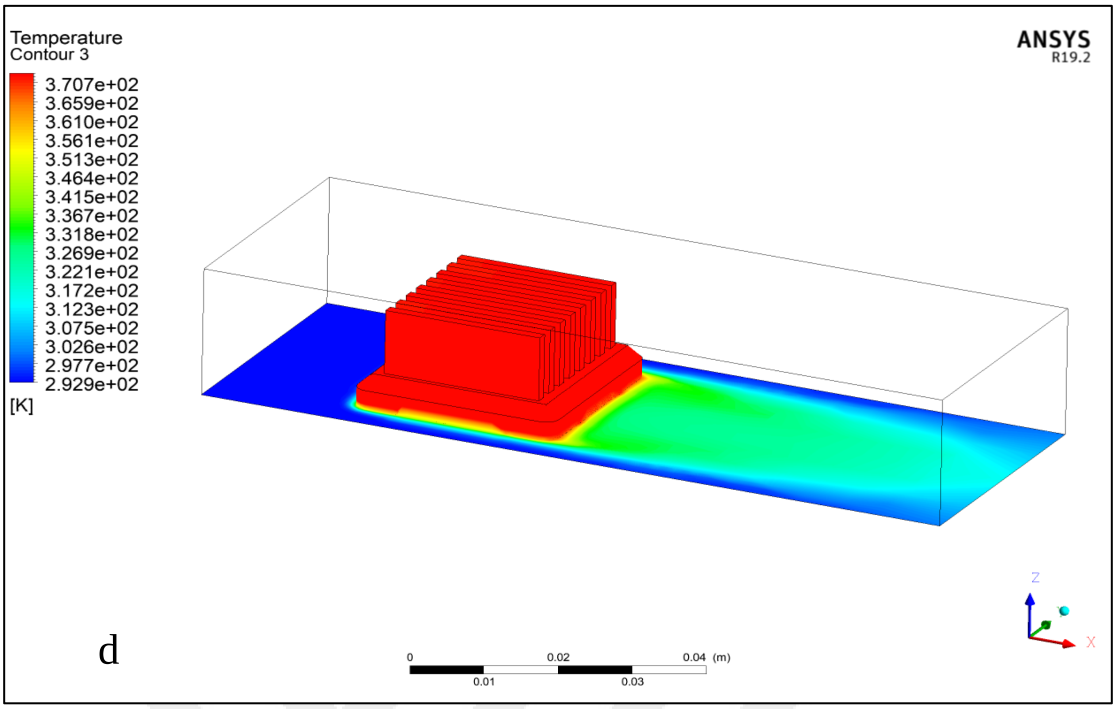

Figure 4.11: Temperature Profiles of Heat Sink With Eight Fin Numbers (A) Top View; B) Temperature Contour Along The Wall, C) Heat Sink Bottom Side and D) Overview).

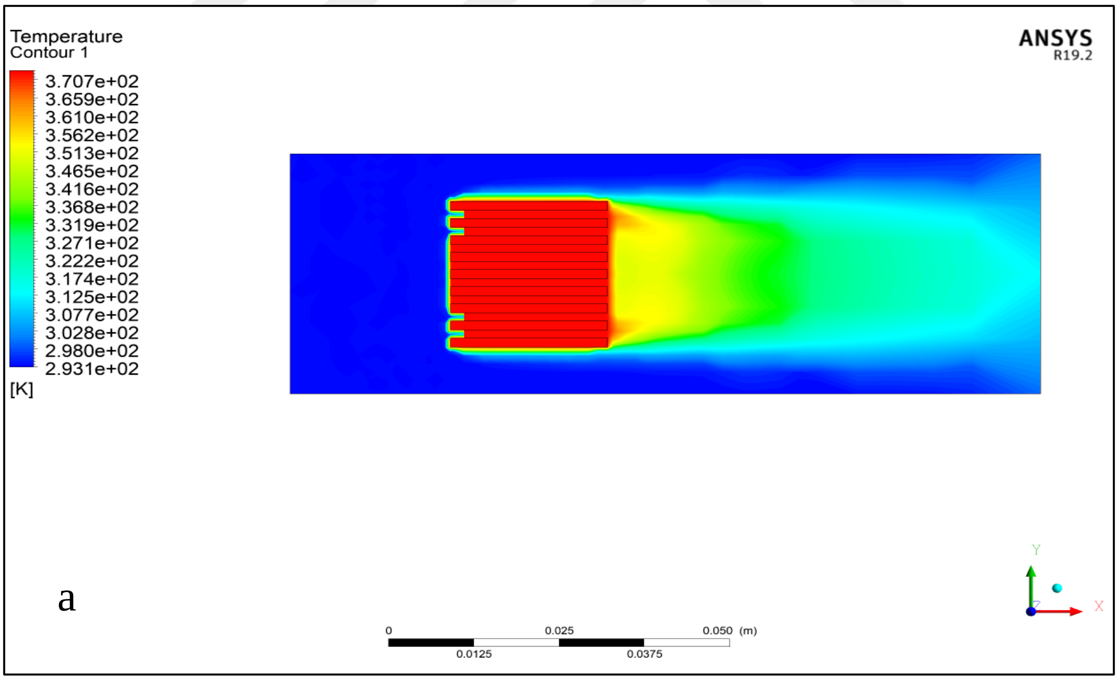

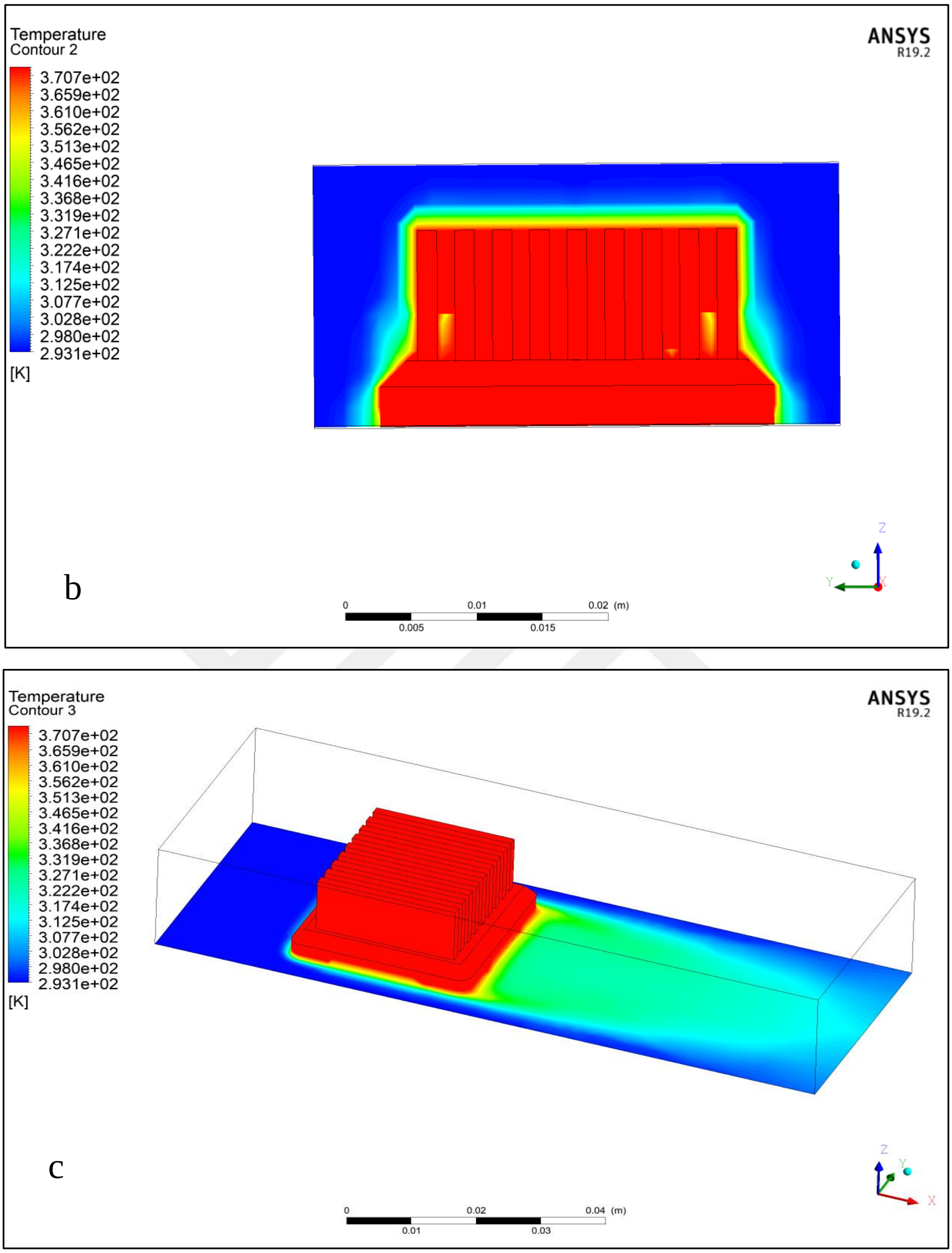

Figure 4.12: Temperature Profiles of Heat Sink With Nine Fin Numbers (A) Top View; B) Temperature Contour Along The Wall and Heat Sink and C) Overview).

Based on the obtained results demonstrated in Figures 4.13, increasing the fins number for heat sink from 5 to 6 and 8 reduce the temperature of heat sink for the system from, where the temperature in case of using 5 fins was 58.7 degree centigrade. While increasing the fins number to 7 or 9 have no significant change on temperature reduction, the outlet temperature reduced to be 58.65 degree centigrade when use 6 and 8 fins. The lowest temperature of the outlet heat sink is 19.95 degree centigrade when using 5, 7 and 9 fins and the lowest heat sink temperature reduced to be 19.75 degree centigrade when use 6 or 8 fins number. The amount of power that is used by the CPU is highly reliant on the temp and is an essential design component. This is shown by the number of studies that examine logic design and alternative implementations to restrict hotspots in order to decrease caused by thermal leakage [121]–[123]. Temp is the primary factor that determines the amount of leakage, although it has only a marginal impact on the dynamic power of the CPU. In earlier generations of central processing units, such as 0.35-to-0.18-micron technologies, the leakage accounted for only a small portion of the total power. However, due to the continued shrinking of geometries in the silicon, which shortens the paths along which leakage can occur, the leakage has increased to the point where it can account for as much as fifty percent [124], thirteen percent of the total power. The designers of CPUs now face the problem of maintaining leaking at or below the 50% limit despite ever-decreasing geometries in their designs.

The obtained results from ANSYS software is differing from the COMSUL software, in spite of ANSYS results give higher senility to temperature, the effect of fins number on temperature is more clear in ANSYS software, therefore, the author suggest that using COMSUL software to investigate the effect on design on CFD and ANSYS software is used to get more reasonable results based on Kepekci and Asma [125] the geometry of the fins is more effective than the materials of the fins itself.

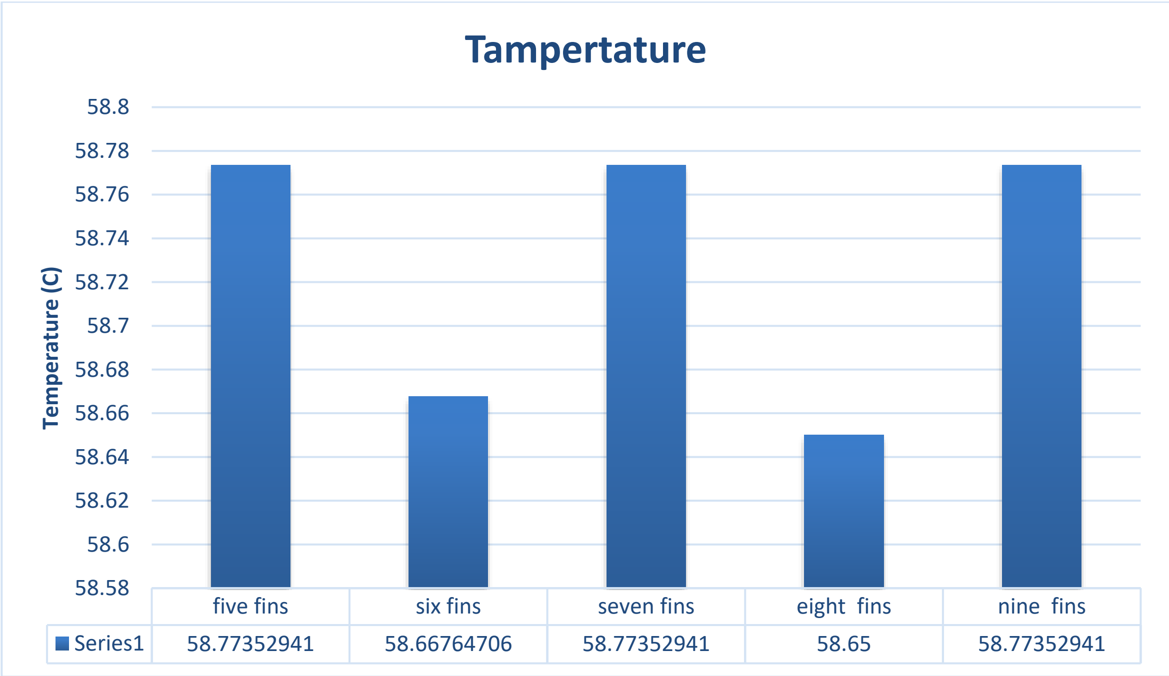

Figure 4.13: Effect of Fins Number on Temperature.

4.2.2 Effect of Fins Number on Velocity

Figures 4.14-4.18 shows the velocity contour for each case with different temperatures values that obtained from ANSYS software that cases differs in fins number first case with five fins and case five with nine fins. Based on figures below the fins number very effective on velocity distribution.

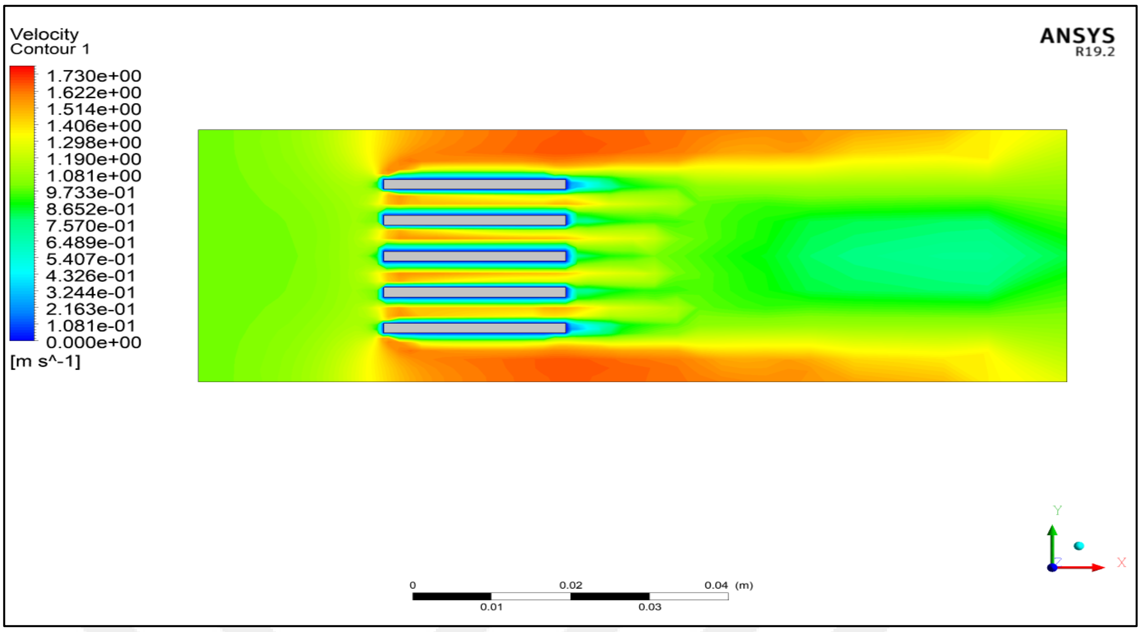
Velocity
Contour 1
1.730e+00
1.622e+00
1.514e+00
1.406e+00
1.298e+00
1.190e+00
1.081e+00
9.733e-01
8.652e-01
7.570e-01
6.489e-01
5.407e-01
4.326e-01
3.244e-01
2.163e-01
1.081e-01
0.000e+00
[m s^-1]
ANSYS
R19.2
0
0.01
0.02
0.03
0.04 (m)
Y
X

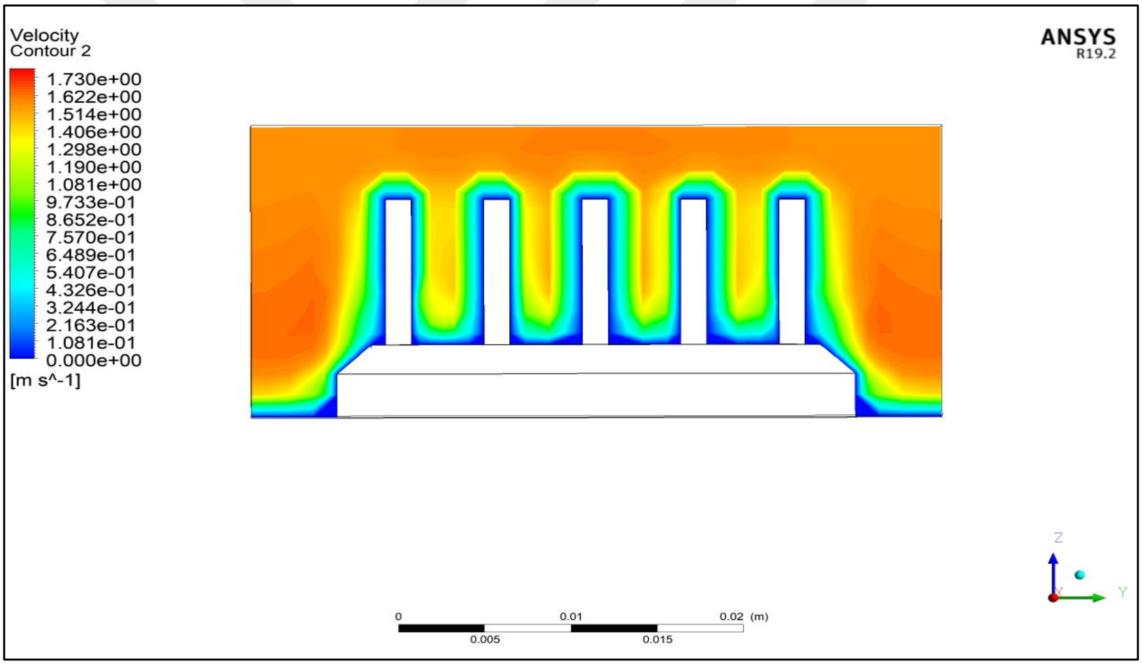
Velocity
Contour 2
1.730e+00
1.622e+00
1.514e+00
1.406e+00
1.298e+00
1.190e+00
1.081e+00
9.733e-01
8.652e-01
7.570e-01
6.489e-01
5.407e-01
4.326e-01
3.244e-01
2.163e-01
1.081e-01
0.000e+00
[m s^-1]
ANSYS
R19.2
0
0.005
0.01
0.015
0.02 (m)
Z
Y

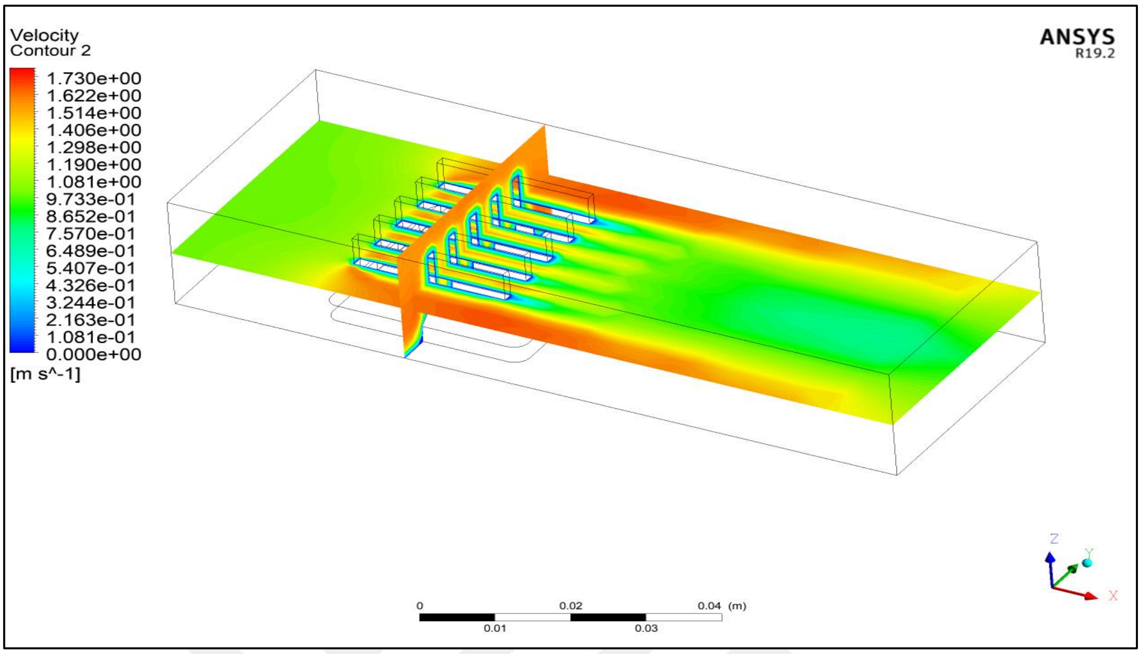

Figure 4.14: Velocity Profiles of Heat Sink With Five Fin Numbers (A) Top View; B) Velocity Contour Along The Wall and Heat Sink and C) Overview).

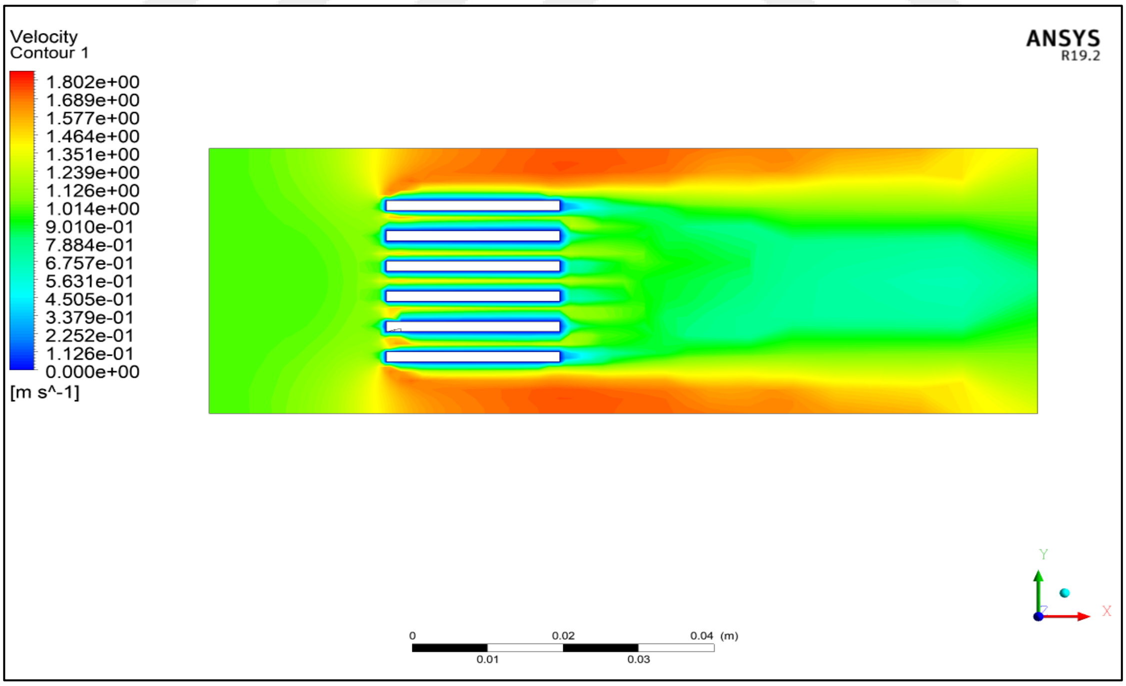

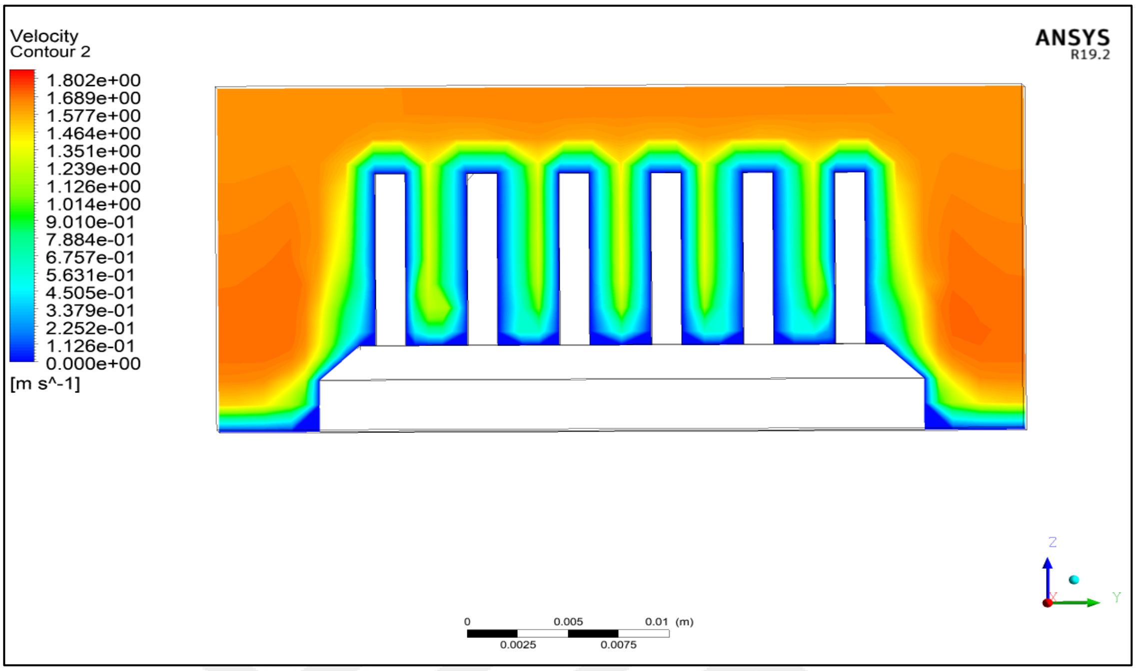

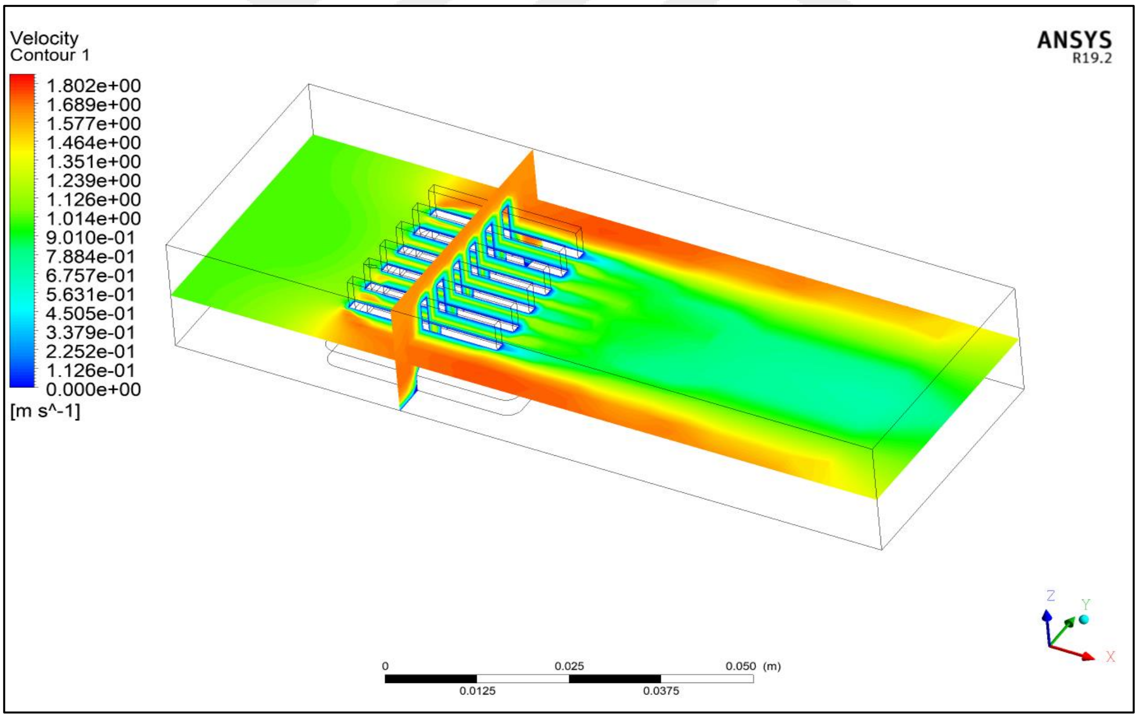

Figure 4.15: Velocity Profiles of Heat Sink With Six Fin Numbers (A) Top View; B) Velocity Contour Along The Wall and Heat Sink and C) Overview).

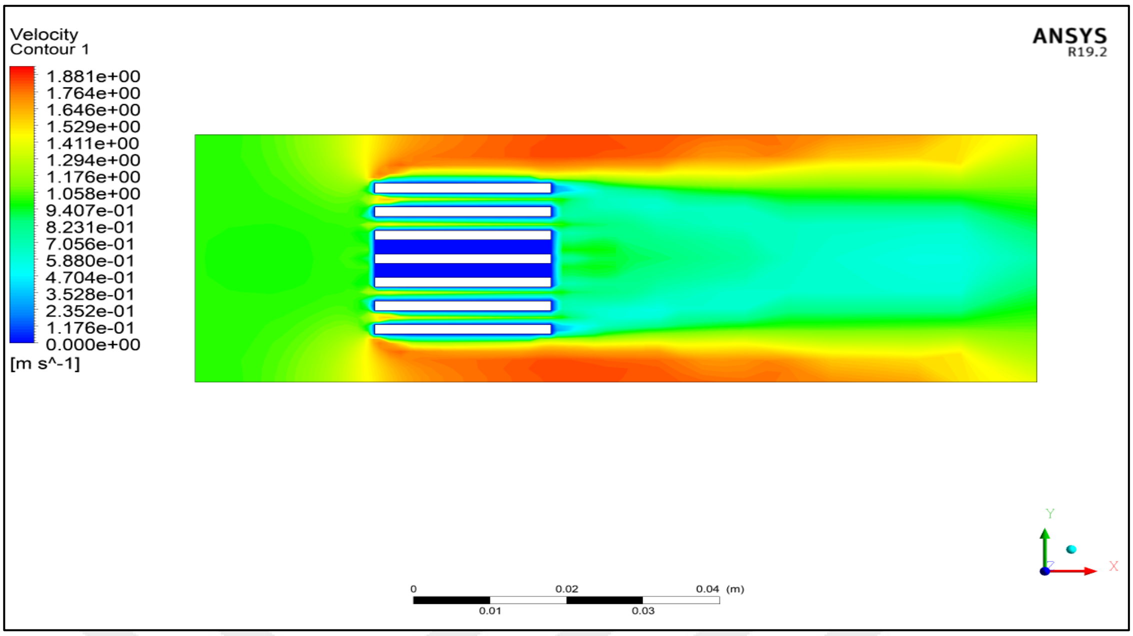
Velocity
Contour 1
1.881e+00
1.764e+00
1.646e+00
1.529e+00
1.411e+00
1.294e+00
1.176e+00
1.058e+00
9.407e-01
8.231e-01
7.056e-01
5.880e-01
4.704e-01
3.528e-01
2.352e-01
1.176e-01
0.000e+00
[m s^-1]
ANSYS
R19.2
0
0.02
0.04 (m)
0.01
0.03

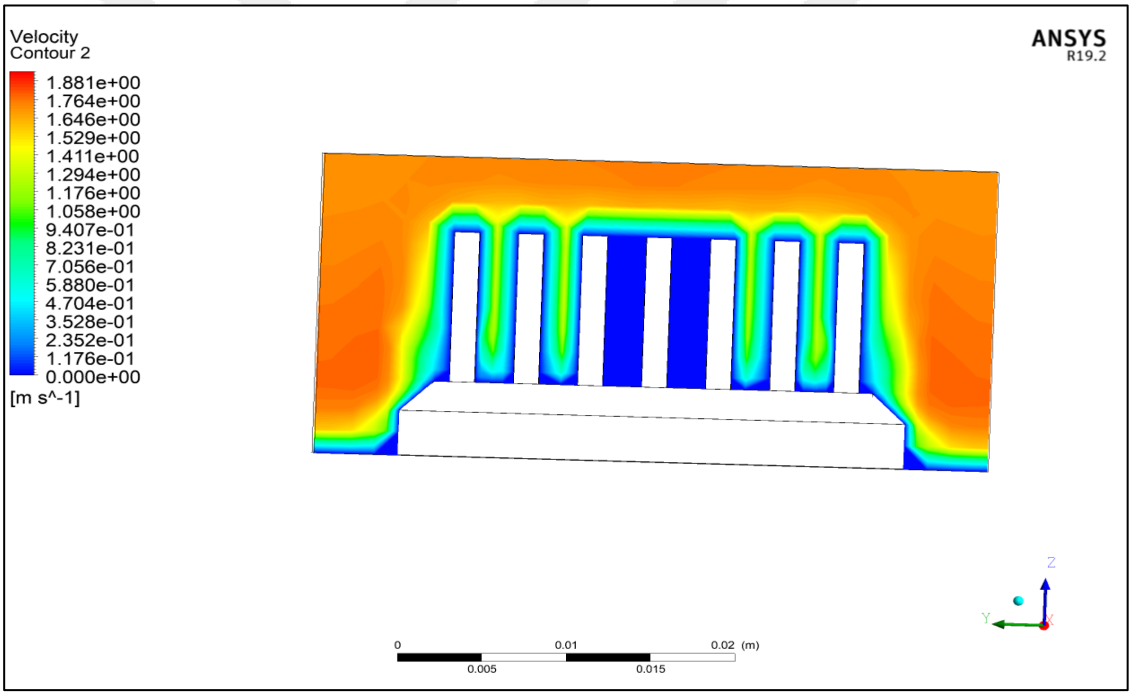
Velocity
Contour 2
1.881e+00
1.764e+00
1.646e+00
1.529e+00
1.411e+00
1.294e+00
1.176e+00
1.058e+00
9.407e-01
8.231e-01
7.056e-01
5.880e-01
4.704e-01
3.528e-01
2.352e-01
1.176e-01
0.000e+00
[m s^-1]
ANSYS
R19.2
0
0.01
0.02 (m)
0.005
0.015

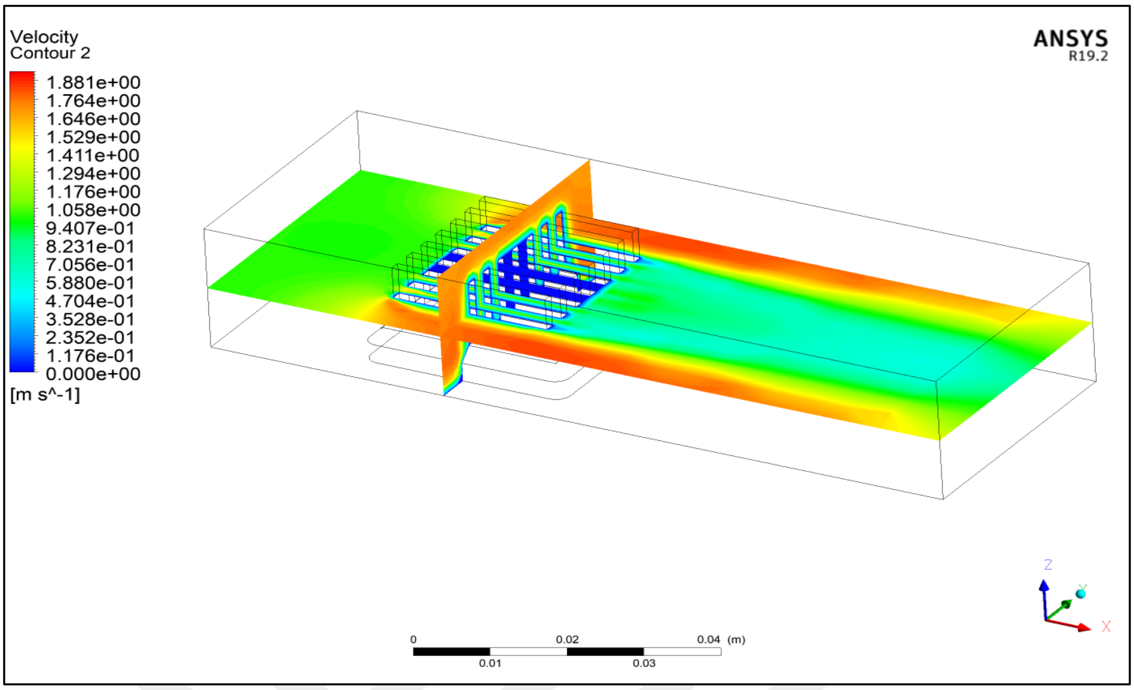

Figure 4.16: Velocity Profiles of Heat Sink With Seven Fin Numbers (A) Top View; B) Velocity Contour Along The Wall and Heat Sink and C) Overview).

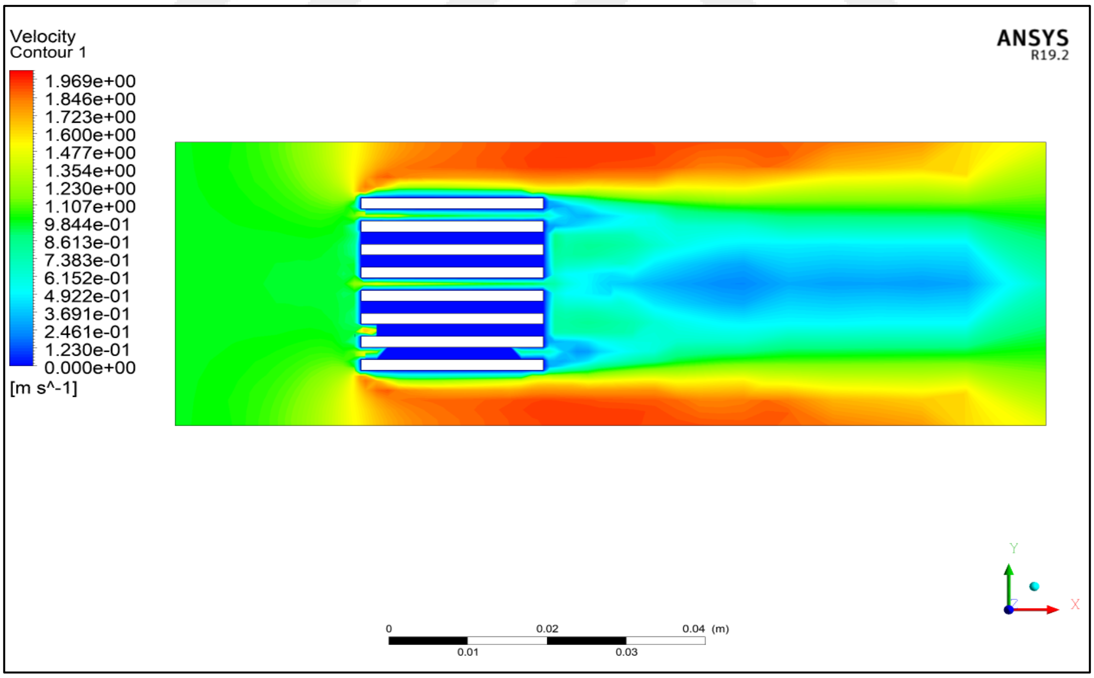

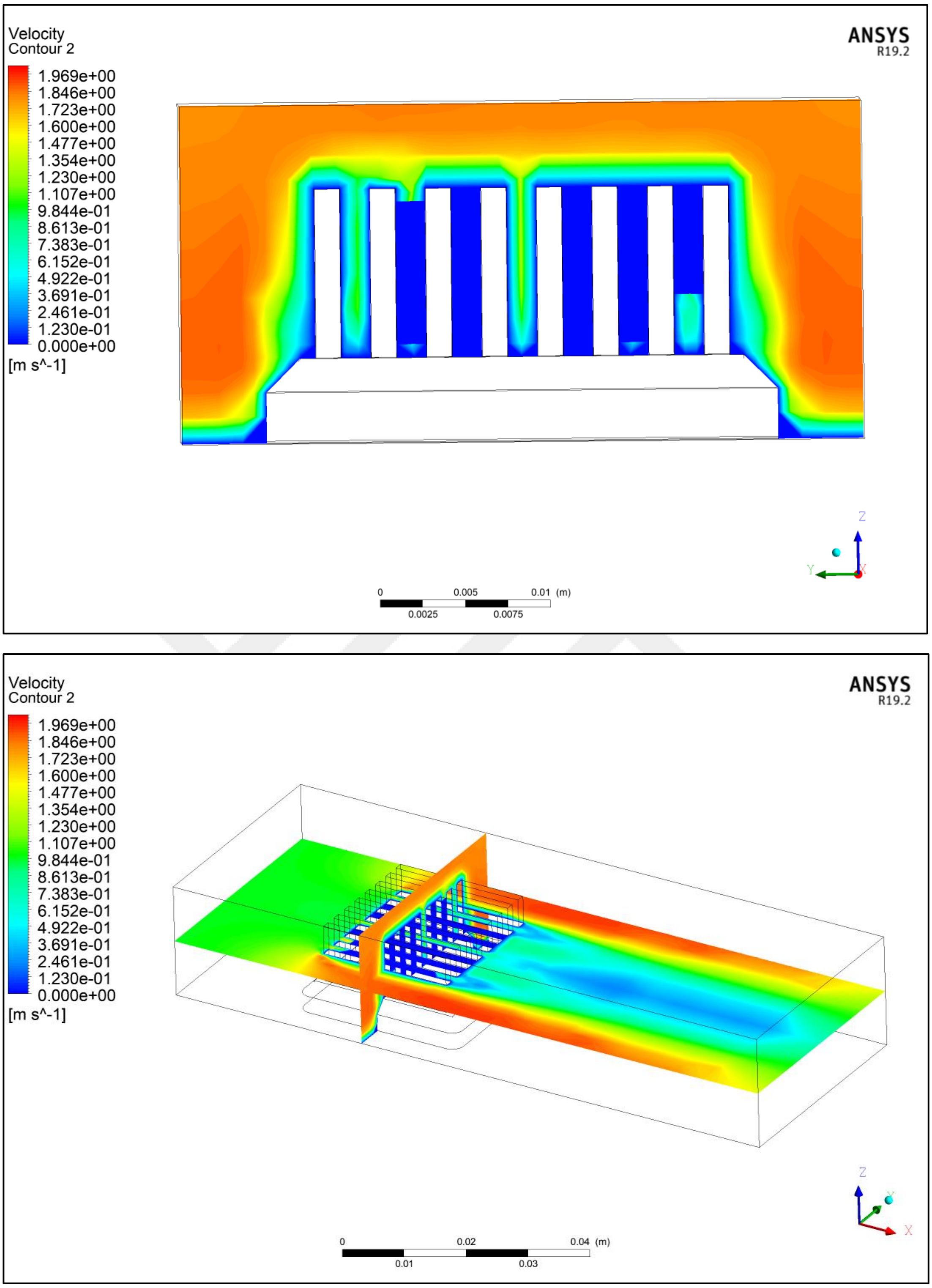

Figure 4.17: Velocity Profiles of Heat Sink With Eight Fin Numbers(A) Top View; B) Velocity Contour Along The Wall and Heat Sink and C) Overview).

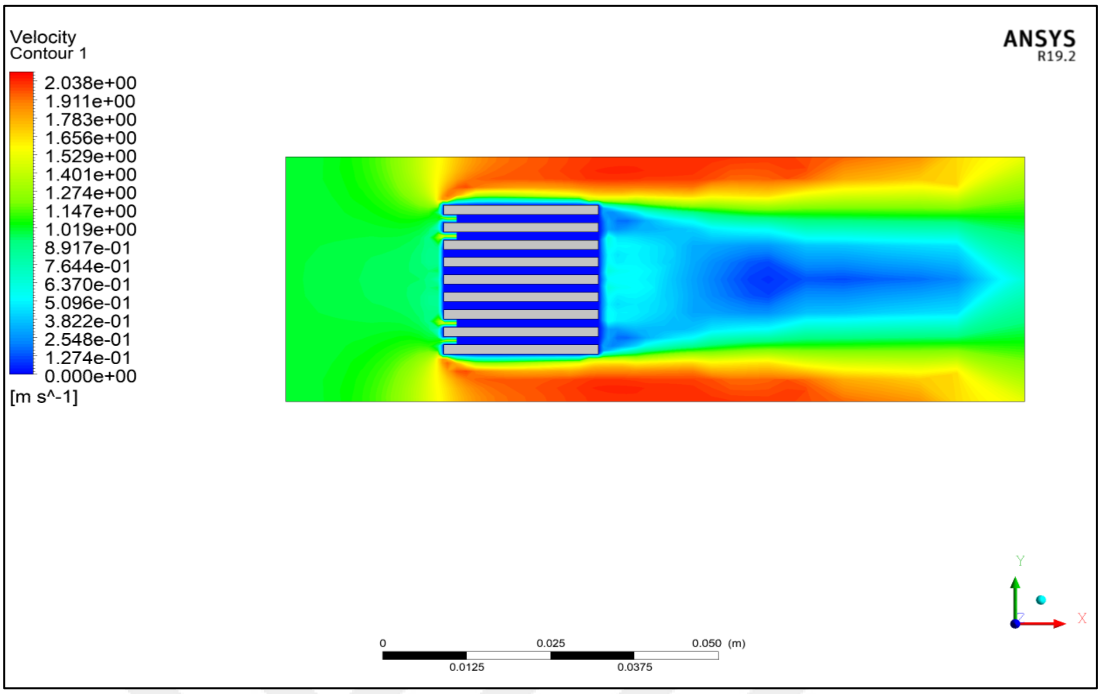
Velocity
Contour 1
2.038e+00
1.911e+00
1.783e+00
1.656e+00
1.529e+00
1.401e+00
1.274e+00
1.147e+00
1.019e+00
8.917e-01
7.644e-01
6.370e-01
5.096e-01
3.822e-01
2.548e-01
1.274e-01
0.000e+00
[m s^-1]
ANSYS
R19.2
0
0.025
0.050 (m)
0.0125
0.0375

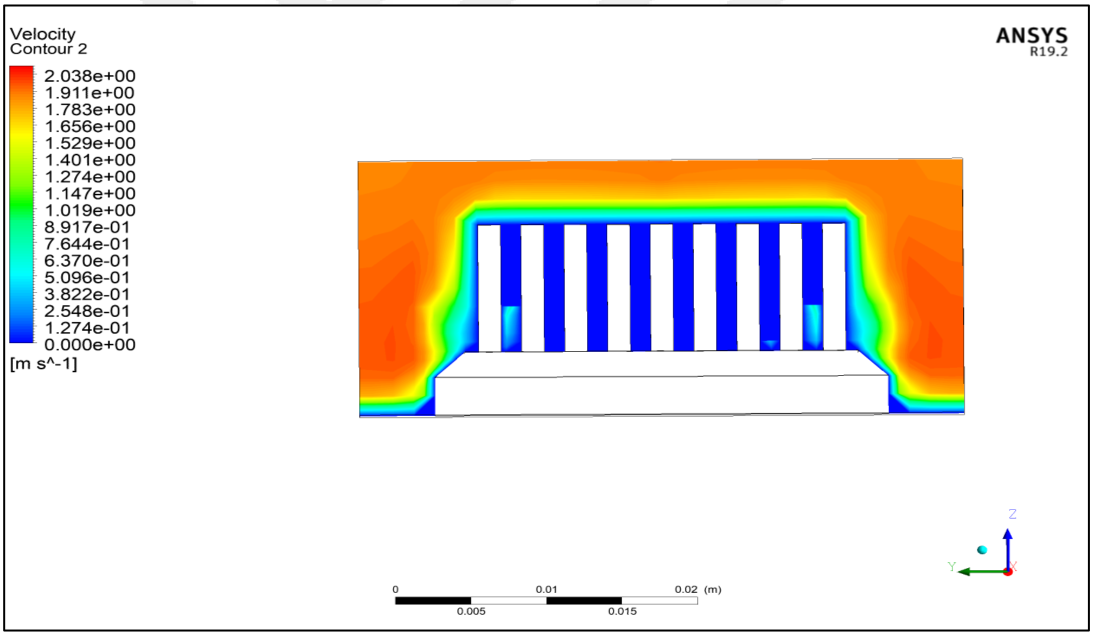
Velocity
Contour 2
2.038e+00
1.911e+00
1.783e+00
1.656e+00
1.529e+00
1.401e+00
1.274e+00
1.147e+00
1.019e+00
8.917e-01
7.644e-01
6.370e-01
5.096e-01
3.822e-01
2.548e-01
1.274e-01
0.000e+00
[m s^-1]
ANSYS
R19.2
0
0.01
0.02 (m)
0.005
0.015

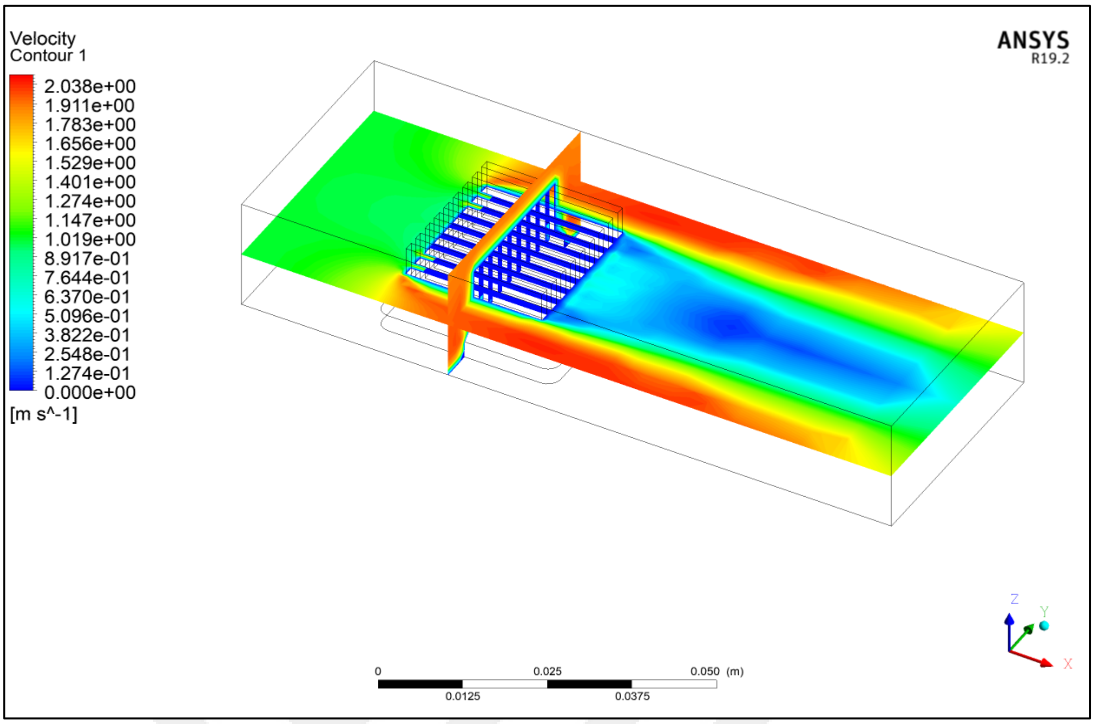

Figure 4.18: Velocity Profiles of Heat Sink With Nine Fin Numbers (A) Top View; B) Velocity Contour Along The Wall and Heat Sink and C) Overview).

The average velocity was increased with increasing the fins number due to increasing the fluid flow path as demonstrated in Figure 4.19, the increasing the fins number for heat sink from 5 to 6, 7, 8 and 9 lead to increase the average velocity. The highest and lowest average velocity magnitude was changed based on the fins number, in case of using 5 fins the average velocity was 0.89 m/s while increase the fins number to 9 lead to increase the average velocity to 1.9 m/s. [126] for velocity ANSYS software give better results and more reasonable on than COMSOL.

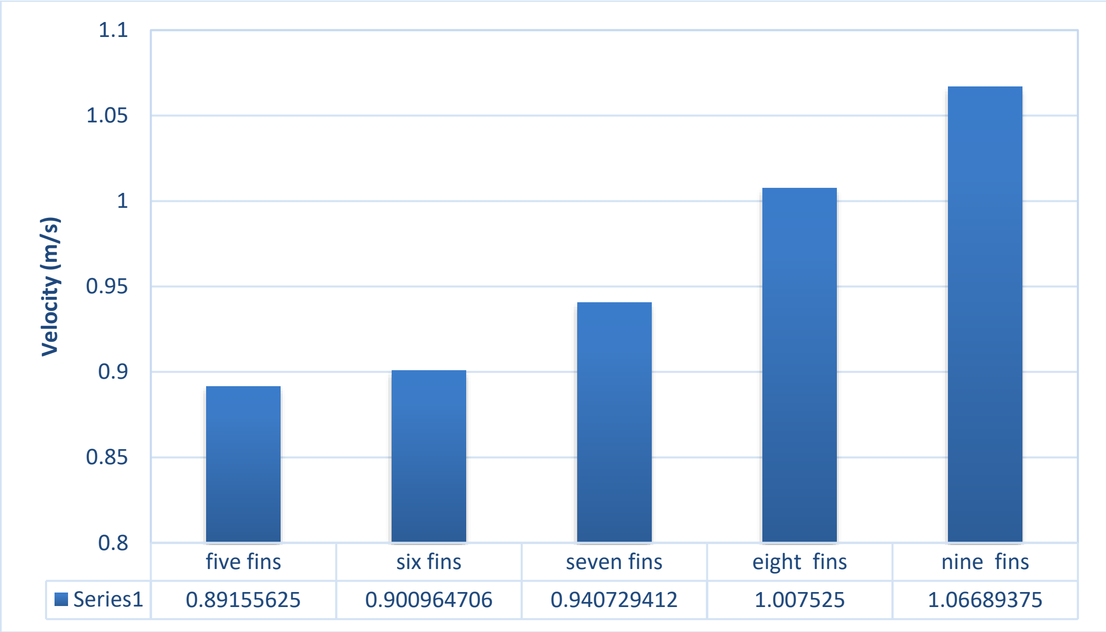

Figure 4.19: Effect of Fins Number on Velocity.

4.2.3 Effect of fines number on Pressure

Figures 4.20-4.24 shows the pressure contour for each case with different temperatures values that obtained from ANSYS software that cases differs in fins number first case with five fins and case five with nine fins. Based on figures below the fins number very effective on velocity distribution.

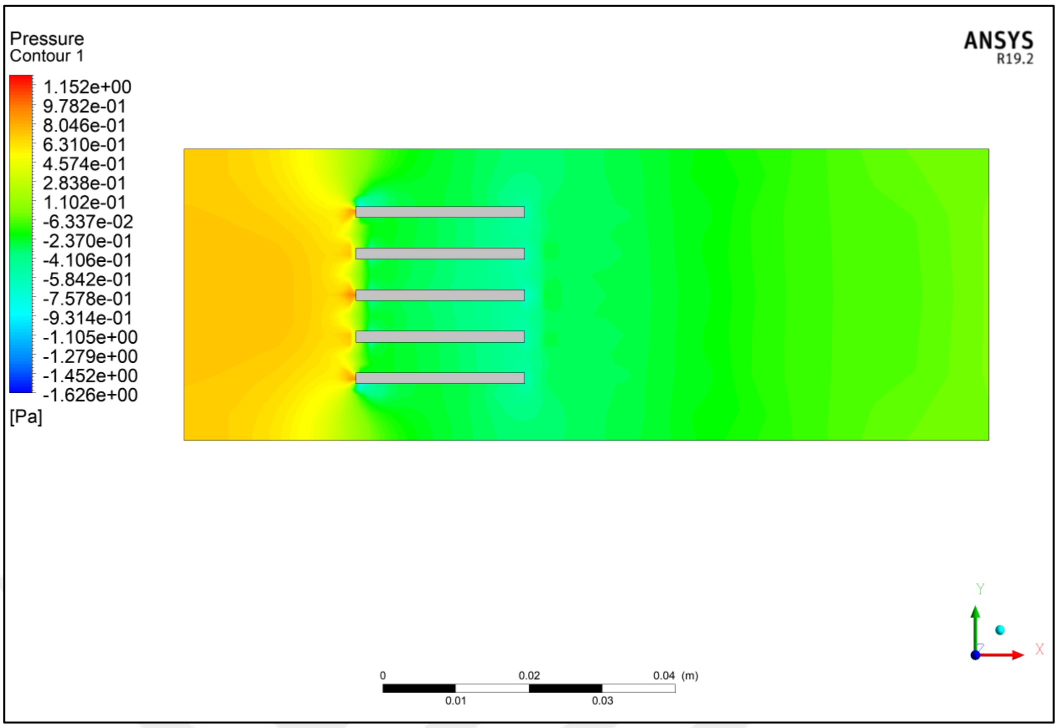

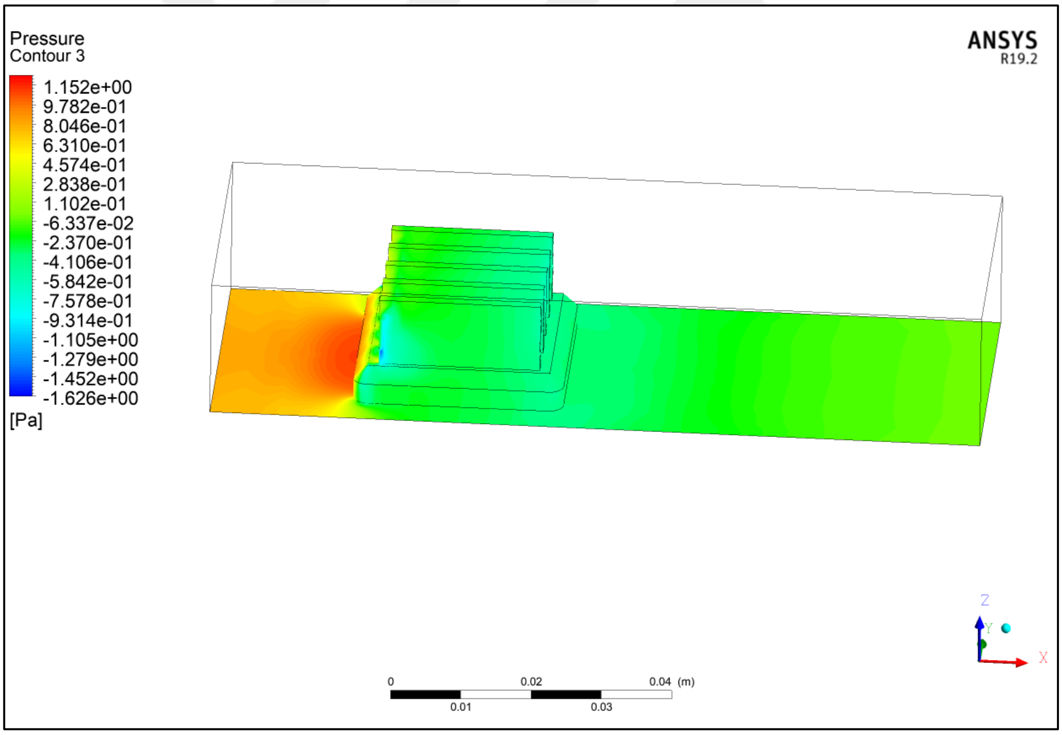

Figure 4.20: Pressure Profiles of Heat Sink With Five Fin Numbers (A) Top View; B) Overview).

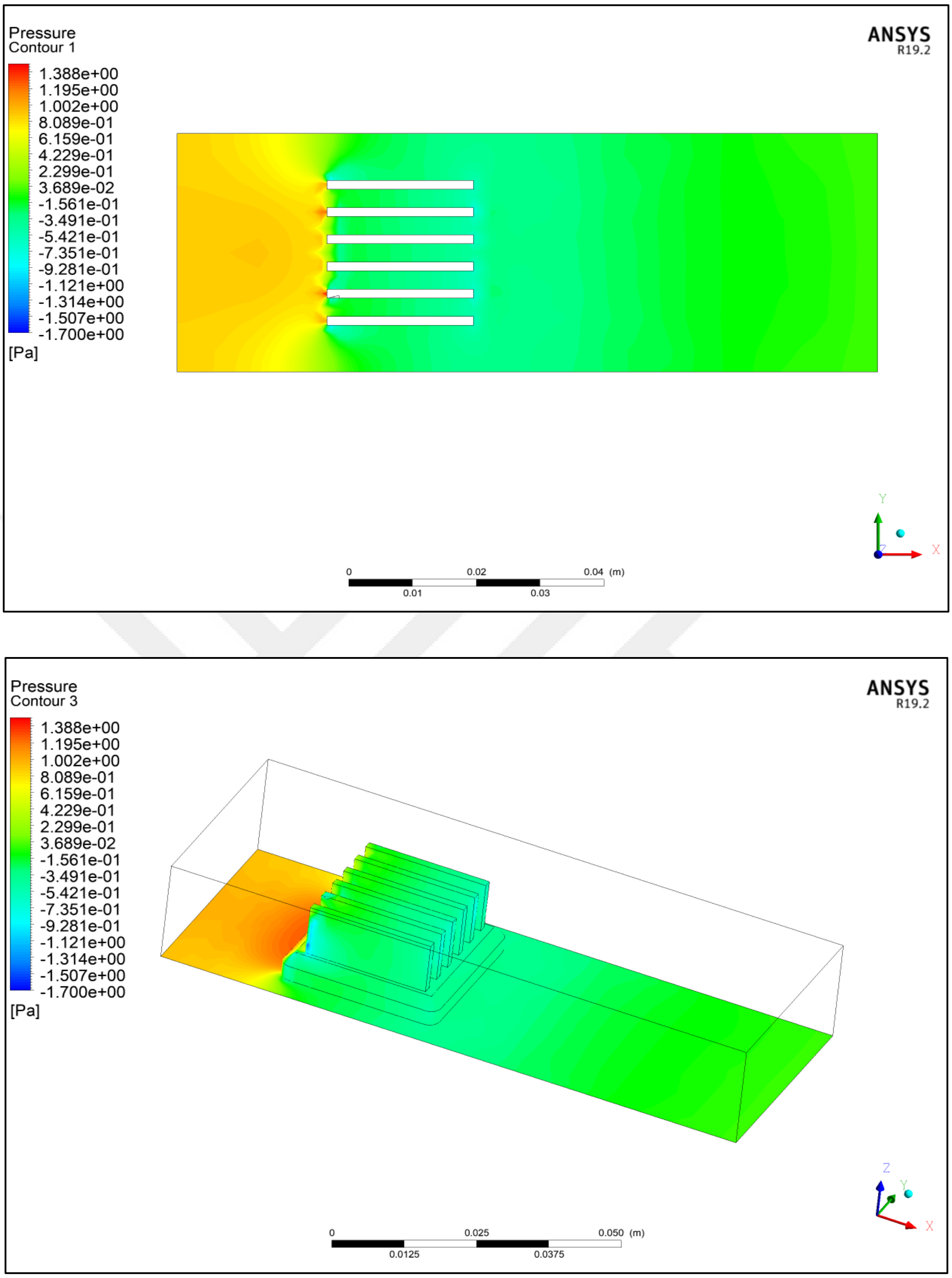

Figure 4.21: Pressure Profiles of Heat Sink With Six Fin Numbers (A) Top View; B) Overview).

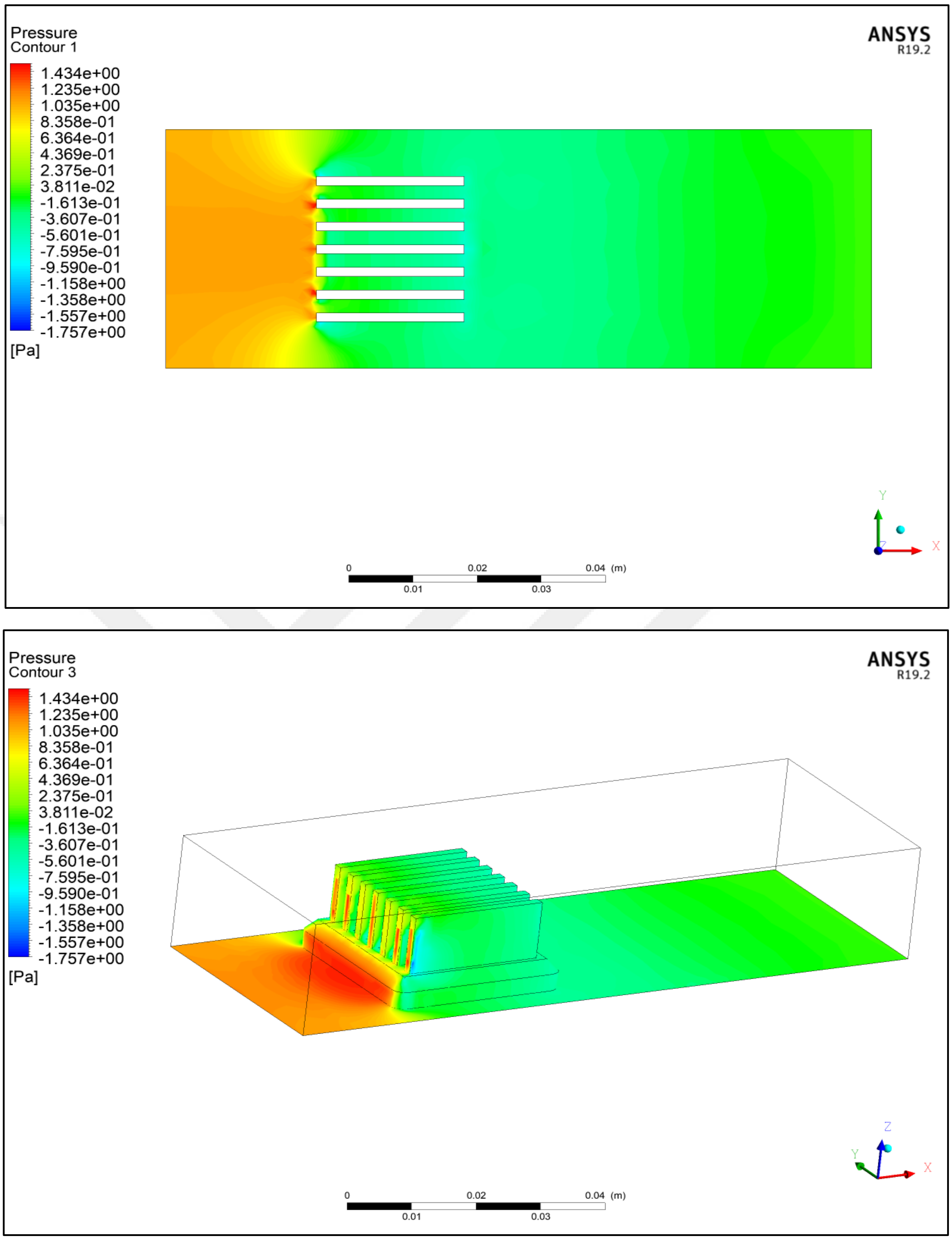

Figure 4.22: Pressure Profiles of Heat Sink With Seven Fin Numbers (A) Top View; B) Overview).

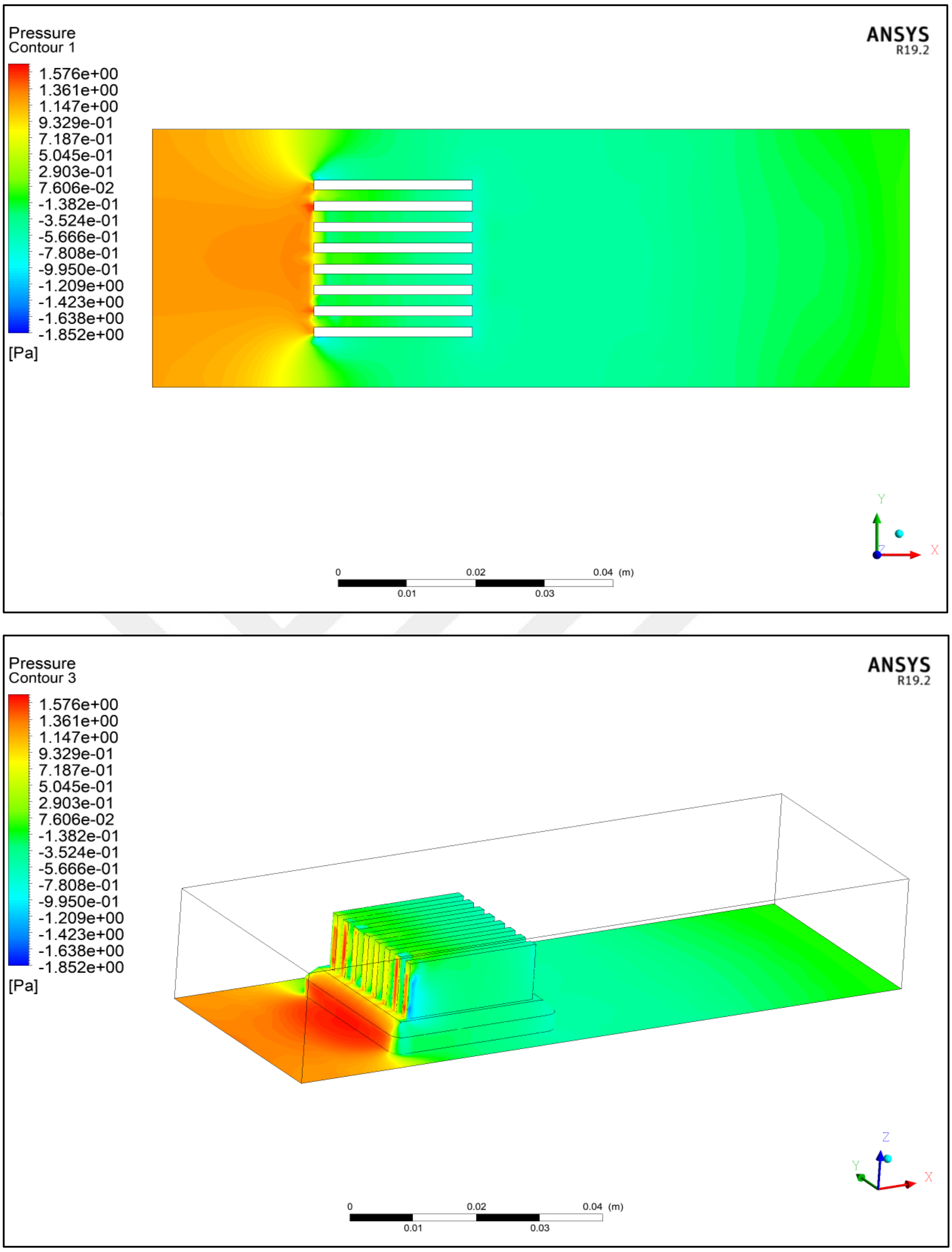

Figure 4.23: Pressure Profiles of Heat Sink With Eight Fin Numbers (A) Top View; B) Overview).

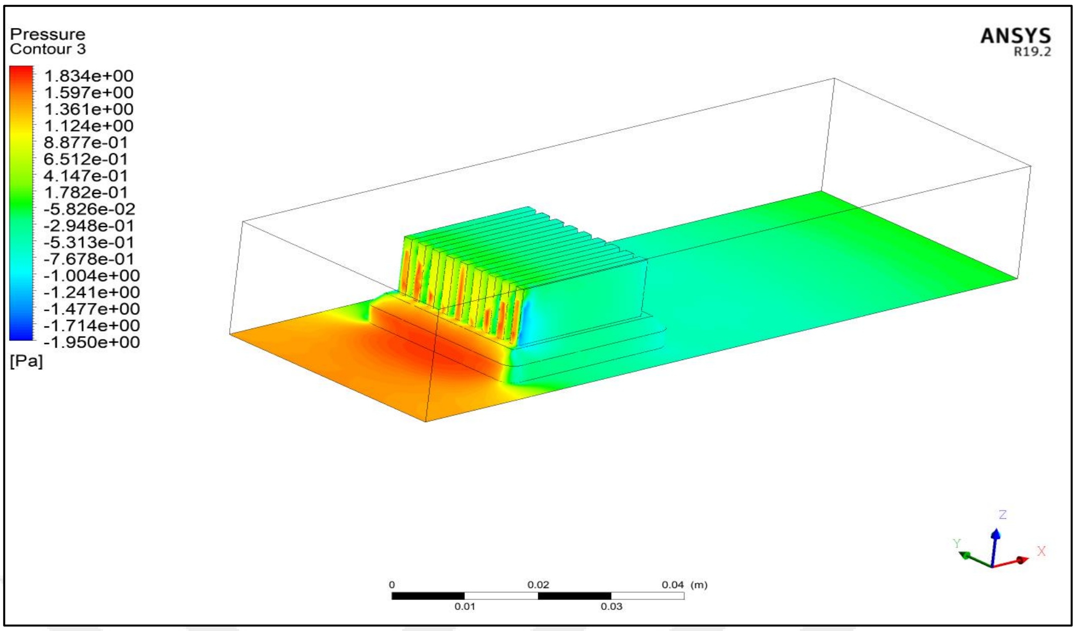
Pressure
Contour 3
1.834e+00
1.597e+00
1.361e+00
1.124e+00
8.877e-01
6.512e-01
4.147e-01
1.782e-01
-5.826e-02
-2.948e-01
-5.313e-01
-7.678e-01
-1.004e+00
-1.241e+00
-1.477e+00
-1.714e+00
-1.950e+00
[Pa]
ANSYS
R19.2
0
0.02
0.04 (m)
0.01
0.03
Z
Y
X

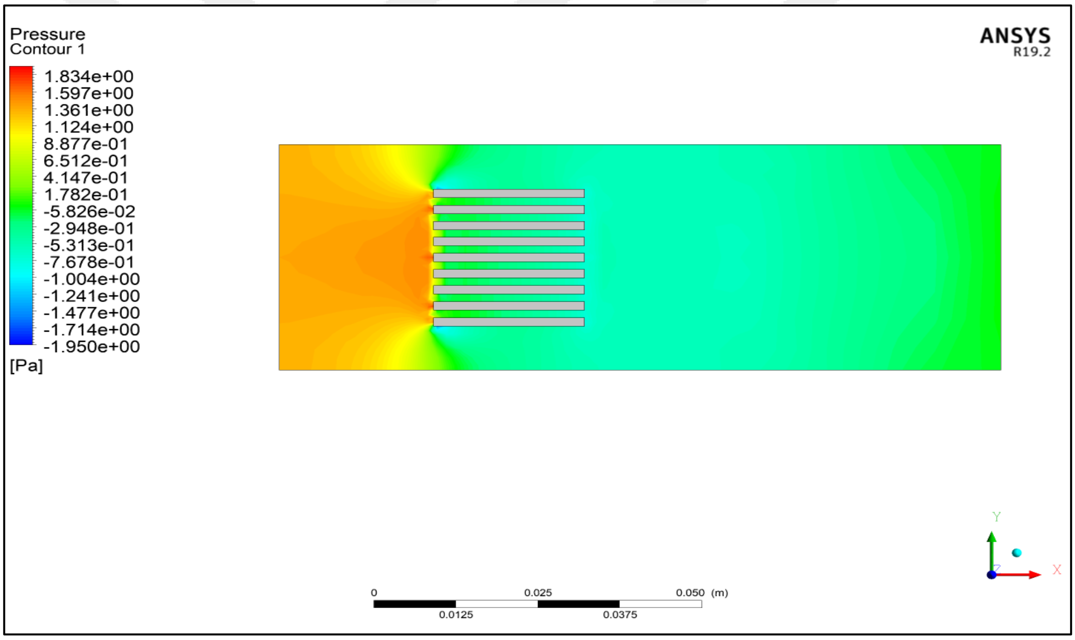
Pressure
Contour 1
1.834e+00
1.597e+00
1.361e+00
1.124e+00
8.877e-01
6.512e-01
4.147e-01
1.782e-01
-5.826e-02
-2.948e-01
-5.313e-01
-7.678e-01
-1.004e+00
-1.241e+00
-1.477e+00
-1.714e+00
-1.950e+00
[Pa]
ANSYS
R19.2
0
0.025
0.050 (m)
0.0125
0.0375
Y
X

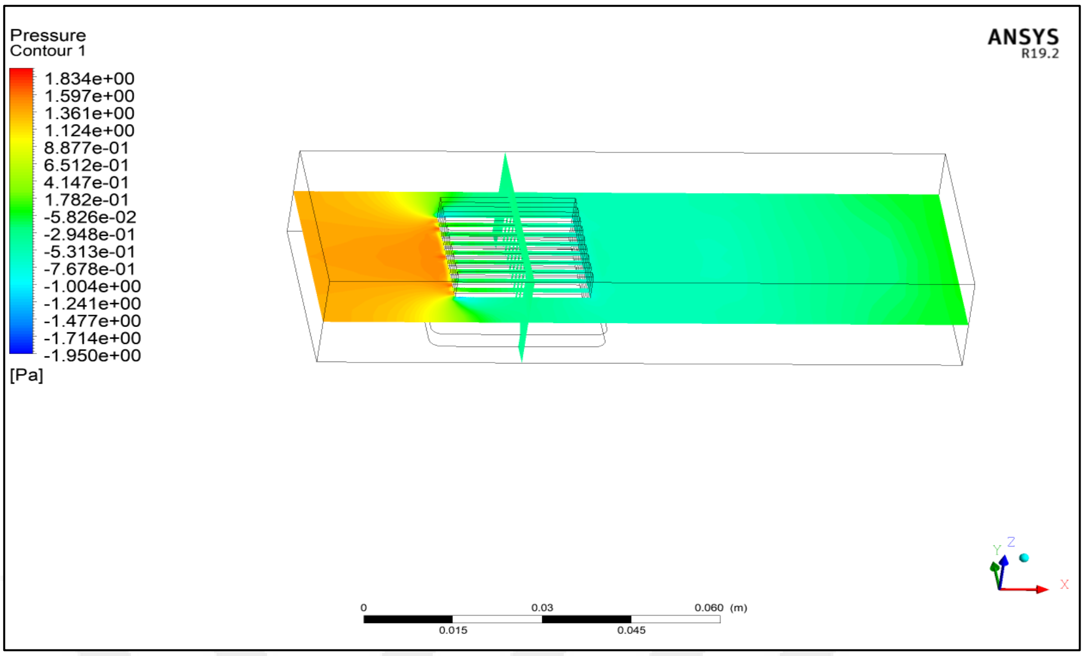

Figure 4.24: Pressure Profiles of Heat Sink With Nine Fin Numbers (A) Top View; B) Pressure Distribution Contour Along The Wall and Heat Sink and C) Overview).

The average pressure was increased with increasing the fins number due to increasing the fluid flow path as demonstrated in Figure 4.25, the increasing the fins number for heat sink from 5 to 6, 7, 8 and 9 lead to decrease the average pressure. The highest and lowest average velocity magnitude was changed based on the fins number, in case of using 5 fins the average velocity was 0.89 m/s while increase the fins number to 9 lead to increase the average velocity to 1.9 m/s. [126] for velocity ANSYS software give better results and more reasonable on than COMSOL

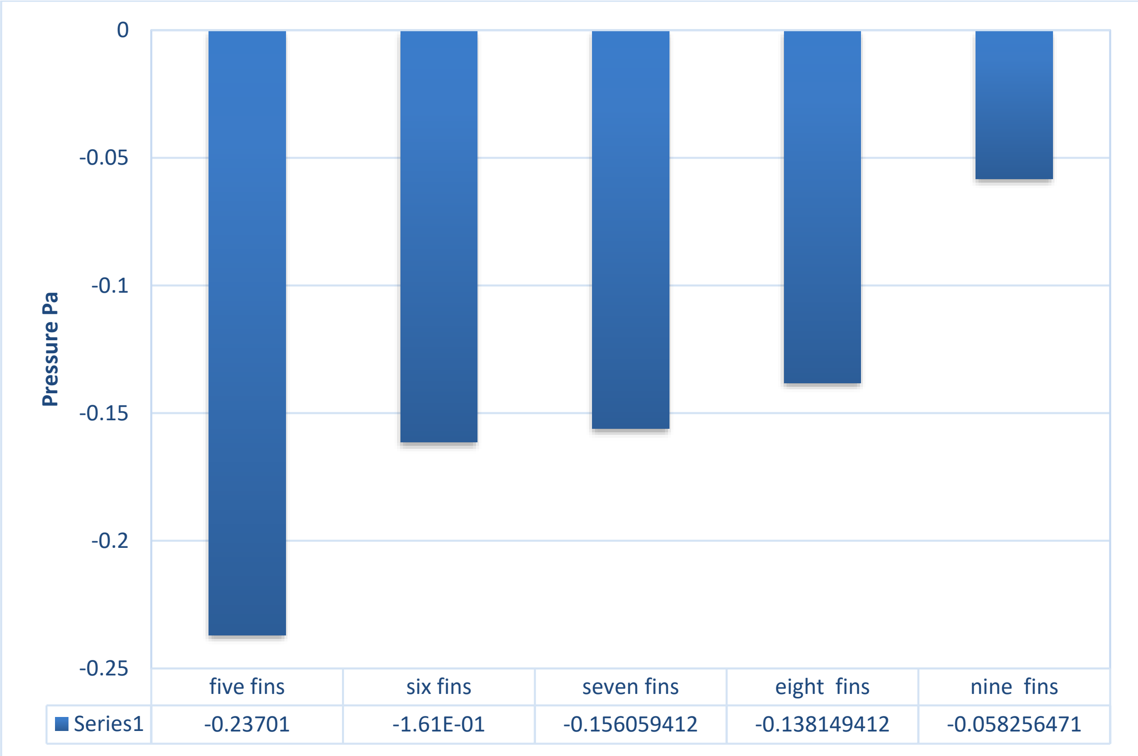

Figure 4.25: Effect of Fins Number on Pressure.

5. CONCLUSION AND RECOMMENDATION

5.1 CONCLUSION

This research project's overarching objective was to develop a numerical method for testing various heatsink geometries utilizing CFD software. A secondary objective of the project was to develop simple and exotic heatsink fin designs that enhance the thermal performance of the heatsink that was the subject of this project's investigation. The veracity of several suggested models developed by other researchers operating in this sector was investigated. The conventional rectangular plate fin heat sink, which is utilized extensively by thermal engineers for the cooling of electronic components, was chosen as the benchmark for performance comparison because the vast majority of researchers believe that this model heat sink is effective in terms of both its performance and its ease of manufacture.

The choice of a certain heat sink type is greatly influenced by the thermal budget allotted for the heat sink as well as the environment in which the heat sink is located. The goal of the present study is to create heat sinks with various fins in order to determine the optimal models, such as the ones listed below:

i. Increasing inlet velocity reduces the components temp of heating generation, and the relation between temperature and inlet velocity is a negative linear relationship.
ii. Increasing the fins number from 5 to 9 leads to increasing the velocity and temperature of the heat sink in the immersion cooling system.
iii. An increase in the number of fans leads to a decrease released temperature significantly.
iv. The pressure of the whole system improved when applied heat sink and increase the fin number caused an increase in the pressure.

5.2 RECOMMENDATION

In the future, we will be working to optimize the performance of heat sinks by conducting simulations on exotic or more complicated heat sink designs. These simulations will make use of our understanding of heat transfer, fluid mechanics, and additive manufacturing or 3D manufacturing capabilities. Additional ideas for future work include the following: • Carry out an investigation by operating simulations with various working fluids.

i. Identify the optimum number of fins for both the plate and pin fin heat sink designs in order to achieve the highest possible level of performance.

ii. Carry out the CFD simulation with the flow in the turbulent regime, and then investigate the differences in the results between the laminar regime and the turbulent regime.

iii. Use a 3D printer to produce heat sink models and then carry out experimental tests on those models.

iv. Do out flow analysis in order to get a deeper comprehension of the flow process that occurs via the fins of heat sinks.

REFERENCES

[1] K. Ebrahimi, G. F. Jones, and A. S. Fleischer, “Thermo-economic analysis of steady state waste heat recovery in data centers using absorption refrigeration,” *Appl. Energy*, vol. 139, pp. 384–397, 2015.

[2] N. Lei and E. R. Masanet, “Global Data Center Energy Demand and Strategies to Conserve Energy,” *Data Cent. Handb. Plan, Des. Build, Oper. a Smart Data Cent.*, pp. 15–26, 2021.

[3] P. K. Kresl, *The City and Quality of Life*. Edward Elgar Publishing, 2021.

[4] K. Cho, H. Chang, Y. Jung, and Y. Yoon, “Economic analysis of data center cooling strategies,” *Sustain. Cities Soc.*, vol. 31, pp. 234–243, 2017.

[5] J. Dai, M. M. Ohadi, D. Das, and M. G. Pecht, *Optimum cooling of data centers*. Springer, 2014.

[6] E. CHIAVAZZO, M. FASANO, L. BERGAMASCO, and R. RAVALLI, “Critical overview and feasibility study of two-phase immersion cooling systems for power electronics,” 2022.

[7] X. Kang, Y. Wang, Q. Huang, Y. Cui, X. Shi, and Y. Sun, “Study on direct-contact phase-change liquid immersion cooling dense-array solar cells under high concentration ratios,” *Energy Convers. Manag.*, vol. 128, pp. 95–103, 2016.

[8] J. L. Gess, S. H. Bhavnani, and R. W. Johnson, “Experimental investigation of a direct liquid immersion cooled prototype for high performance electronic systems,” *IEEE Trans. Components, Packag. Manuf. Technol.*, vol. 5, no. 10, pp. 1451–1464, 2015.

[9] J. M. Shah, R. Eiland, A. Siddarth, and D. Agonafer, “Effects of mineral oil immersion cooling on IT equipment reliability and reliability enhancements to data center operations,” in *2016 15th IEEE Intersociety Conference on Thermal and Thermomechanical Phenomena in Electronic Systems (ITherm)*, 2016, pp. 316–325.

[10] S. J. Self, B. V Reddy, and M. A. Rosen, “Geothermal heat pump systems: Status review and comparison with other heating options,” *Appl. Energy*, vol. 101, pp. 341–348, 2013.

[11] C.-C. Cheng, P.-C. Chang, H.-C. Li, and F.-I. Hsu, “Design of a single-phase immersion cooling system through experimental and numerical analysis,” *Int. J. Heat Mass Transf.*, vol. 160, p. 120203, 2020.

[12] X. C. Tong, “Liquid cooling devices and their materials selection,” in *Advanced materials for thermal management of electronic packaging*, Springer, 2011, pp. 421–475.

[13] R. C. Chu, R. E. Simons, M. J. Ellsworth, R. R. Schmidt, and V. Cozzolino, “Review of cooling technologies for computer products,” *IEEE Trans. Device Mater. Reliab.*, vol. 4, no. 4, pp. 568–585, 2004.

[14] I. W. Kuncoro, N. A. Pambudi, M. K. Biddinika, I. Widiastuti, M. Hijriawan, and K. M. Wibowo, “Immersion cooling as the next technology for data center cooling: A review,” in *Journal of Physics: Conference Series*, 2019, vol. 1402, no. 4, p. 44057.

[15] A.-C. Iradukunda, D. R. Huitink, and F. Luo, “A review of advanced thermal management solutions and the implications for integration in high-voltage packages,” *IEEE J. Emerg. Sel. Top. Power Electron.*, vol. 8, no. 1, pp. 256–271, 2019.

[16] S. M. Khanvilkar, “Design and CFD analysis of a tank solution for natural convection based single-phase immersion cooling of servers.” The University of Texas at Arlington, 2021.

[17] N. A. Pambudi, A. Sarifudin, R. A. Firdaus, D. K. Ulfa, I. M. Gandidi, and R. Romadhon, “The immersion cooling technology: Current and future development in energy saving,” *Alexandria Eng. J.*, vol. 61, no. 12, pp. 9509–9527, 2022.

[18] H. Coles and M. Herrlin, “Immersion cooling of electronics in DoD installations,” CALIFORNIA UNIV BERKELEY BERKELEY United States, 2016.

[19] J. M. Shah, “Reliability challenges in airside economization and oil immersion cooling.” 2016.

[20] S. M. S. Murshed and C. A. N. De Castro, “A critical review of traditional and emerging techniques and fluids for electronics cooling,” *Renew. Sustain. Energy Rev.*, vol. 78, pp. 821–833, 2017.

[21] A. C. Kheirabadi and D. Groulx, “Experimental evaluation of a thermal contact liquid cooling system for server electronics,” *Appl. Therm. Eng.*, vol. 129, pp. 1010–1025, 2018.

[22] J. Hwang and T. Lee, “Study on the Design and Operation of an Outdoor Air-Cooling System for a Computer Room,” *Energies*, vol. 14, no. 6, p. 1670, 2021.

[23] P. Sagar, P. Teotia, A. D. Sahlot, and H. C. Thakur, “Heat transfer analysis and optimization of engine fins of varying geometry,” *Mater. Today Proc.*, vol. 4, no. 8, pp. 8558–8564, 2017.

[24] R. K. Mohammed, Y. Xia, R. A. Sahan, and Y.-F. Pang, “Performance improvements of air-cooled thermal tool with advanced technologies,” in *2012 28th Annual IEEE Semiconductor Thermal Measurement and Management Symposium (SEMI-THERM)*, 2012, pp. 354–361.

[25] J. Choi and M. Jeong, “Compact, lightweight, and highly efficient circular heat sink design for high-end PCs,” *Appl. Therm. Eng.*, vol. 92, pp. 162–171, 2016.

[26] J. Cho and J. Woo, “Development and experimental study of an independent row-based cooling system for improving thermal performance of a data center,” *Appl. Therm. Eng.*, vol. 169, p. 114857, 2020.

[27] J. Ni and X. Bai, “A review of air conditioning energy performance in data centers,” *Renew. Sustain. energy Rev.*, vol. 67, pp. 625–640, 2017.

[28] J. Koomey, “Growth in data center electricity use 2005 to 2010,” *A Rep. by Anal. Press. Complet. Req. New York Times*, vol. 9, no. 2011, p. 161, 2011.

[29] A. Haywood, J. Sherbeck, P. Phelan, G. Varsamopoulos, and S. K. S. Gupta, “Thermodynamic feasibility of harvesting data center waste heat to drive an absorption chiller,” *Energy Convers. Manag.*, vol. 58, pp. 26–34, 2012.

[30] K. G. Brill, “The invisible crisis in the data center: The economic meltdown of Moore’s law,” *white Pap. Uptime Inst.*, pp. 2–5, 2007.

[31] T. Gao *et al.*, “A study of direct liquid cooling for high-density chips and accelerators,” in *2017 16th IEEE Intersociety Conference on Thermal and*

Thermomechanical Phenomena in Electronic Systems (ITherm), 2017, pp. 565–573.

[32] C. Nadjahi, H. Louahlia, and S. Lemasson, “A review of thermal management and innovative cooling strategies for data center,” *Sustain. Comput. Informatics Syst.*, vol. 19, pp. 14–28, 2018.

[33] H. Zhang, S. Shao, H. Xu, H. Zou, and C. Tian, “Free cooling of data centers: A review,” *Renew. Sustain. Energy Rev.*, vol. 35, pp. 171–182, 2014.

[34] W. Jiang, Z. Jia, S. Feng, F. Liu, and H. Jin, “Fine-grained warm water cooling for improving datacenter economy,” in *2019 ACM/IEEE 46th Annual International Symposium on Computer Architecture (ISCA)*, 2019, pp. 474–486.

[35] M. Salim and R. Tozer, “Data Centers’ Energy Auditing and Benchmarking-Progress Update.,” *ASHRAE Trans.*, vol. 116, no. 1, 2010.

[36] A. Shehabi, S. J. Smith, E. Masanet, and J. Koomey, “Data center growth in the United States: decoupling the demand for services from electricity use,” *Environ. Res. Lett.*, vol. 13, no. 12, p. 124030, 2018.

[37] N. Ottman *et al.*, “Soil exposure modifies the gut microbiota and supports immune tolerance in a mouse model,” *J. Allergy Clin. Immunol.*, vol. 143, no. 3, pp. 1198–1206, 2019.

[38] I. W. Kuncoro, N. A. Pambudi, M. K. Biddinika, and C. W. Budiyanto, “Optimization of immersion cooling performance using the Taguchi Method,” *Case Stud. Therm. Eng.*, vol. 21, p. 100729, 2020.

[39] P. Birbarah *et al.*, “Water immersion cooling of high power density electronics,” *Int. J. Heat Mass Transf.*, vol. 147, p. 118918, 2020.

[40] N. A. Pambudi, A. M. Yusuf, and A. Sarifudin, “The Use of Single-Phase Immersion Cooling by Using Two Types of Dielectric Fluid for Data Center Energy Savings,” *Energy Eng. J. Assoc. Energy Eng.*, vol. 119, no. 1, pp. 275–286, 2021.

[41] Y. Zhang, S. L. Ho, and W. Fu, “Applying response surface method to oil-immersed transformer cooling system for design optimization,” *IEEE Trans. Magn.*, vol. 54, no. 11, pp. 1–5, 2018.

[42] M. S. Patil, J.-H. Seo, and M.-Y. Lee, “A novel dielectric fluid immersion cooling technology for Li-ion battery thermal management,” *Energy Convers. Manag.*, vol. 229, p. 113715, 2021.

[43] X. Kang, C. Wang, Y. Wang, and Y. Kang, “Nature of substrate modification effect on thermal performance of simulated solar cells over phase-change immersion cooling under high concentration ratios,” *Energy Convers. Manag.*, vol. 177, pp. 511–518, 2018.

[44] B. B. Kanbur, C. Wu, S. Fan, and F. Duan, “System-level experimental investigations of the direct immersion cooling data center units with thermodynamic and thermoeconomic assessments,” *Energy*, vol. 217, p. 119373, 2021.

[45] M. Lionello, M. Rampazzo, A. Beghi, D. Varagnolo, and M. Vesterlund, “Graph-based modelling and simulation of liquid immersion cooling systems,” *Energy*, vol. 207, p. 118238, 2020.

[46] G. Xia, L. Cao, and G. Bi, “A review on battery thermal management in electric vehicle application,” *J. Power Sources*, vol. 367, pp. 90–105, 2017.

[47] P. Chen, S. Harmand, and S. Ouenzerfi, “Immersion cooling effect of dielectric liquid and self-rewetting fluid on smooth and porous surface,” *Appl. Therm. Eng.*, vol. 180, p. 115862, 2020.

[48] T. Muthuramalingam, “Effect of diluted dielectric medium on spark energy in green EDM process using TGRA approach,” *J. Clean. Prod.*, vol. 238, p. 117894, 2019.

[49] A. Maleki, A. Haghighi, M. E. H. Assad, I. Mahariq, and M. A. Nazari, “A review on the approaches employed for cooling PV cells,” *Sol. Energy*, vol. 209, pp. 170–185, 2020.

[50] P. Dwivedi, K. Sudhakar, A. Soni, E. Solomin, and I. Kirpichnikova, “Advanced cooling techniques of PV modules: A state of art,” *Case Stud. Therm. Eng.*, vol. 21, p. 100674, 2020.

[51] W. Yuan *et al.*, “Comparison study of the performance of two kinds of photovoltaic/thermal (PV/T) systems and a PV module at high ambient temperature,”

Energy, vol. 148, pp. 1153–1161, 2018.

[52] Z. Peng, M. R. Herfatmanesh, and Y. Liu, “Cooled solar PV panels for output energy efficiency optimisation,” *Energy Convers. Manag.*, vol. 150, pp. 949–955, 2017.

[53] A. K. Suresh, S. Khurana, G. Nandan, G. Dwivedi, and S. Kumar, “Role on nanofluids in cooling solar photovoltaic cell to enhance overall efficiency,” *Mater. Today Proc.*, vol. 5, no. 9, pp. 20614–20620, 2018.

[54] D. Kulkarni, X. Tang, S. Ahuja, R. Dischler, and R. Mahajan, “Experimental study of two-phase cooling to enable large-scale system computing performance,” in *2018 17th IEEE Intersociety Conference on Thermal and Thermomechanical Phenomena in Electronic Systems (ITherm)*, 2018, pp. 596–601.

[55] R. Eiland, J. Edward Fernandes, M. Vallejo, A. Siddarth, D. Agonafer, and V. Mulay, “Thermal performance and efficiency of a mineral oil immersed server over varied environmental operating conditions,” *J. Electron. Packag.*, vol. 139, no. 4, 2017.

[56] U. Mukhopadhyay, A. Skjellum, O. Hambolu, J. Oakley, L. Yu, and R. Brooks, “A brief survey of cryptocurrency systems,” in *2016 14th annual conference on privacy, security and trust (PST)*, 2016, pp. 745–752.

[57] W. Pan, F. Zheng, Y. Zhao, W.-T. Zhu, and J. Jing, “An efficient elliptic curve cryptography signature server with GPU acceleration,” *IEEE Trans. Inf. Forensics Secur.*, vol. 12, no. 1, pp. 111–122, 2016.

[58] A. Kampl, “Bitcoin 2-phase immersion cooling and the implications for high performance computing,” *Electron. Cool. Mag.*, vol. 1, 2014.

[59] L. Campbell and P. Tuma, “Numerical prediction of the junction-to-fluid thermal resistance of a 2-phase immersion-cooled IBM dual core POWER6 processor,” in *2012 28th Annual IEEE Semiconductor Thermal Measurement and Management Symposium (SEMI-THERM)*, 2012, pp. 36–44.

[60] P. D. Lund, J. Lindgren, J. Mikkola, and J. Salpakari, “Review of energy system flexibility measures to enable high levels of variable renewable electricity,” *Renew. Sustain. energy Rev.*, vol. 45, pp. 785–807, 2015.

[61] L. Ding *et al.*, “Effect of temperature on compression behavior of polypropylene

separator used for Lithium-ion battery," *J. Power Sources*, vol. 466, p. 228300, 2020.

[62] P. Dubey, G. Pulugundla, and A. K. Srouji, "Direct comparison of immersion and cold-plate based cooling for automotive Li-ion battery modules," *Energies*, vol. 14, no. 5, p. 1259, 2021.

[63] O. S. Dmitrieva, G. R. Patrakova, and A. V Dmitriev, "Evaluation of the cooling system calculation technique for oil-immersed transformers," in *2017 International Conference on Industrial Engineering, Applications and Manufacturing (ICIEAM)*, 2017, pp. 1–4.

[64] T. H. Wang, C.-C. Lee, and Y.-S. Lai, "Thermal characteristics evaluation for board-level high performance flip-chip package equipped with vapor chamber as heat spreader," *Microelectron. Eng.*, vol. 87, no. 12, pp. 2463–2467, 2010.

[65] P. Naphon, S. Wongwises, and S. Wiriyasart, "On the thermal cooling of central processing unit of the PCs with vapor chamber," *Int. Commun. Heat Mass Transf.*, vol. 39, no. 8, pp. 1165–1168, 2012.

[66] Y. Wang, B. Wang, K. Zhu, H. Li, W. He, and S. Liu, "Energy saving potential of using heat pipes for CPU cooling," *Appl. Therm. Eng.*, vol. 143, pp. 630–638, 2018.

[67] G. Xiahou, J. Zhang, R. Ma, and Y. Liu, "Novel heat pipe radiator for vertical CPU cooling and its experimental study," *Int. J. Heat Mass Transf.*, vol. 130, pp. 912–922, 2019.

[68] N. Zhao, L. Guo, C. Qi, T. Chen, and X. Cui, "Experimental study on thermo-hydraulic performance of nanofluids in CPU heat sink with rectangular grooves and cylindrical bugles based on exergy efficiency," *Energy Convers. Manag.*, vol. 181, pp. 235–246, 2019.

[69] P. Naphon, S. Wongwises, and S. Wiriyasart, "Application of two-phase vapor chamber technique for hard disk drive cooling of PCs," *Int. Commun. Heat Mass Transf.*, vol. 40, pp. 32–35, 2013.

[70] T. Yousefi, S. A. Mousavi, B. Farahbakhsh, and M. Z. Saghir, "Experimental investigation on the performance of CPU coolers: Effect of heat pipe inclination angle and the use of nanofluids," *Microelectron. Reliab.*, vol. 53, no. 12, pp. 1954–1961, 2013.

[71] C. Dang, L. Jia, and Q. Lu, “Investigation on thermal design of a rack with the pulsating heat pipe for cooling CPUs,” *Appl. Therm. Eng.*, vol. 110, pp. 390–398, 2017.

[72] K. Zhu *et al.*, “Experimental study of energy saving performances in chip cooling by using heat sink with embedded heat pipe,” *Energy Procedia*, vol. 105, pp. 5160–5165, 2017.

[73] P. Naphon and S. Wiriyasart, “Liquid cooling in the mini-rectangular fin heat sink with and without thermoelectric for CPU,” *Int. Commun. Heat Mass Transf.*, vol. 36, no. 2, pp. 166–171, 2009.

[74] S. Wiriyasart, C. Hommalee, and P. Naphon, “Thermal cooling enhancement of dual processors computer with thermoelectric air cooler module,” *Case Stud. Therm. Eng.*, vol. 14, p. 100445, 2019.

[75] D. Liu, F.-Y. Zhao, H.-X. Yang, and G.-F. Tang, “Thermoelectric mini cooler coupled with micro thermosiphon for CPU cooling system,” *Energy*, vol. 83, pp. 29–36, 2015.

[76] A. Siricharoenpanich, S. Wiriyasart, A. Srichat, and P. Naphon, “Thermal management system of CPU cooling with a novel short heat pipe cooling system,” *Case Stud. Therm. Eng.*, vol. 15, p. 100545, 2019.

[77] L. Zhu, R. F. Boehm, Y. Wang, C. Halford, and Y. Sun, “Water immersion cooling of PV cells in a high concentration system,” *Sol. Energy Mater. Sol. Cells*, vol. 95, no. 2, pp. 538–545, 2011.

[78] S. Mehrotra, P. Rawat, M. Debbarma, and K. Sudhakar, “Performance of a solar panel with water immersion cooling technique,” *Int. J. Sci. Environ. Technol.*, vol. 3, no. 3, pp. 1161–1172, 2014.

[79] H. Kiani, D.-W. Sun, and Z. Zhang, “The effect of ultrasound irradiation on the convective heat transfer rate during immersion cooling of a stationary sphere,” *Ultrason. Sonochem.*, vol. 19, no. 6, pp. 1238–1245, 2012.

[80] Y. Sun, Y. Wang, L. Zhu, B. Yin, H. Xiang, and Q. Huang, “Direct liquid-immersion cooling of concentrator silicon solar cells in a linear concentrating photovoltaic

receiver," *Energy*, vol. 65, pp. 264–271, 2014.

[81] A. Trimbake, C. P. Singh, and S. Krishnan, "Mineral oil immersion cooling of lithium-ion batteries: an experimental investigation," *J. Electrochem. Energy Convers. Storage*, vol. 19, no. 2, 2022.

[82] N. A. Pambudi *et al.*, "Preliminary experimental of GPU immersion-cooling," in *E3S web of conferences*, 2019, vol. 93, p. 3003.

[83] C. Liu and H. Yu, "Evaluation and Optimization of a Two-Phase Liquid-Immersion Cooling System for Data Centers," *Energies*, vol. 14, no. 5, p. 1395, 2021.

[84] I. Levin, A. Dordopulo, A. Fedorov, and Y. Doronchenko, "Design Technology for Reconfigurable Computer Systems with Immersion Cooling," in *Russian Supercomputing Days*, 2018, pp. 554–564.

[85] I. I. Levin, A. I. Dordopulo, A. M. Fedorov, and A. A. Gulenok, "Reconfigurable computer based on Virtex UltraScale+ FPGAs with immersion cooling system," in *International Conference on Parallel Computational Technologies*, 2017, pp. 27–41.

[86] X. Li, L. Lv, X. Wang, and J. Li, "Transient thermodynamic response and boiling heat transfer limit of dielectric liquids in a two-phase closed direct immersion cooling system," *Therm. Sci. Eng. Prog.*, vol. 25, p. 100986, 2021.

[87] D. V. Gandhi, "Computational analysis for thermal optimization of server for single phase immersion cooling," vol. 2, p. 89, 2019.

[88] B.-K. Lee, "Computational fluid dynamics in cardiovascular disease," *Korean Circ. J.*, vol. 41, no. 8, pp. 423–430, 2011.

[89] N. R. Saber *et al.*, "Progress towards patient-specific computational flow modeling of the left heart via combination of magnetic resonance imaging with computational fluid dynamics," *Ann. Biomed. Eng.*, vol. 31, pp. 42–52, 2003.

[90] J.-P. Kone, X. Zhang, Y. Yan, G. Hu, and G. Ahmadi, "Three-dimensional multiphase flow computational fluid dynamics models for proton exchange membrane fuel cell: A theoretical development," *J. Comput. Multiph. Flows*, vol. 9, no. 1, pp. 3–25, 2017.

[91] V. Malviya, R. Mishra, and J. Fieldhouse, "CFD investigation of a novel fuel-saving device for articulated tractor-trailer combinations," *Eng. Appl. Comput. Fluid Mech.*,

vol. 3, no. 4, pp. 587–607, 2009.

[92] L. Marshall and P. Bemis, “Using CFD for data center design and analysis,” *Appl. Math Model. White Pap.*, 2011.

[93] A. H. Almaneea, “Thermal analysis of liquid immersed electronics for data centres.” University of Leeds, 2014.

[94] S. Hari, *Computational Fluid Dynamics (CFD) simulations of dilute fluid-particle flows in aerosol concentrators*. Texas A&M University, 2003.

[95] K. Wang and H. Wang, “A fast characteristic finite difference method for fractional advection–diffusion equations,” *Adv. Water Resour.*, vol. 34, no. 7, pp. 810–816, 2011.

[96] T. Norton and D.-W. Sun, “Computational fluid dynamics (CFD)–an effective and efficient design and analysis tool for the food industry: a review,” *Trends Food Sci. Technol.*, vol. 17, no. 11, pp. 600–620, 2006.

[97] V. Jagota, A. P. S. Sethi, and K. Kumar, “Finite element method: an overview,” *Walailak J. Sci. Technol.*, vol. 10, no. 1, pp. 1–8, 2013.

[98] F. Arbeiter *et al.*, “Thermal-hydraulics of helium cooled First Wall channels and scoping investigations on performance improvement by application of ribs and mixing devices,” *Fusion Eng. Des.*, vol. 109, pp. 1123–1129, 2016.

[99] S. Alkharabsheh *et al.*, “A brief overview of recent developments in thermal management in data centers,” *J. Electron. Packag.*, vol. 137, no. 4, p. 40801, 2015.

[100] Y. M. Manaserh, M. I. Tradat, A. R. Gharaibeh, B. G. Sammakia, and R. Tipton, “Shifting to energy efficient hybrid cooled data centers using novel embedded floor tiles heat exchangers,” *Energy Convers. Manag.*, vol. 247, p. 114762, 2021.

[101] Y. Fulpagare and A. Bhargav, “Advances in data center thermal management,” *Renew. Sustain. Energy Rev.*, vol. 43, pp. 981–996, 2015.

[102] R. Mittal and G. Iaccarino, “Immersed boundary methods,” *Annu. Rev. Fluid Mech.*, vol. 37, pp. 239–261, 2005.

[103] H. Ito, “Flow in curved pipes,” *JSME Int. J.*, vol. 30, no. 262, pp. 543–552, 1987.

[104] L. Zhang and Z. Chen, “Convective heat transfer in cross-corrugated triangular ducts under uniform heat flux boundary conditions,” *Int. J. Heat Mass Transf.*, vol. 54, no. 1–3, pp. 597–605, 2011.

[105] G. S. Constantinescu and K. D. Squires, “LES and DES investigations of turbulent flow over a sphere at Re= 10,000,” *Flow, Turbul. Combust.*, vol. 70, pp. 267–298, 2003.

[106] T. Hiramatsu, M. Kawasaki, and K. Saikawa, “On the estimation of gravitational wave spectrum from cosmic domain walls,” *J. Cosmol. Astropart. Phys.*, vol. 2014, no. 02, p. 31, 2014.

[107] M. Petrov, S. Utyuzhnikov, A. Chikitkin, and V. Titarev, “On extension of near-wall domain decomposition to turbulent compressible flows,” *Comput. Fluids*, vol. 210, p. 104629, 2020.

[108] I. Ahmed, S. Rostom, A. Lanza, and H. De Lasa, “Computational fluid dynamics study of the CREC riser simulator: mixing patterns,” *Powder Technol.*, vol. 316, pp. 641–649, 2017.

[109] R. Anwar, V. V. Vermol, S. Rahman, O. H. Hassan, and T. W. Dung, “Reformulating local ceramic stoneware with alumina as replacement material for the heat sink,” in *Proceedings of the International Symposium on Research of Arts, Design and Humanities (ISRADH 2014)*, 2015, pp. 507–516.

[110] M. Imran and S. A. Moeed, “Design and Simulation of Heat Sink for Different Components Geometry with Various Heat Capacities.”

[111] T. C. Ashrae, “Thermal guidelines for data processing environments,” *Am. Soc. Heat. Refrig. Air-Conditioning Eng. Tech. Rep*, vol. 9, p. 205, 2004.

[112] C. E. Bash, C. D. Patel, and R. K. Sharma, “Efficient thermal management of data centers—Immediate and long-term research needs,” *HVAC&R Res.*, vol. 9, no. 2, pp. 137–152, 2003.

[113] H. M. Daraghmeh and C.-C. Wang, “A review of current status of free cooling in datacenters,” *Appl. Therm. Eng.*, vol. 114, pp. 1224–1239, 2017.

[114] L. Gimeno *et al.*, "Oceanic and terrestrial sources of continental precipitation," *Rev. Geophys.*, vol. 50, no. 4, 2012.

[115] Y. Gong, F. Zhou, G. Ma, and S. Liu, "Advancements on mechanically driven two-phase cooling loop systems for data center free cooling," *Int. J. Refrig.*, 2022.

[116] W. Feist, J. Schnieders, V. Dorer, and A. Haas, "Re-inventing air heating: Convenient and comfortable within the frame of the Passive House concept," *Energy Build.*, vol. 37, no. 11, pp. 1186–1203, 2005.

[117] J. L. Niu, L. Z. Zhang, and H. G. Zuo, "Energy savings potential of chilled-ceiling combined with desiccant cooling in hot and humid climates," *Energy Build.*, vol. 34, no. 5, pp. 487–495, 2002.

[118] R. R. Schmidt, K. C. Karki, K. M. Kelkar, A. Radmehr, and S. V Patankar, "Measurements and predictions of the flow distribution through perforated tiles in raised floor data centers," *Proc. Pacific Rim/ASME Int. Electron. Packag. Tech. Conf. (IPACK), Kauai, HI*, 2001.

[119] P. Lin, J. Niemann, and L. Long, "Choosing between direct and indirect air economization for data centers," *White Pap.*, vol. 215, 2015.

[120] H. Shrigondekar, Y.-C. Lin, and C.-C. Wang, "Investigations on performance of single-phase immersion cooling system," *Int. J. Heat Mass Transf.*, vol. 206, p. 123961, 2023.

[121] M. Ni and S. O. Memik, "Thermal-induced leakage power optimization by redundant resource allocation," in *Proceedings of the 2006 IEEE/ACM international conference on Computer-aided design*, 2006, pp. 297–302.

[122] R. Mukherjee, S. O. Memik, and G. Memik, "Peak temperature control and leakage reduction during binding in high level synthesis," in *Proceedings of the 2005 international symposium on Low power electronics and design*, 2005, pp. 251–256.

[123] A. Agarwal, S. Mukhopadhyay, C. H. Kim, A. Raychowdhury, and K. Roy, "Leakage power analysis and reduction: models, estimation and tools," *IEE Proceedings-Computers Digit. Tech.*, vol. 152, no. 3, pp. 353–368, 2005.

[124] F. Fallah and M. Pedram, “Standby and active leakage current control and minimization in CMOS VLSI circuits,” *IEICE Trans. Electron.*, vol. 88, no. 4, pp. 509–519, 2005.

[125] H. Kepekci and A. Asma, “Comparative Analysis Of Heat Sink Performance Using Different Materials,” *Am. J. Eng. Res.*, vol. 9, no. 4, pp. 204–210, 2020.

[126] C. G. Popovici, S. V. Hudişteanu, T. D. Mateescu, and N.-C. Chereches̹, “Efficiency improvement of photovoltaic panels by using air cooled heat sinks,” *Energy procedia*, vol. 85, pp. 425–432, 2016.